Isotope Workshop Volume, ESIR XVIth Workshop

Book · July 2023

Ana-Voica Bojar
University of Salzburg
147 PUBLICATIONS 1,419 CITATIONS

Gottfried Tichy
University of Salzburg
5 PUBLICATIONS 21 CITATIONS

Lasocin Lublin

Budapest Portorož

Kraków Tallinn

Seggauberg Leipzig

Cluj-Napoca Złotniki Lubańskie

Budapest Freiberg

Zadar Băile Govora

Lublin

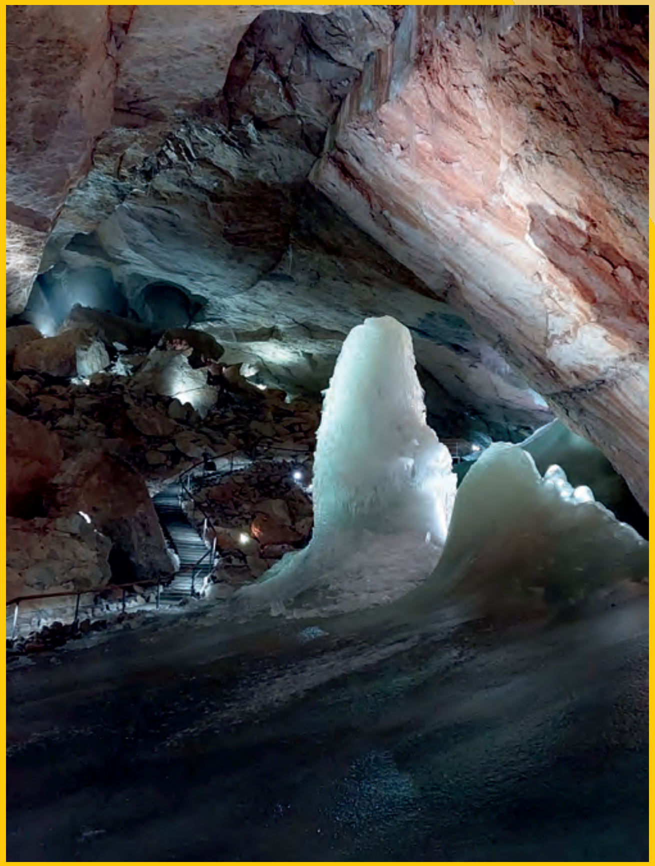

Mineralogie
Studienzentrum Naturkunde
Universalmuseum Joanneum

ESIR

ESIR Isotope Workshop XVI
July, 2023
Graz, Austria

European Society for Isotope Research (ESIR) XVI

European Society for Isotope Research

ESIR XVI
Graz

July 10th to 14th 2023

Isotope Workshop Volume

European Society for Isotope Research

Isotope Workshop Volume
ESIR
XVIth Workshop
Graz, July 10th to 14th 2023

Hosted by:
Universalmuseum Joanneum
Department of Mineralogy

Ana-Voica Bojar, Gottfried Tichy., Hans-Peter Bojar, Bernd Moser, Artur Wojtowicz, Andrzej Pelc, Franz Neubauer, 2023: Abstract and Geological Trip XVIth; Workshop of the European Society for Isotope Research, Graz, Austria (organisation, redaction, design, layout, excursion guide and homepage) 156 pages.

What can the sediments of a cooling pond say about liquid ^{14}C aqueous discharges from the nuclear power plant: case study Lake Drūkšiai, Ignalina nuclear power plant cooling pond

Barisevičiūtė R., Ežerinskis Ž., Šapolaitė J., Butkus L.
State Research Institute Center for Physical Sciences and Technology, Savanorių Ave. 231, LT-02300 Vilnius, Lithuania

Mažeika J.
State Research Institute Nature Research Centre, Akademijos 2, Vilnius, LT 08412, Lithuania

Radiocarbon is produced in nuclear reactors through neutron-induced reactions with ^{14}N, ^{17}O, and ^{13}C isotopes present in the materials of fuel, moderator and coolant of reactors [1]. Areas in close proximity to nuclear power plants are most affected by airborne releases. Normally, liquid effluents are considered to contain relatively low amounts of ^{14}C.

The Ignalina nuclear power plant (INPP) operated two RBMK-1500 units (design electric power 1500 MW_e and decreased to 1350 MWe due to safety concerns after the Chernobyl accident). For 26 years, Lake Drūkšiai served as a cooling basin for the INPP. Unit 1 came online in December 1983 and was shut down on December 31, 2004. Unit 2 was put into operation in August 1987 and shut-down on December 31, 2009. An official monitoring of ^{14}C in liquid releases from the Ignalina nuclear power plant was never performed.

Any official data concerning liquid ^{14}C releases from the other RBMK-type reactors are not available. However, the INPP was one of the rarer cases when the nuclear power plants used the lake as a pond for cooling and industrial discharges. Furthermore, the relatively long water residence time in the lake (of 3 y) allowed reconstruction of the routine ^{14}C liquid releases from the INPP to its cooling pond Lake Drūkšiai with sufficiently high temporal resolution by analysing the radiocarbon vertical distribution in sediment core samples, taken in the main sedimentation area of the lake.

In this work, we had the possibility to compare the radiocarbon distribution in three sediment cores (one taken in 2013 and two in 2019). Comparison of the vertical distribution of radiocarbon in the three undisturbed bottom sediment cores taken within an area of 50-100 m size in the deepest depression of Lake Drūkšiai revealed some differences in ^{14}C activity concentration profiles. Typically, radiocarbon distribution studies are not performed on multiple sediment cores from the same lake site, as it is simply not expected that the carbon cycle at the closely located sites would be affected by different factors [2,3]. Cores taken in 2019 showed a permament^{14}C release rate of 0.76±0.06 GBq/y all eight years after the closure of the INPP. The ^{14}C release rate established from radiocarbon measurements in both cores did not differ by more than 0.8 GBq/y. However, including data from the core taken several years ago, the estimated radiocarbon release rate values varied within 1.3 GBq/y.

It must be considered that carbon isotopic composition in the lake ecosystem was also influenced by other factors associated with anthropogenic activity not related to ^{14}C pollution, including hydrological changes in the lake, an increase in the temperature that affected all processes in the lake's ecosystem. All of such factors could lead to variation of the estimated liquid radiocarbon discharges from INPP.

References

[1] International Atomic Energy Agency Technical Report 421. 2004.
[2] Mischke S, Weynell M, Zhang C, Wiechert U. Quat. Int. 313–314 (2013) 147–155.
[3] Hou J, D'Andrea WJ, Liu Z. Quat. Sci. Rev. 48 (2012) 67–79.

$\delta^{13}C$ and intrinsic water use efficiency (iWUE) for trees in various health conditions – case study for Świerklaniec Forest District

Benisiewicz B., Pawełczyk S., Kłusek M.
Institute of Physics – CSE, Silesian University of Technology, Konarskiego 22B, 44-100 Gliwice, Poland

The research was carried out for two pines growing side by side in the Świerklaniec Forest District. One tree was in good health condition, the other pine had damaged crown and was destined to be cut down. Tree cores were subjected to dendrochronological analysis. Based on these studies, cores were divided into annual increments and subjected to chemical preparation. Carbon isotopic composition of α-cellulose samples was determined using mass spectrometer coupled to the elemental analyzer. Additionally, based on the $\delta^{13}C$ values, the iWUE values were calculated, and trees sensitivity to change of temperature and sum of precipitation was checked. Isotopic studies covered the years 1967-2020.

Until the end of the 1990s, the record of $\delta^{13}C$ had significantly lower values for a healthy tree than for a damaged tree. The isotope record of a healthy tree since 1980 is characterized by a horizontal trend, in the case of a damaged tree there is a clear downward trend from 1985 to 2000. Correlation coefficients between isotopic and climatic data indicate different sensitivity of trees to climatic factors. Apart from climatic factors, pollutant emissions could have had an impact on tree growth and $\delta^{13}C$ values, especially since there is a zinc smelter near the sampling site. The characteristics of the trend can be justified by the number of pollutants emitted by industrial plants (especially SO_2), which were the highest in the 1970s and 1980s, and significantly decreased in the 1990s. Differences in iWUE, calculated from data sets, representing two trees are significant.

The CO_2-rich gas-emissions from the Carpathians: constraints from noble gas isotopic compositions

Boglárka-Mercedesz Kis
Babeș-Bolyai University, Department of Geology, M. Kogălniceau 1, 400084 Cluj-Napoca, Romania

László Palcsu
Szabolcs Harangi, MTA-ELTE Volcanology Research Group, ELTE University Budapest, Pázmány sétány 1/C, Budapest, H-1117, Hungary

Antonio Caracausi
Istituto Nazionale di Geofisica e Vulcanologia, Sezione di Palermo, Via Archirafi 36, 90123, Palermo, Italy.

Roland Szalay
Babeș-Bolyai University, Department of Geology, M.Kogălniceau 1, 400084 Cluj-Napoca, Romania

The mountain range of the Carpathians hosts several gas emissions, that are present especially close to the volcanic centres of the range or within the folded structures (e.g. the Ceahlau-Severin nappe systems in Romania and the Magura nappe systems in Poland). These are mainly carbon-dioxide-dominated emissions, but other gas-species, like methane, nitrogen or hydrogen-sulphur are also present [1, 2, 3]. The gas emissions apper as free gases, mofettes or they are transported to the surface through groundwater and form CO_2-rich mineral water springs or bubbling pools.

The gas emissions, named mofettes, are also used for their curative effects at several places within the Carpathians, (e.g.in Poland and in Romania) [1, 3].

In our study we try to constrain the origin of the gases from their noble gas isotopic composition, especially the helium and neon. Their isotopic signatures reflect multiple sources for these gases, like mantle/magmatic degassing, having R/R_a ratios up to 3, thermal metamorphism of subducted carbonate rocks, having R/R_a values around 1 and $^{13}C\text{-}CO_2$ isotopic signatures typical for limestone and even significant contribution from decomposition of organic material hosted in the flysch deposits, with R/R_a values of typical crustal gases and depleted $^{13}C\text{-}CO_2$.

The origin of the gases is strongly related to the geodynamic and tectonic setting of the Carpathian range and suggest that the possible source for the CO_2 gas is the recycled carbon that formed when subduction processes were active in the Carpathian range. Within the range we find several anomalies, like the area of Ciomadul (Eastern Carpathians, Romania), where the R/R_a reach the highest values within the Carpathian range (R/R_a=3.2), suggesting the importance of mantle upwelling in the area.

Acknowledgements

This work was supported by a grant of the Romanian Ministry of Education and Research, CNCS -UEFISCDI, project number PN-III-P1-1.1-TE-2019-1908, within PNCDI III, contract number TE 63/2020.

References

[1] Vaselli, O., Minissale, A., Tassi, F., Magro, G., Seghedi, I., Ioane, D., Szakács, A., Chemical Geology (182), 637-654

[2] Kis, B., Caracausi, A., Palcsu, L., Baciu, C., Ionescu, A., Futó, I., Sciarra, A., Harangi, Sz., 2019, Geochemistry, Geophysics, Geosystems, 20.

[3] Kotarba, M.J., Sumino, H., Nagao, K., 2020, Applied Geochemistry (122), 104732

Hydrothermal vent fauna, Manus Basin, Papua New Guinea: diet and ecology evidence from multi-element stable isotope geochemistry and arenic speciation

Ana-Voica Bojar[1,2], Christophe Lécuyer[3,4], William Maher[5], Hans-Peter Bojar[2], François Fourel[6], Ștefan Vasile[7]
[1] *Department of Environment and Biodiversity, Salzburg University, Hellbrunnerstrasse 34, A-5020, Salzburg, Austria*
[2] *Department of Mineralogy, Universalmuseum Joanneum, Weinzöttlstrasse 16, A-8045, Graz, Austria*
[3] *Laboratoire de Géologie de Lyon, CNRS UMR 5276, Université Claude Bernard Lyon 1, 69622 Villeurbanne, France*
[4] *Institut Universitaire de France, 103 Boulevard, Saint-Michel, 75005 Paris, France*
[5] *Research School of Earth Sciences, Australian National University, Canberra 2000 Australia*
[6] *Laboratoire d'Ecologie des Hydrosystèmes Naturels et Anthropisés, LEHNA UMR CNRS 5023, Université Claude Bernard Lyon 1, 69622 Villeurbanne, France*
[7] *Department of Geology, Mineralogy, and Paleontology, Faculty of Geology and Geophysics, University of Bucharest, 1 Nicolae Bălcescu Avenue, 010041 Bucharest, Romania*

Vent endemic animals depend on the primary production of symbiotic microorganisms, with life cycles driven by chemosynthesis, instead of photosynthesis. Hydrothermal fluids contain H_2, CH_4, H_2S, NO_3^- , As and metal ions, which are used as energy sources for bacteria in order to fulfil their own and host needs [1], [2], [3]. It has been proposed that the local fluid chemical composition drives the local vent ecology [4] thus symbiosis between chemosynthetic bacteria and invertebrates at deep-sea hydrothermal vents offers opportunities to study the effects of water chemistry, niche segregation and the relationship between symbionts, hosts and diet. An overview of the identified *ε*- and *γ-Proteobacteria* symbiotic chemoautotrophs and associated pathways are given by [5], [6].

In the Western Pacific, four hydrothermal vent sites, with associated chemosynthetic communities have been described: the Manus Basin, the North Fiji Basin, the Lau Basin and the Mariana Trough. The biological assemblages associated with these vents are different from those occurring in the East Pacific and Mid-Atlantic Ridge. Indeed, in the Western Pacific the prevailing gastropods are primary consumers. Situated close to the fast-spreading rift zone (>100 mm/year) of the Manus Basin (Fig. 1), one of the most extended and active hydrothermal fields is Vienna Woods that hosts a faunal assemblage consisting of snails, barnacles, bythograeid crabs, bresiliid shrimps, vestimentiferans, corals and sea anemones [7], [8], [9]. Among the most abundant macro-organisms living at this site, *Alviniconcha hessleri* and *Ifremeria nautilei* occupy niches in the immediate vicinity of the vent and *Eochionelasmus ohtai manusensis* in the distal position.

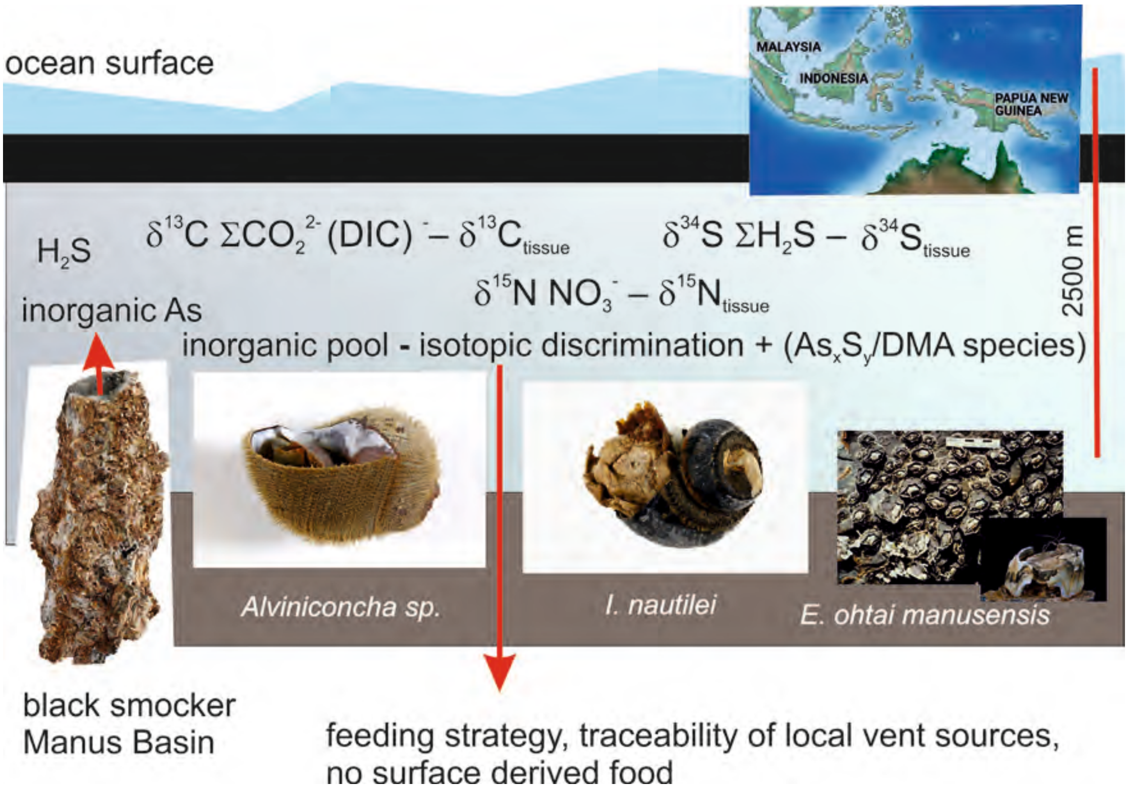

Figure. Location of the investigated site and species in the Western Pacific. The investigated isotope systems as well as arsenic speciation and their relationship with the living organisms are displayed.

In the Western Pacific, four hydrothermal vent sites, with associated chemosynthetic communities have been described: the Manus Basin, the North Fiji Basin, the Lau Basin and the Mariana Trough. The biological assemblages associated with these vents are different from those occurring in the East Pacific and Mid-Atlantic Ridge. Indeed, in the Western Pacific the prevailing gastropods are primary consumers. Situated close to the fast-spreading rift zone (>100 mm/year) of the Manus Basin, one of the most extended and active hydrothermal fields is Vienna Woods that hosts a faunal assemblage consisting of snails, barnacles, bythograeid crabs, bresiliid shrimps, vestimentiferans, corals and sea anemones [7], [8], [9]. Among the most abundant macro-organisms living at this site, *Alviniconcha hessleri* and *Ifremeria nautilei* occupy niches in the immediate vicinity of the vent and *Eochionelasmus ohtai manusensis* in the distal position.

In the present study, in order to determine diets and survival strategies at the active hydrothermal site Vienna Woods, we report $\delta^{13}C$, $\delta^{15}N$, $\delta^{34}S$ data for the dominant assemblage represented by *Alviniconcha* sp., *I. nautilei* and *E. ohtai manusensis.* The isotopic measurements applied to soft tissues and shells allow determining the isotopic discrimination between inorganic water compounds used by organism as nutritional sources and symbiont/host itself. The determined isotopic discrimination provides further information into the type of symbiont of each investigated species and food pathway. A further aim was to provide insights into the process of arsenic (As) bioaccumulation and biotransformation in the investigated marine organisms. As is abundant at hydrothermal vent sites as it is commonly associated with S and can be used by microorganisms that are known to be present in some hydrothermal organisms as symbionts e.g., worms as an alternative energy source [10]. The acquired data allow making comparisons with adjacent vent areas of the Manus Basin such as Solwara 1 and PACMANUS, in order to identify the mechanisms acting at regional scale and asses sources and pathways of nutrients at the investigated site [11, 12].

References

[1] Felbeck, H., Childress, J.J., Somero, G.N., 1981. Calvin-Benson cycle and sulphide oxidation enzymes in animals from sulphide-rich habitats. Nature 293, 291–293.

[2] Nakagawa, S., Takai, K., 2008. Deep-sea vent chemoautotrophs: diversity, biochemistry and ecological significance. FEMS Microbiol. Ecol. 65 (1), 1–14. [3] Le Bris, N., Yücel, M., Das, A., Sievert, S.M., LokaBharathi, P., Girguis, P.R., 2019. Hydrothermal energy transfer and organic carbon production at the deep seafloor. Front. Mar. Sci. 5.

[4] Luther III, G.W., Rozan, T.F., Taillefert, Martial, Nuzzio, D.B., Di Meo, C., Shank, T.M., Lutz, R.A., Cary, S.C., 2001. Chemical speciation drives hydrothermal vent ecology. Nature 410, 813–816.

[5] Yamamoto, M., Takai, K., 2011. Sulfur metabolisms in epsilon- and gamma-proteobacteria in deep-sea hydrothermal fields. Front. Microbiol. 2, 192

[6] Nunoura, T., Takaki, Y., Kazama, H., Kakuta, J., Shimamura, S., Makita, H., Hirai, M., Miyazaki, M., Takai, K., 2014. Physiological and genomic features of a novel sulfur-oxidizing gammaproteobacterium belonging to a previously uncultivated symbiotic lineage isolated from a hydrothermal vent. PLoS One 9 (8).

[7] Lisitsyn, A.P., Crook, K.A.W., Bogdanov, Y.A., Zonenshayn, L.P., Murav'yev, K.G., Tufar, W., Gurvich, Y.G., Gordeyev, V.V., Ivanov, G.V., 1993. A hydrothermal field in the rift zone of the Manus Basin, Bismark Sea. Int. Geol. Rev. 35 (2), 105–126.

[8] Galkin, S.V., 1997. Megafauna associated with hydrothermal vents in the Manus Back Arc basin (bismarck sea). Mar. Geol. 142 (1–4), 197–206.

[9] Collins, P.C., Kennedy, R., Van Dover, C.L., 2012. A bilogical survey method applied to seaflor massive sulphides (SMS) with contagiously distributed hydrothermal-vent fauna. Mar. Ecol. Prog. Ser. 452, 89–107.

[10] Maher, W.A., Duncan, E., Dilly, G., Foster, S., Krikowa, F., Lombi, E., Scheckel, Girguis K. P., 2016. Arsenic concentrations and species in three hydrothermal vent worms, *Ridgeia piscesae, Paralvinella sulficola* and *Paralvinella palmiformis*. Deep-Sea Res. Part I Oceanogr. Res. Pap. 116, 41–48.

[11] Bojar, A.-V., Lécuyer, C., Bojar, H.-P., Fourel, F., Vasile, Ș., 2018. Ecophysiology of the hydrothermal vent snail *Ifremeria nautilei* and barnacle *Eochionelasmus ohtai manusensis*, Manus Basin, Papua New Guinea: insights from shell mineralogy and stable isotope geochemistry. Res. Part I Oceanogr. Res. Pap. 133, 49–58.

[12] Bojar, A.-V., Lécuyer, C., Maher, W., Bojar, H.-P., Fourel, F., Vasile, Ș., 2023. Multi-element stable isotope geochemistry and arsenic speciation of hydrothermal vent fauna (*Alviniconcha* sp., *Ifremeria nautilei* and *Eochionelasmus ohtai manusensis)*, Manus Basin, Papua New Guinea. Chemosphere 324, 138258.

Patterns of Isotopic and Biogeochemical Signatures in *Picea abies* L. Stands in Southern Romania: Implications for Nutrient and Metal Dynamics

Botoran O.R.[1], Costinel D.[1], Miricioiu M.[1], Nechita C.[2], Iordache A.M.[1], Badea S.L[1], Zaharioiu A.M.[1], Sandru C[1], Ionete R.E.[1]
[1]*National Research and Development Institute for Cryogenics and Isotopic Technologies - ICSI Râmnicu Vâlcea, 4th Uzinei Street, 240050 Râmnicu Vâlcea, Romania*
[2]*National Research and Development Institute for Forestry "Marin Drăcea" – INCDS, 128 Eroilor Boulevard, 077190, Voluntari, Romania*

In the post-industrial era, human activities have significantly impacted the nitrogen (N) and carbon (C) cycles, leading to a visible increase in inputs in water and terrestrial ecosystems. The use of N-containing fertilizers is the primarily reason of this growth. Additionally, reactive N (NO_y and NH_x) emissions from burning fossil fuels have led to transboundary pollution and redistributed nitrogen in terrestrial environments. As a result, eutrophication, biodiversity loss, acidification, and emissions of greenhouse gases such as N_2O will occur. The impact of N enrichment has long been debated, particularly regarding possible mitigation strategies for reducing nitrogen in terrestrial ecosystems. This process enhances photosynthesis and plant growth, leading to increased terrestrial net carbon (C) sequestration in soil and biomass, which helps to limit global carbon dioxide emissions. The promotion of carbon storage processes is primarily linked to the availability of essential nutrients such as nitrogen and phosphorus (P), as well as other environmental factors including temperature, water, light, and pH. The adaptability of the ecosystem's carbon to nitrogen (C:N) ratios and processes at regional scales is attributed to the consistent predictability of temperate and boreal forest stoichiometry, biological nitrogen fixation, and the loss of nitrogen within the ecosystem. The natural forest ecosystems in Romania are experiencing a knowledge gap regarding the feedback between the carbon, nitrogen, and phosphorus cycles. Various studies have investigated limitations in nutrient availability, carbon sequestration, net primary productivity, and the impact of toxic metals on soil and forest production. However, the interdependent relationships and dynamics of elements other than carbon (C), nitrogen (N), and phosphorus (P) were not extensively studied. The challenge of this study was to determine the primary control mechanism of these elements on *Picea abies* L needles, bark, litter, and soil. Specifically, the investigation aimed to assess the initial effects of litter and soil solution chemistry on *Picea abies* L bark and needles in the Cozia National Park in Romania. Furthermore, the study included an analysis of the impact on C:N:P stoichiometry ratios and nutrient pool, as well as an in-depth assessment of interactions with metal accumulation and mobility.

The study investigated the stable carbon and nitrogen isotope ratios ($\delta^{13}C$ and $\delta^{15}N$) and nutrient ratios (C:N, C:P, and C:H) of various matrices, including needles, bark, litter, and soil samples from 17 evergreen coniferous forest sites in the Southern Carpathians, spanning an altitudinal range between 521 and 1554 m. The $\delta^{13}C$ varied widely in needles (-32.09 ‰ to -27.23 ‰) and bark (-28.24 ‰ to -23.84 ‰), with a higher range observed in the needle (4.86 ‰) and bark (4.40 ‰). The $\delta^{15}N$ values showed a decreasing trend from the lower layers of the soil to the litter, and the mean value was negative in needles (-1.27±1.05 ‰) compared with bark (1.42±1.77 ‰). The C:N ratio ranged widely across the matrices, with the highest values observed in the needles (28 to 90.4) and bark (70.5 to 112.29) and the lowest values in the soil samples (0.45 to 14.09). Carbon and nitrogen are fundamental elements that play critical roles in plant growth and ecosystem functioning. Carbon is important for energy transfer and nutrient cycling, while nitrogen is essential for protein synthesis and other metabolic processes in plant cells. The ratio of carbon to nitrogen (C:N) is an important indicator of nutrient use efficiency in plants. A higher C:N ratio suggests that nitrogen is used more efficiently, whereas a lower C:N ratio is associated with faster microbial decomposition and the release of nitrogen into the environment. The C:P ratio was highest in the litter (0.80±0.61) and decreased in bark (0.26±0.06) and needles (0.12±0.08), while the C:H ratio had comparable mean values for needles, bark, and litter and decreased in the soil samples. In the current study, the individual role of each element examined is linked to multiple physiological and photosynthetic responses rather than a single mode of action. Moreover, the investigation has identified significant differences between the various matrices (needles, bark, litter, and soil) for each element, suggesting that the relationships and sources are intricate and multifaceted.

This research revealed significant differences in the chemical profiles of soil, litter, needles, and bark, indicating differences in nutrients, heavy metals, and toxic metals. These differences can be attributed to both natural and human-induced factors, with high levels of certain nutrients, such as calcium and potassium, or low levels of sodium, potentially indicating an imbalance in the nutrient cycle caused by human disturbances. Low C:N ratios were observed in both soil and litter, indicating low levels of residue return and organic carbon and nitrogen accumulation. The interactions between nutrients and other compounds, such as heavy metals and toxic elements, were found to have mainly negative relationships, which contributed to the heterogeneity observed in the various matrices. The variance between matrices differed significantly, indicating that the turnover processes of organic layers are influenced by tree inputs on soil organic matter quality and mineral content. The high C nutrient ratio observed in needles allows for increased carbon storage per unit nutrient in the forest ground ecosystem, but may have a negative impact on the regional climate.

Keywords: isotopic fingerprint, chemical profile, evergreen forest, altitude trend

Acknowledgement

This work has been financed by the Ministry of Research, Innovation and Digitization through Program 1 - Development of the national research and development system, Subprogram 1.2 - Institutional performance - Projects for financing excellence in R&D, Contract no. 19PFE/2021, and NUCLEU Program, grant number PN 19110302: „*Research on the variation trends specific to stable isotopes in different tree species: deepening the fractionation mechanisms and chemical processes interconnected on the soil-water-plant chain*” and project PN 23150301 „*Implementation of integrated isotopic-chemical-nuclear analytical methodologies for authentication the traditional Romanian food products*”.

Isotope biogeochemistry of carbonate-bearing sinter in the Anthropocene

Michael Ernst Böttcher[1,2,3*], Tamina Bruhnke[1], Cátia M. Ehlert von Ahn[1], Peter Escher[1,4], Marko Lipka[1,5], Patricia Roeser[1,6], Iris Schmiedinger[1], Vera Winde[1,7], and Zijun Wu[1,8]

[1]*Geochemistry & Isotope Biogeochemistry, Leibniz Institute for Baltic Sea Research (IOW), Germany*
[2]*Marine Geochemistry, University of Greifswald, Germany*
[3]*Interdisciplinary Faculty, University of Rostock, Germany*
[4]*Present address: Ecoandmore, Freiburg, Germany*
[5]*Present address: UKA Nord Projektentwicklung, Rostock, Germany*
[6]*Present address: University of Bonn, Environmental Geosciences, Germany*
[7]*Present address: Hydroisotop, Schweitenkirchen, Germany*
[8]*Present address: State Key Laboratory of Marine Geology, Tongji University, PRC*

Introduction

Processes in the dissolved carbonate system of fresh surface waters may contribute and are sensitive to variations of boundary conditions associated with climate change in the Anthropocene. Groundwaters saturated in $CaCO_3$ and supersaturated in carbon dioxide (when it comes into contact with the atmosphere) that emerge from springs start to degas carbon dioxide to the atmosphere. This process leads to the development of calcite supersaturation of the aqueous solution. When exceeding a critical value, solid disequilibrium carbonates precipitate, thereby linking the present terrestrial, with the past marine carbon cycles. The distribution of trace elements and different stable isotopes associated to the mineral precipitation fractionations is linked to non-equilibrium processes, impacted by the initial solution composition, hydrodynamics, and possible biological activity in the stream beds and leads to the development of characteristic geochemical signals. A comparison of trace element discrimination with experimental calibrations allows for an estimate of in-situ precipitation rates (e.g., [1, 2]). In case of anoxic ground water appearance, iron ochre formation may further occur, that is controlled by oxygen uptake, carbon dioxide degassing, and potential microbial activity of iron-oxidizing bacteria. Most pronounced anthropogenically induced carbonate formation conditions are found upon concrete weathering, when hyperalkaline solutions develop allowing for the absorption of atmospheric carbon dioxide (the reversed process when compared to the hard water creek development [3]) and the abiotic formation of $CaCO_3$. Stable isotope discrimination, in particular, allows to understand the processes leading to the relative contributions from loss/gain of CO_2 to/from the atmosphere and/or the biosphere, the fixation into carbonate minerals, and the residual dissolved carbon fluxes towards rivers and the coastal sea [3, 5, 6]. Since these fresh waters may be enriched in nutrients, metals, and dissolved inorganic carbon, the discharge to coastal waters is potentially linked to societal issues, like the change in buffer capacity which is associated to the consequences of *rising green-house gas levels* and *surface ocean water acidification*.

Study sites and isotope geochemical and physico-chemical analyses

Examples for hard water creeks and ferruginous springs in the temperate climate zone showing recent active sinter formation were chosen from Rügen Island (Site R), sites close to Meschendorf (Site M, [6, 7]), both located at the southern Baltic Sea. The results are compared to a site close to Westerhof (Site W) where a long research history is documented (e.g. [2, 4, 5]) that allow for a look on the potential reflection of environmental changes by the isotope geochemical signals. As examples for active chemical carbonate precipitation driven by the absorption of atmospheric CO_2, which is a typical by product of concrete degradation [8], weathered World War II bunker systems (Site B) from the North Sea coastline were investigated.

Besides physical in-situ parameters (temperature, pH, electric conductivity, major and trace elements), nutrients, and the stable isotope (H, C, O, S) composition of dissolved and solid phases were analyzed by ICP-OES, nutrient analyzer, gas irmMS, and CRDS techniques. A physicochemical characterization of the aqueous solution was carried out by using the PHREEQC code. Carbonate precipitation rates are estimated based on measured trace element distribution coefficients in comparison to calibrated experimental studies. Textural and chemical compositions of solid phases were furthermore analyzed by SEM-EDX.

Results and discussion

All hard-water creeks at Sites R and W sites are characterized by a two-stage developement of the surface waters that can be differentiated in: 1. An induction period starting at the spring, where degassing of carbon dioxide takes place, followed 2. by a stage where calcite formation from the highly supersaturated solution is continuously driven by further degassing. In both phases, the liberation of CO_2 is associated with an enrichment of the heavy carbon isotope in the remaining dissolved inorganic carbon. Trace element (Li, Na, Mg, Sr, Ba, SO_4) discrimination between the aqueous solutions and recent calcite precipitates along the flow path yield distribution coefficients that are compared to calibrated experimental studies to estimate calcite precipitation rates. The trace-element based rate estimates for Site W are higher than published direct measurements [2], which is presumably due to hydrodynamic boundary conditions impacting the in-situ growth experiments. Stable isotope signatures (^{13}C, ^{18}O, ^{34}S) allow for an element source identification and mechanistic interpretation of the processes controlling the carbonate system. The geochemical results at Site W can be compared with observations dating back to the late 60s [2, 4, 5].), now allowing for an analysis for ecosystem changes during more than 5 decades. Whereas, C and O isotope signatures are surprisingly similar through time, the sulfur isotope signals indicate differences within this time period, likely reflecting changes in the atmospheric sulfur cycle. Besides carbonates, idiomorphic $BaSO_4$ was observed in recent carbonate sinters at Sites R and W for the first time, in accordance with slight physicochemical supersaturation found for the hard water creeks. This new finding indicates that trace element and stable isotope signatures in fresh water barite may have a, to be further explored, proxy potential. At Sites R and M the stream finally end in the coastal brackish Baltic Sea. The excess in dissolved CO_2 compared to the atmosphere enhances the degassing capacity of the mixed coastal waters, which may partly be buffered by thew dissolution of mechanically eroded carbonate rocks from the carbonate cliffs.

Concrete degradation leads to the fixation of atmospheric CO_2 marked by the development of extreme disequilibrium isotope signatures that are kinetically controlled by the chemical hydroxylation of absorbed CO_2 into the hyperalkaline solutions followed by the very fast precipitation of the solid [e.g., 3, 8].

In the case of anoxic groundwater discharge, the isotope hydrogeochemical composition indicates that the development of the spring water is controlled by the initial uptake of biogenic carbon dioxide in the unsaturated soil zone of the catchment area followed by the dissolution of carbonate and pyrite in the aquifers. Discharge of these fresh waters along the coastline leads to a surface flow towards the Baltic Sea, which is accompanied by a subsurface submarine ground water discharge (SGD) component. The contact with the atmosphere is associated with a release of isotopically light CO_2, the uptake of gaseous oxygen, the microbially promoted precipitation of FeOOH and calcite, adsorption of P and trace elements. The development of the calcite-supersaturation level along the surface flow-path is balanced by a delicate interplay of the different pH-impacting processes. The developing temporal iron curtain acts as an element sink in the beach sediments that may be transported into the Baltic Sea coastal waters during erosion events [6] that are expected to increase in frequency upon rising seawater level.

Therefore, carbonate-precipitating fresh waters act as a source for atmospheric CO_2, although they are forming carbonate-bearing deposits on land, but the degradation of concrete installations may lead to a minor fixation of atmospheric CO_2, similar to the weathering of ultramafic coastal sands [9].

Acknowledgements

The presented studies were partly supported by the DFG research training group BALTIC TRANSCOAST and the carbon part belongs partly to the BMBF project COOLSTYLE as part of CARBOSTORE. All parts were further supported by Leibniz IOW. Participants of the Greifswald Aquatic Environmental Geochemistry (GAEG) class are acknowledged for their enthusiastic field support. The authors further wish to thank O. Dellwig, A. Köhler, R. Bahlo, and S. Plewe for expert ICP-OES and SEM-EDX support.

References

[1] Böttcher M.E., Dietzel M., 2010. Metal-ion partitioning during low-temperature precipitation and dissolution of anhydrous carbonates and sulfates. EMU Notes in Mineralogy 10, 139-187.

[2] Dreybrodt W., Buhmann D., Michaelis J., Usdowski E., 1992. Geochemically controlled calcite precipitation by CO_2 outgassing: Field measurements of precipitation rates in comparison to theoretical predictions. Chem. Geol. 97, 285-297.

[3] Böttcher M.E., Neubert N., Escher P., von Allmen K., Samankassou E., Nägler, T.F., 2018. Multi-isotope (Ba, C, O) partitioning during experimental carbonatization of a hyperalkaline solution. Geochemistry, 78, 241-247.

[4] Savelli C., Wedepohl K.-H., 1967. Geochemische Untersuchungen an Sinterkalken (Travertinen), Contr. Mineral. Petrol. 21, 238-256.

[5] Michaelis J., Usdowski E., Menschel G., 1985. Partitioning of ^{13}C and ^{12}C on the degassing of CO_2 and the precipitation of calcite – Rayleigh-type fractionation and a kinetic model. Am. J. Sci. 285, 318-327.

[6] Lipka M., Böttcher M.E., Wu Z., Sültenfuß J., Jenner A.-K., Westphal, J., Dellwig, O., Escher P., Schmiedinger I., Winde V, Struck U., 2018. Ferruginous groundwaters as a source for P, DIC, and Fe in coastal waters of the southern Baltic See: Isotope hydrobiogeochemistry and the role of an iron curtain. E3S Web Conf. 54, 1-5.

[7] Ehlert von Ahn C. M., Scholten J., Malik C., Feldens P., Liu B., Dellwig O., Jenner A.-K., Papenmeier S., Schmiedinger I., Zeller M.A., Böttcher M.E., 2021. A multi-tracer study of fresh submarine and surface water sources for a temperate urbanized coastal bay. Front. Environm. Sci., 9: 642346.

[8] Dietzel, M., Usdowski, E., Hoefs, J., 1992. Chemical and $^{13}C/^{12}C$- and $^{18}O/^{16}O$-isotope evolution of alkaline drainage waters and the precipitation of calcite. Appl. Geochem. 7, 177–184.

[9] Bernier P., Guidi J.-B., Böttcher M.E., 1997. Coastal progradation and very early diagenesis of ultramafic sands as a result of rubble discharge from asbestos excavations (North Corsica, France). Mar. Geol. 144, 163-175

A stable isotope look on benthic sources for dissolved inorganic carbon in the North Sea: The Skagerrak example

Michael Ernst Böttcher[1,2,3*], Carla Nantke[1], Antonia Schell[1], Donald E. Canfield[4], Cátia M. Ehlert von Ahn[1], and Iris Schmiedinger[1]

[1]*Geochemistry & Isotope Biogeochemistry, Leibniz Institute for Baltic Sea Research (IOW), Germany*
[2]*Marine Geochemistry, University of Greifswald, Germany*
[3]*Interdisciplinary Faculty, University of Rostock, Germany*
[4]*Institute of Biology, University of Southern Denmark, Odense M, Denmark*

Introduction

Marine sediments may act as a sink for carbon. Substrate and electron donor availabilities, sedimentology, as well as biological activity may influence the carbon cycling, impacting the release of TA and DIC. The North Sea is a highly dynamic system with shallow tidal areas and fresh water tributaries delivering nutrients and dissolved carbon. For the southern part, benthic DIC sources have been identified [1], with tidal areas being further hot spots [2], some being impacted by submarine fresh water discharge [3]. The Skagerrak provides the unique opportunity of studying benthic DIC production under the impact of different dominant electron acceptors [4, 5, 6, 7]. Potential transformation of carbonates may impact release of TA and DIC.

Study sites and isotope geochemical and physico-chemical analyses

Here, we focused on the role of different electron acceptors [4] in sediments from the North Sea, with a special focus on the Skagerrak. The pelagic and benthic system was investigated for the DIC source function and carbon storage capacity. Water column, pore water, and sediment samples were investigated to understand the processes controlling the benthic production and release of TA and DIC. The carbon (and oxygen) isotope composition of dissolved and solid phases was used to understand the specific biogeochemical processes dominating benthic mineralization and carbonate dissolution.

Besides physical in-situ parameters (temperature, pH, electric conductivity, major and trace elements), nutrients, and the stable isotope (H, C, O) composition of dissolved and solid phases were analyzed by ICP-OES, nutrient analyzer, gas irmMS, and CRDS techniques. Sediments were further analyzed for organic and inorganic carbon contents, as well as extractable major, and trace elements.

Results

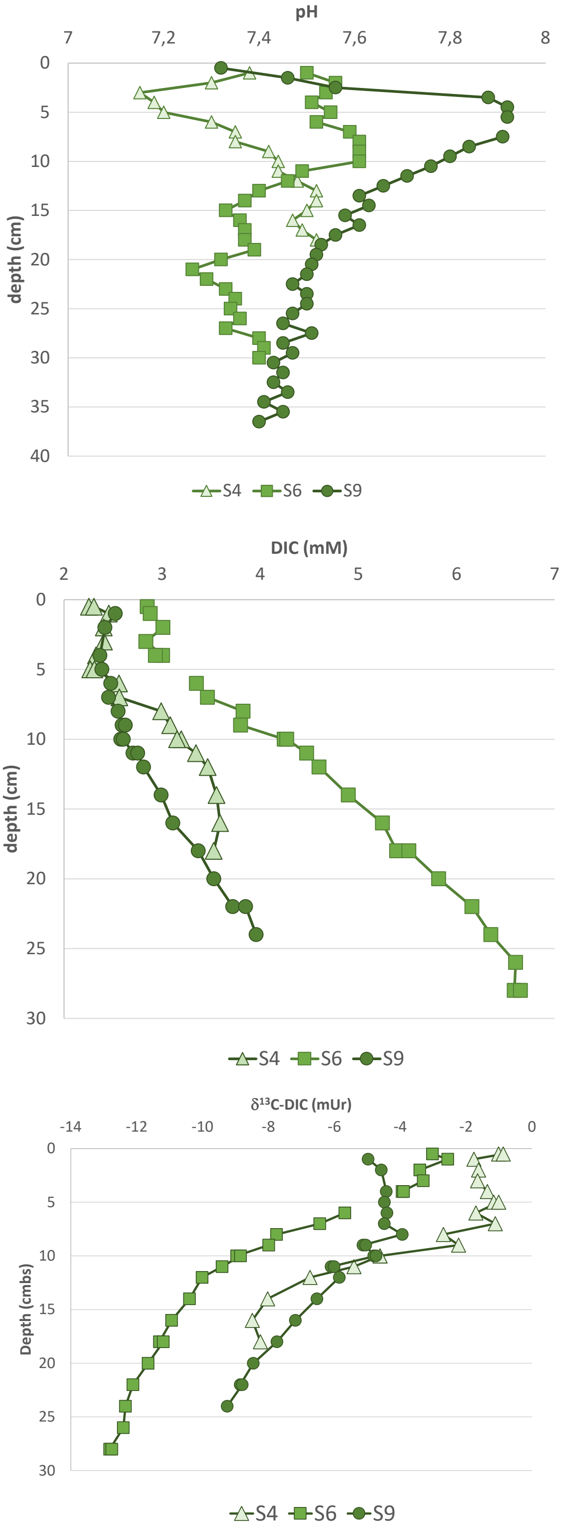

Figures: Downcore variations of pore water variables in sediments of Sites S4, S6, and S9 [4] demonstrate the role of different mineralization processes for the release of DIC and the resulting flux of isotopically light across the sediment-water interface

Acknowledgements

The present study was supported by the BMBF project COOLSTYLE as part of CARBOSTORE, and by Leibniz IOW. We wish to thank the captain and crew of RV Skagerrak and Denise Otto for on-board support.

References

[1] Burt et al. (2016) Limnol. Oceanogr. 61, 666-683.
[2] Schwichtenberg et al. (2020) Biogeosciences, 17, 4223-4245.
[3] Winde V. et al. (2014) J. Mar. Sys. 129, 394-402.
[4] Canfield D.E. et al. (1993) Geochim Cosmochim Acta 57, 3867-2883.
[5] Reyes C.et al. (2016) FEMS Microbiol Ecol. 92, fiw054
[6] Reyes C. et al. (2017) Mar Biotechnol 19, 175-190
[7] Reyes C. et al. (2017) Geomicr. J. 34, 840-850

Hydro- and isotope geochemistry of a ferruginous spring

Elke Bozau[1], Martina Jutta Weichmann[1], Michael Ernst Böttcher[2,3,4]
[1]*TU Clausthal, IGP, Leibnizstr. 10, 38678 Clausthal-Zellerfeld, Germany*
[2]*Leibniz-Institut für Ostseeforschung, Seestr. 15, 18119 Warnemünde, Germany*
[3]*Marine Geochemistry, University of Greifswald, Germany*
[4]*Interdisciplinary Faculty, University of Rostock, Germany*

Introduction

Iron oxyhydroxide precipitation at springs is a well-known biogeochemical process and often accompanied by the degassing of carbon dioxide. Both processes are associated with changes in pH and the concentration of dissolved ions. Furthermore, a significant kinetic ^{13}C enrichment occurs during CO_2 degassing in the water along the flow path in contact with the atmosphere [1]. Physicochemical equilibrium is seldomly reached under natural conditions and kinetics are impacted by many factors, including hydrodynamics, microbial activity and the initial composition of the solution. To understand the main processes underlying the hydrochemical development of such a ferruginous spring system in the Harz Mountains, water samples were analysed and experimental investigations were carried out.

Figure 1: The iron spring (tube = sample 1, channel: sample 2 & 3, outflow to the ditch = sample 4)

Study site, sampling, analytical methods and modelling

The so-called "Eisenquelle" (iron spring) is located near the hiking trail "Hexenstieg" in the Harz Mountains (Germany) and discharges from an aquifer at the border of fractured quartzite and greywacke with siliceous and argillaceous shales. The runoff of the spring is varying from 0.02 up to 6 L/s. Bog iron stabilised by organic ligands and weathered silicate minerals of the aquifer rocks are considered to be the source of iron in the spring water.

Water quality of the iron spring (Figure 1) has been investigated for about 50 years [2 - 5]. The spring water was sampled at the tube (sample 1). To get more information about CO_2 degassing and iron precipitation, additional samples have been taken along the flow path since February 2019. Temperature, pH, specific electrical conductivity (SEC), major ions, trace metals and isotope data (δ^2H, δ^{13}C, δ^{18}O, δ^{34}S) were analysed as described by [2 - 5]. Saturation indices and CO_2 partial pressures for the sampled spring water were calculated using the PHREEQC package [6] and the thermodynamic database “phreeqc.dat”.

Results and discussion

The main chemical data of all sampling campaigns measured in several studies [2 - 5] are given in Table 1. The pH value of the iron spring ranges from 5.1 up to 7.8, SEC values range between 61 and 171 µS/cm. The water is dominated by sodium and bicarbonate. The measured variations indicated by the concentration of dissolved ions and SEC can be explained by the seasonal variation of the precipitation rate. Comparing the historical evolution of the ionic composition starting in the 1970s until now shows that besides seasonal dynamics, in particular the sulphate concentrations decreased similar to many European watersheds with short residence times due to the reduction of sulphur emissions since the 1990s of the last century [7]. The average sulphate concentration in the iron spring was 24 mg/L in the 70s whereas less than 8 mg/L were measured between 2010 and 2019. Sulphate concentrations in precipitation measured in a nearby study site [8] showed 0.3 - 3.3 mg sulphate/L in 2014. Iron concentrations in the iron spring range between 0.5 - 9 mg/L. Analyses of filtered (0.45 µm) and unfiltered samples at the tube indicate that the fraction of dissolved iron is about 90 %. The highest SEC values (171 µS/cm) and most of the ions (except for iron) were observed after a long dry period in 2018.

Tab. 1: Water quality variations of the iron spring (1972 - 2019)

Sampling year	1972 – 1973 (7)	1997 (4)	2010 – 2019 (10)
(Number of samples)	Min … Median … Max	Min … Median … Max	Min … Median … Max
pH	5.1 … 5.7 …6.5	6.5 … 6.5 … 6.8	5.2 … 6.2 … 7.8
SEC (µS/cm)	61 … 79 … 94	104 … 124 … 142	73 … 113 … 171
Ca^{++} (mg/L)	2.3 … 3.0 … 4.0	3.9 … 4.9 … 9.4	3.3 … 5.1 … 16
Mg^{++}	2.6 … 2.7 … 3.2	2.2 … 2.4 … 4.2	1.5 … 2.8 … 3.6
Na^+	5.8 … 6.4 … 8.1	4.9 … 5.2 … 8.5	7.6 … 9.6 … 11
HCO_3^-	24 … 31 … 43	n.a.	32 … 36 … 49
Cl^-	4.9 … 6.5 … 14	11 … 12 … 14	7.1 … 15 … 21
SO_4^{--}	8.0 … 24 … 28	7.6 … 10 … 13	5.5 … 7.4 … 8.4
Fe_{total}	0.5 … 2.0 … 5.5	2.3 … 5.8 … 8.2	1.1 … 3.2 … 6.6
Reference	Alicke (1974)	Weller (1998)	Bozau et al. (2013, 2021)

DOC was measured on selected occasions between 2010 and 2012 [4] and displays wide seasonal changes (1.8 - 7.0 mg C/L) with higher concentrations during the vegetation period. The δ^{18}O and δ^2H values of the spring water correspond to the values of the regional atmospheric precipitation [4, 5]. Compared to other springs of the Upper Harz Mountains, a relatively wide range of these values is found (δ^{18}O: -9.7 … -8.5 ‰ VSMOW) which may be explained by a relatively fast response of the spring water to precipitation events. In February 2019, September 2021 and March 2022, the carbon isotope composition (δ^{13}C values between -22 ‰ and -15 ‰ VPDB) indicates that the main source of DIC is dissolved soil CO_2 originating from root respiration and the degradation of C3 organic matter [9 - 11].

Tab. 2: Hydrogeochemical data along the flow path of the iron spring measured in December 2021

Sample	1 - Tube	2	3	4 - Outflow
pH	5.8	6.0	6.0	6.1
SEC (µS/cm)	127	127	126	126
Ca^{++} (mg/L)	5.66	5.68	5.76	5.80
Mg^{++}	2.97	2.91	2.93	2.96
Na^{+}	10.6	10.6	10.6	10.7
HCO_3^- (mg/L)	34.2	34.1	34.1	33.9
Cl^-	15.0	15.1	15.0	15.1
SO_4^{--}	4.67	4.70	4.73	4.69
Fe_{total} (mg/L)	2.85	2.92	2.86	2.79

The δ^{34}S values of 2.1 ‰ (February 2019) and 0.5 ‰ VDCT (March 2022) for sulphate in the spring water are slightly lower than the average values of atmospheric sulphate [11 - 12], probably due to some discriminating sorption processes or minor water-rock interaction before discharge. The chemical changes along the flow path were investigated in December 2021. The data (Table 2) display only small changes of pH, SEC, dissolved iron and bicarbonate, indicating relatively slow precipitation of the metal oxyhydroxides. Batch tests and PHREEQC modelling results showed that chemical equilibrium is not reached. Whereas the outgassing of CO_2 leads to slightly decreasing DIC along the flow path, an increase of δ^{13}C values is clearly seen due to the preferential degassing of light isotopes [1, 9]. In March 2022, the δ^{13}C value increased by -1.5 ‰ along the flow path.

Conclusions

The hydrogeochemical parameters of the studied iron spring are changing on a seasonal scale. Iron oxyhydroxide precipitation and carbon dioxide degassing are observed along the flow path. Chemical equilibrium conditions are not established until the end of the flow channel due to the continuous reactions with atmospheric gases at high flow rates. The δ^{13}C values of the DIC can be used as a particularly sensitive tracer for disequilibrium processes of the carbonate system. It is planned to investigate the iron precipitates along the flow channel for trace metals, oxygen and iron isotopes to get further insights of the microbial activity in the spring system.

Acknowledgements

The authors acknowledge analytical support by the TUC and IOW laboratories, in particular S. Schlenczek, F. Funke, I. Schmiedinger and A. Koehler.

References

[1] Michaelis J., Usdowski E., Menschel G., 1985. Partitioning of ^{13}C and ^{12}C on the degassing of CO_2 and the precipitation of calcite – Rayleigh-type fractionation and a kinetic model. Am. J. Sci. 285, 318-327.

[2] Alicke R., 1974. Die hydrochemischen Verhältnisse im Westharz in ihrer Beziehung zu Geologie und Petrographie. Clausthaler Geol. Abh. 20.

[3] Weller L., 1998. Die hydrogeologischen und hydrogeochemischen Verhältnisse am NW-Hang des Bruchberges südöstlich von Altenau. Diploma thesis, TU Clausthal.

[4] Bozau E., Stärk H.-J., Strauch G., 2013. Hydrogeochemical characteristics of spring water in the Harz Mountains, Germany. Chemie der Erde 73, 283-292.

[5] Bozau E., Bauer G., Licha T., Lojen S., 2021. Hydrochemical response of spring and mine waters in the Upper Harz Mountains (Germany) after dry periods and heavy rain events. ZDGG 172(1), 73-82.

[6] Parkhurst D.L., Appelo C.A.J., 1999. User's Guide to PHREEQC (Version 2). US Geological Survey, Water Resources Investigations Report 99-4259.

[7] Veselý J., Majer V., Norton S.A., 2002. Heterogeneous response of central European streams to decreased acidic atmospheric deposition. Environ. Pollut. 120, 272-281.

[8] Bozau E., Azoños Figueroa A., Licha T., Wiegand B., 2015. Chemische Zusammensetzung des atmosphärischen Eintrags. Grundwasser 20, 163-168.

[9] Spence J., Telmer K., 2005. The role of sulfur in chemical weathering and atmospheric CO_2 fluxes: Evidence from major ions, $\delta^{13}C_{DIC}$, and $\delta^{34}S_{SO4}$ in rivers of the Canadian Cordillera. Geochim. Cosmochim. Acta 69, 5441-5458.

[10] Boutton T.W., Archer S.R., Midwood A.J., Zitzer S.F., Bol R., 1998. $\delta^{13}C$ values of soil organic carbon and their use in documenting vegetation change in a subtropical savanna ecosystem. Geoderma 82, 5-41.

[11] Böttcher M.E., 1999. The stable isotopic geochemistry of the sulfur and carbon cycles in a modern karst environment. Isotopes Environ. Health Stud. 35, 39-61.

[12] Tichomirowa M., Haubrich F., Klemm W., Matschullat J., 2007. Regional and temporal (1992–2004) evolution of air-borne sulphur isotope composition in Saxony, southeastern Germany, central Europe. Isotopes Environ. Health Stud. 43, 295-3

Experimental study on $\delta^{13}C$ and $\delta^{15}N$ in conifer plant materials - investigation of their potential as markers for geographical and botanical origin

Costinel D., Ionete R.E., Botoran O.R.., Miricioiu M.G., Mathiu T.M.
National Research and Development Institute for Cryogenics and Isotopic Technologies - ICSI Rm. Valcea, Uzinei Street no. 4, 240050, Romania

Stable isotope analysis has long proven to be a useful tool in the study of forest ecology, as it sheds light on the carbon and nitrogen cycling in forest ecosystems. In addition to soil and water samples, the stable isotopic composition of plant tissues can provide valuable information on trophic interactions, nutrient cycling, ecosystem processes, and environmental conditions. Carbon and nitrogen stable isotopes ($\delta^{13}C$ and $\delta^{15}N$) are commonly used as tracers in ecological and environmental studies since they can reveal information on the biogeochemical cycling of these elements in different ecosystems. This work sought to understand the relationship between the values of $\delta^{15}N$ and $\delta^{13}C$ in various plant materials related to conifers from different varieties and areas in Romania, as well as their potential as indicators of the geographical and botanical origin of the trees, to comprehend the cycling of C and N in ecological systems. Therefore, conifer samples from the mountain ranges of Romani-Bistrița, Romani-Buila, and Voineasa-Haneș, in the Southern Carpathians, which span a wide range of environmental gradients (579 to 1300 m), were examined. The samples were collected in 2021, between May and June. During the sample collection period, the air temperatures ranged from 10 to 18 °C, with an average of 100 mm of precipitation per day. The sampled biological materials were represented by bark, needles, and branches, from *Picea abies L.* (spruce), *Abies alba mill* (fir), *Pseudotsuga menziesii* (Douglas Pine tree), *Pinus sylvestris L.* and *Larix decidua ssp carpatica* conifers. Continuous Flow Isotope Ratio Mass Spectrometry (CF-IRMS), a very sensitive analytical technique that requires very little amounts of sample and has great accuracy and precision in measurements of $\delta^{15}N$ and $\delta^{13}C$ values (± 0.3 ‰), was used to get the isotopic fingerprints. Standard operating protocols were followed to acquire a representative and homogeneous sample for the CF-IRMS analysis, starting with the quartering of plant materials, drying, and grinding the samples [1].

We observed a dissociation of the measured values of $\delta^{13}C$ and $\delta^{15}N$ from different types of conifer bark along with variety (spruce, pine, and fir) and geographical origin (geo-climatic influences). Analyzing the $\delta^{13}C$ and $\delta^{15}N$ values of spruce branches (*Picea abies L.)* originating from the same region (Voineasa-Hanes), but collected from different altitudes (1300 m, 1309 m and 1316 m, respectively), a concentration in carbon 13 was observed for samples from the base of the tree to their top. In terms of nitrogen 15, samples taken from the middle of the tree were found to be more enriched than those taken from the base and the top, and there was also an altitude-related difference (an enrichment in nitrogen 15 for samples collected from areas located at a high altitude). The increase in carbon 13 content was observed especially in bark and branches sampled from the upper part of the spruce tree, followed by a decrease in content towards the base of the tree. The levels of carbon 13 in the soil samples exhibit minimal variations across the different altitudes where the sampling was conducted. However, the nitrogen 15 content displayed significant changes, ranging from -1.26 ‰ at 1300 m altitude to +0.55 ‰ at 1309 m altitude. This is attributed to the presence of varying deposits of compost in the soil [2]. The isotopic signature of $\delta^{13}C$ and $\delta^{15}N$ in the conifer branch samples obtained from all study areas (Voineasa, Bistrita, and Buila) showed a notable impact of the local geo-climatic factors such as altitude, latitude, and temperature. Additionally, the wood samples collected from Voineasa, an area situated at a greater altitude than the other two studied forest regions, displayed a heightened concentration of nitrogen 15.

The data we have collected provides further evidence of the positive correlation between altitude and $\delta^{13}C$ levels in evergreen conifers. However, we have uncovered discrepancies in the rate of increase among species, with *Picea abies* L exhibiting the highest level of $\delta^{13}C$ plasticity across varying altitudes. We have also observed variations in the relationship between $\delta^{15}N$ and $\delta^{13}C$ levels among different species, suggesting that plants utilize a range of strategies to acquire limited resources in different environmental conditions. The correlation observed can facilitate the application of ecosystem models across different species and complex terrain, by providing a means to translate the impact of leaf structure on photosynthetic function. Further research is necessary to fully comprehend the importance of species interactions under a changing climate by distinguishing the effects of atmospheric and soil drivers on trait variation.

Keywords: carbon 13, nitrogen 15, conifer plant, geographical and botanical origin

Acknowledgements

This work has been financed by the Ministry of Research, Innovation and Digitization through Program 1 - Development of the national research and development system, Subprogram 1.2 - Institutional performance - Projects for financing excellence in R&D, Contract no. 19PFE/2021, and NUCLEU Program, grant number PN 19110302: „*Research on the variation trends specific to stable isotopes in different tree species: deepening the fractionation mechanisms and chemical processes interconnected on the soil-water-plant chain*" and PN 23150301 „*Implementation of integrated isotopic-chemical-nuclear analytical methodologies for authentication the traditional Romanian food products*".

References

[1] IAEA-TECDOC-1870, 2019, p.3-28

[2] Marshall J.D., Brooks J.R., Lajtha K., Stable Isotopes in Ecology and Environmental Science, 2007 (Ed II), chapter 2, p. 22-50;

Clumped isotope temperatures obtained from snail shells and earthworm biospheriods from the Dunaszekcső loess record: comparability and the effect of sample preparation methods

Andrea Czébely[1,2], Marianna Túri[3], Diána Kiss[3], Gábor Újvári[4], László Rinyu[3]
1. University of Debrecen, Doctoral School of Earth Sciences, Egyetem tér 1., H-4032 Debrecen, Hungary
2. Isotoptech Zrt., Bem tér 18/c., H-4026 Debrecen, Hungary
3. Isotope Climatology and Environmental Research Centre (ICER), Institute for Nuclear Research (ATOMKI), Bem tér 18/c., H-4026 Debrecen, Hungary
4. Institute for Geological and Geochemical Research, Research Centre for Astronomy and Earth Sciences, H-1112 Budapest, Hungary

Carbonates are common target materials of paleoclimate reconstructions, as ambient temperature is recorded in their isotopic composition during carbonate formation and recrystallization. In addition to the traditionally widely used molluscs, foraminifera and coccoliths, research has recently focused on biospheroids, which are secondary carbonates secreted by earthworms.

Major drawback of the traditional oxygen isotope thermometry is that the oxygen isotopic composition of the fluid from which the carbonate precipitated must be known. In most cases only rough estimates are available resulting in high uncertainties in reconstructed temperatures. Carbonate clumped isotope thermometry [1,2,3], in contrast to the traditional method, examine the relative excess in binding of the ^{13}C and ^{18}O isotopes in the lattice structure. The formation of the $^{13}C^{18}O^{16}O^{2-}{}_2$ ion group in the crystal lattice of carbonate minerals shows a strong temperature dependence: higher abundance ratios are expected and observable at low temperatures, as it is thermodynamically more favourable.
This study is aimed at testing the usefulness of earthworm's biospheroid as a temperature proxy by comparing it to formerly studied land snails. We have selected the Dunaszekcső loess record in southern Hungary for this purpose, which is an extensively studied section with a high resolution ^{14}C chronology [4,5,6], revealing stadial-interstadial variations in sedimentation rates. In addition, clumped isotope paleotemperature data from soil carbonates and molluscs [6,7] are also available from this loess record.

Eight samples were collected in 10 cm resolution from the loess layers between 850-770 cm representing the GI-5.1 period and surrounding stadials [7]. The associated temperature was calculated previously between 8-15 °C [7] based on the clumped isotope results obtained from mollusc shells of these layers (*Trochulus hispidus, Succinella oblonga*).

Outcomes of the Δ_{47} measurements may potentially be influenced by the method of sample preparations. Thus, two different sample preparation methods were tested on individuals of the snail species recovered from the mentioned loess layers. Újvári et al. [7] prepared their snail shells samples for Δ_{47} analyses by ultrasonic cleaning and using 1-2% HCl solution [7]. By contrast, our treatment involved ultrasonic bath/cleaning under vacuum and 2% H_2O_2 solution. Both methods were pre-tested on IAEA C2 standard samples with well-known isotopic composition. Clumped isotope analysis was also performed on biospheroid samples from the same layers, and the calculated temperatures were compared with those obtained from the snail shells by Újvári et al. [7]. Our primary goal with the earthworm biospheroid Δ_{47} measurements is to find out whether the Δ_{47} compositions are affected by the so-called vital effect and to what extent the formation of biospheroid carbonates is influenced by kinetic effects.

References:

[1] Wang, Z., Schauble, E. A. and Eiler, J. M. 2004, Equilibrium thermodynamics of multiply substituted isotopologues of molecular gases. Geochimica et Cosmochimica Acta, Vol. 68: 4779–4797.

[2] Eiler J.M. and Schauble E. 2004, $^{18}O^{13}C^{16}O$ in Earth’s atmosphere, Geochimica et Cosmochimica Acta, Vol. 68, No. 23, 4767–4777.

[3] Eiler, J.M. 2007, “Clumped-isotope” geochemistry - The study of naturally-occurring, multiply-substituted isotopologues, Earth and Planetary Science Letters, Vol. 262, 309–327.

[4] Újvári, G., Molnár, M., Novothny, Á., Páll-Gergely, B., Kovács, J. and Várhegyi, A. 2014, AMS ^{14}C and OSL/IRSL dating of the Dunaszekcső loess sequence (Hungary): chronology for 20 to 150 ka and implications for establishing reliable ageedepth models for the last 40 ka, Quaternary Science Review Vol. 106, 140-154.

[5] Újvári, G., Molnár, M. and Páll-Gergely, B. 2016, Charcoal and mollusc shell ^{14}C-dating of the Dunaszekcso} loess record, Hungary, Quaternary Geochronology Vol. 35, 43-53.

[6] Újvári, G., Kele, S., Bernasconi, S.M., Haszpra, L., Novothny, Á. and Bradák, B. 2019, Clumped isotope paleotemperatures from MIS 5 soil carbonates in southern Hungary, Palaeogeography, Palaeoclimatology, Palaeoecology Vol. 518, 72–81.

[7] Újvári, G., Bernasconi, S.M., Stevens, T., Kele S., Páll-Gergely B., Surányi G., and Demény A. 2021, Stadial-Interstadial Temperature and Aridity Variations in East Central Europe Preceding the Last Glacial Maximum, AGU, Advancing Earth and Space Science, Paleoceanography and Paleoclimatology, Volume 36, Issue 8, 10.1029/2020PA004170

Cave monitoring in Hungarian: preliminary results from Ca and Mg isotopes analyses of drip water

Czuppon Gy., Demény A.
Institute for Geological and Geochemical Research, Research Centre for Astronomy and Earth Sciences, ELKH, Budapest, Hungary

Palcsu L., Braun M.
Isotope Climatology and Environmental Research Centre (ICER), Institute for Nuclear Research, ELKH, Debrecen, Hungary

Stieber J.
Stieber Environmental Ltd,, Budapest, Hungary

Dobosy P.
Department of Hydrogeology and Engineering Geology, Institute of Environmental Management, University of Miskolc, Miskolc, H-3515, Hungary

Speleothems formed in caves are one of the most important climate archives from continental areas. In order to use speleothems in the reconstruction of past climate and environmental changes it is necessary to understand the environmental and hydrological processes that determine the physico-chemical conditions of carbonate precipitation and hence speleothem formation. Therefore cave monitoring researches have been conducting in three caves in Hungary since 2013: Csodabogyós Cave in Keszthely Mt (West Hungary), Béke and Baradla caves in Aggtelek (Northeast Hungary). To expand the set of speleothem-based proxies the monitoring activities, which included monitoring of climatological parameters (e.g., temperature, CO_2) measured inside and outside the caves, drip rate, the chemical, trace element, stable hydrogen and oxygen isotopic compositions of drip waters, stable carbon and oxygen isotope analyses of newly formed carbonates, was complemented with calcium and magnesium isotope measurments of drip waters and newly formed carbonets since 2022.

Climatological investigation revealed seasonality in CO_2 concentration related to outside temperature variation indicating variable ventilation regime in the studied caves. The comparision of the stabe isotope composition of the drip waters and the amount-weighted precipitation indicated that the epikarst above the studied sites is generally well mixed and the dominant infiltration takes place during the winter half year. Moreover, the long-term monitoring of the stable isotope composition of drip water in Baradla Cave and the precipitaiton indicate that slight changes in the precipitation over the years can be reflected in the composition of the drip waters. Although the seasonal isotopic signal observed in precipitation is generally not transmitted to drip water, inter-annual variability can be recorded in drip water and hence in the precipitating carbonate (e.g., speleothem).

The Mg isotope analyses of the drip water revealed systematic differences among the caves. In addition, the prelimary results suggest that the isotopic composition variability depend on the hydrological conditions.

The "overshoot" following 8.2 ky event recorded in speleothem from Béke Cave (NE Hungary)

Czuppon György, Attila Demény, Máté Karlik, Zoltán Siklósy
Institute for Geological and Geochemical Research, Research Centre for Astronomy and Earth Sciences, ELKH, Budapest, Hungary

Szabolcs Leél-Össy
Department of Geology, Eötvös Loránd University, Budapest, Hungary

Mihály Óvári
Atomic Energy Research Institute, Centre for Energy Research, ELKH, Budapest, Hungary

Gergely Surányi and Mihály Molnár
Isotope Climatology and Environmental Research Centre (ICER), Institute for Nuclear Research, ELKH, Debrecen, Hungary

Ke Lin and Shen Chuan-Chou
High-Precision Mass Spectrometry and Environment Change Laboratory (HISPEC), Department of Geosciences, National Taiwan University, Taipei, Taiwan

During the Holocene several short term climate anomalies occurred, among which the 8.2 k.y. event was the most pronounced. Several proxy records spreading from the North Atlantic to monsoonal regions indicate that this event has a semi-global impact, at least (mostly cooling). Large amount of freshwater release into the North Atlantic has been invoked as a main cause of the slowdown of the oceanic thermohaline circulation, resulted in temperature drop in West and North Europe [1, 2].

Here we present new isotopic and chemical data of calcite and inclusion hosted water of stalagmites from Central Europe (Béke Cave, NE Hungary). The oxygen isotope time series reveals a negative anomaly around 8.2 k.y., while a positive anomaly appears in the following period (8.1 k.y.). Similar patterns are also observed in the hydrogen isotope data series. Assuming that the temperature change was solely responsible for the observed systematics, this data is utilized to calculate the relative temperature increase/decrease. Apparently, 1-2.5°C temperature decrease for the 8.2 k.y. event, while 2°C increase for "8.1 k.y. event" can be given. Moreover, not only the temperature could influence the isotope composition but also the changes of the amount of precipitation and/or its seasonality as well as the shift of the main route of the moisture transportation (Atlantic vs. Mediterranean moisture sources). Calculated d-excess values might indicate some changes during these periods. In addition, the trace element composition suggests increased summer precipitation relative to winter for the period 8.1.

Acknowledgements

The research was financially supported by the National Research, Development and Innovation Office, Hungary (OTKA 101664, OTKA 123871, PD 121387 and FK 138626) and the Hungarian Academy of Sciences (NANOMIN project, KEP-1/2020). We are also grateful for the support and permission of the Aggtelek National Park Directorate and the Duna-Ipoly National Park Directorate. The János Bolyai Research Scholarship of the Hungarian Academy of Sciences financially supported György Czuppon’s work.

References

[1] von Grafenstein U., Erlenkeuser H., Müller J., Jouzel J. Johnsen S. (1998): The cold event 8200 years ago documented in oxygen isotope records of precipitation in Europe and Greenland. Climate Dynamics 14 : 73—81.

[2] Barber D.C, Dyke A., Hillaire-Marcel C., Jennings A. E., Andrews J. T., Kerwin M. W., Bilodeau G., McNeely R., Southon J., Morehead M. D., Gagnon J.-M. (1999) Forcing of the cold event of 8,200 years ago by catastrophic drainage of Laurentide lakes. Nature, 400, 344-348.

Chemical and isotopic charachteristics of springs in Aggtelek Karst, Hungary

Czuppon-Lázár M., Kovács J.
Eötvös University, Doctoral School of Environmental Sciences, Pázmány Péter sétány 1/C, H-1117 Budapest, Hungary

Dobosy P.
Department of Hydrogeology and Engineering Geology, Institute of Environmental Management, University of Miskolc, Miskolc, H-3515, Hungary

Stieber J.
Stieber Environmental Ltd., Nyerges str.6 H-1181 Budapest Hungary

Gruber P.
Directorate of Aggtelek National Park Tengerszem s. 1 H-3758 Jósvafő Hungary

Czuppon Gy.
Institute for Geological and Geochemical Research, Research Centre for Astronomy and Earth Sciences, ELKH, Budapest, Hungary

A detailed research on springs in the Aggtelek karst area (NE Hungary) was conducted in order to better understand the hydrodynamics of karst and the effect of various weather (climate) conditions on the springs as well as to group of the springs. For these purposes, a monitoring network was establish in 2020 that includes 22 wells and springs covering the whole area. The springs are visited every month to measure their physical/chemical field parameters (temperature, pH, electrical conductivity) and collect water samples for chemical and stable isotope analyses. Utilizing this data set, it aimed to group these springs by cluster and discriminant analysis. In case of major hydrological events, sampling was conducted in higher resolution. Furthermore, the combined cluster and discriminant analysis (CCDA) was also applied, because CCDA combines two traditional methods in order to determine the optimal number of groups and the corresponding clustering that occurs during clustering (classification), and to determine not only the similar groups but also the most homogeneous groups among the groups. This investigation gave better understanding of the hydrogeological background of the studied area.

In addition, the analysis of the geochemical time series of each of the studied springs provided an opportunity to reveal the temporal variability of the parameters under study as a function of meteorological conditions. Different behaviours were detected based on the time series of the sources and the response to precipitation events. Our initial results showed that some sources responded rapidly (1-2 days) to a major precipitation event, while others were characterised by a stable state with no change in chemical and isotopic composition over the period studied. Moreover, the stable isotopic composition of the sources seems to indicate that the main infiltration period takes place in the winter half of the year.

The research was supported by Doctoral Student Scholarship Program of the Co-operative Doctoral Program of the Ministry of Innovation and Technology Financed from the National Research, Development and Innovation Fund (KDP-2021 - C1794892 to Márta Czuppon-Lázár). In addition, we are also thankful for the support and permission to the Aggtelek National Park Directorate.

Nitrate removal in contaminated aquifers – laboratory incubations with isotope analyses of NO_3^-, NO_2^- and N_2O

Deb S., Lewicka-Szczebak D.
Institute of Geological Sciences, University of Wrocław, ul. Cybulskiego 30, 50-205 Wrocław, Poland

Nitrogen is one of the most essential nutrients to plant growth and is often added to the soil as nitrogen fertilizers to maximize crop yield. Nitrogen undergoes various transformations in the agricultural ecosystem through nitrification, denitrification, annamox processes, and soil microorganisms play a crucial role in influencing its availability to plants. However, excessive application of nitrogen fertilizers has disrupted the global nitrogen cycle, resulting in nitrogen loss into the environment through leaching of nitrogen into the groundwater (mostly as nitrate), and through emission of gases (mostly as nitrous oxide). Nitrous oxide (N_2O), a potent greenhouse gas, can contribute to global warming, also high nitrogen content in water can harm human health and water quality. Nitrate (NO_3^-) contamination in groundwater is a global concern, nitrate when transformed to nitrite (NO_2^-) may lead to methemoglobinemia - the blue-baby syndrome, and with further possible conversion to nitrosamine which are potent carcinogens [1]. Therefore, it is important to develop strategies to reduce soil residual nitrogen, increase nitrogen-use efficiency by crops, and improve soil fertility to prevent nitrogen loss into the environment [2].

In our study we focused on the research area where sewage from yeast factory is applied as a natural fertilizer. This strategy largely supports agricultural production with elimination of synthetic fertilizers, but at the same time has most probably large impact on the groundwater quality. A very high nitrate concentration above 80 mg L^{-1} was found in the groundwaters sampled from the piezometers in the preliminary sampling conducted in this study area. These waters were then applied to perform laboratory incubation studies, to determine the potential of natural nitrate removal in these waters and to determine the conditions supporting denitrification processes.

Naturally occurring N isotopes $^{15}N/^{14}N$, and $^{18}O/^{16}O$, and their isotope fractionation effects in microbial nitrogen transformation can greatly enhance our knowledge of the nitrogen cycle. Stable isotope studies are a useful tool for determining the various sources and sinks of different molecules in the nitrogen cycling process. Variations in $^{15}N/^{14}N$ in NH_4^+, NO_2^-, and NO_3^- accompanied by variations of $^{18}O/^{16}O$ in NO_2^-, and NO_3^-, can provide insights through different biogeochemical processes that involve these molecules and their removal from the environment [3]. Moreover, the isotopic analyses of N_2O provide three isotope characteristics of this compound, namely, $\delta^{15}N$, $\delta^{18}O$ and SP - Site Preference - which describes the difference in $\delta^{15}N$ between central and peripheral position of the linear N_2O molecule. These analyses give further insight into the N_2O production pathways and hence can also provide information on the progress of denitrification processes [4]. In our studies we combine N_2O analyses with mineral nitrogen analyses to trace the microbial processes of N transformations.

Mineral nitrogen isotope analyses can be performed with the help of microbial mediated methods. Bacterial culture strains *Pseudomonas aureofaciens* [5, 6] and *Stenotrophomonas nitritireducens* [7] are applied for NO_3^- and NO_2^- isotope analyses, respectively. These bacterial strains conduct denitrification with N_2O as the terminal product, as they lack the N_2O reductase gene responsible for the reduction of N_2O to N_2. *Stenotrophomonas nitritireducens*

can selectively reduce NO_2^- to N_2O without reducing NO_3^-. The final product, N_2O, is measured for the isotopic composition using Laser
Spectroscopy - Picarro N_2O Isotope Instrument combined with small sample injection module (SSIM) allowing for measurements of small volume samples.

Different environmental factors such as temperature, pH, and nutrient availability have significant impact on the mechanisms of nitrogen cycling. pH has been demonstrated as a crucial factor on denitrification pathways and affects the microbial production of N_2O through enzyme sensitivity. A pH of between 7.0 and 8.0 has been suggested as optimum for denitrification [8]. Further, in a study by Liu et. al [9], addition of glucose as carbon source had enhanced effect on denitrification. Hence, for a better understanding of the pH effect on nitrogen cycle, a series of experiments were conducted using groundwater samples (anoxic conditions/flushed with N_2) with different pH levels (pH 5, 7, and 9) and incubated in the dark for 2 weeks at optimal groundwater temperature of 15^0C, at 100rpm. After 1 week of incubation, glucose (2 g L^{-1}) was added to the groundwater samples and further incubated. Headspace samples were collected for N_2O Picarro measurements. Also, mineral N samples in groundwater were analysed at the beginning, in the middle i.e., after 1week of incubation, and at the end of the experiment. In addition, to determine the isotopic signature of mineral Nitrogen, these groundwater samples are analysed for bacterial denitrification by *Pseudomonas aureofaciens* and *Stenotrophomonas nitritireducens.* The different pH treatments were tested to find the optimal pH for nitrate removal. However, on contrary to our expectations we have observed significant nitrate production in all pH treatments, most probably due to chemical processes responsible for nitrate generation from dissolved organic nitrogen forms. The isotope analyses, which are currently being performed, should allow for determination of particular processes involved in nitrates transformations.

References:

[1] Yao, S., Liu, L., Zhang, S. and Tang, X., *Water*, *14*(11), p.1759, 2022.

[2] Rütting, T., Aronsson, H. and Delin, S., *Nutrient Cycling in Agroecosystems*, *110*, 1-5, 2018.

[3] Magyar, P.M., Hausherr, D., Niederdorfer, R., Stöcklin, N., Wei, J., Mohn, J., Bürgmann, H., Joss, A. and Lehmann, M.F., *Scientific Reports*, *11*(1), 1-12, 2021.

[4] Lewicka-Szczebak, D., Lewicki, M. P., & Well, R., *Biogeosciences*, *17*(22), 5513–5537, 2020.

[5] Sigman, D. M., Casciotti, K. L., Andreani, M., Barford, C., Galanter, M., & Böhlke, J. K., *Analytical Chemistry*, *73*(17), 4145–4153, 2001.

[6] Casciotti, K. L., Sigman, D. M., Hastings, M. G., Böhlke, J. K., & Hilkert, A., *Analytical Chemistry*, *74*(19), 4905–4912, 2002.

[7] Böhlke, J. K., Smith, R. L., & Hannon, J. E., *Analytical Chemistry*, *79*(15), 5888–5895, 2007.

[8] Giles, M., Morley, N., Baggs, E. M., & Daniell, T. J., *Frontiers in Microbiology*, *3*, 2012.

[9] Liu, R., Xia, L., Liu, M., Gao, Z., Feng, J., You, H., Qu, W., Xing, T., Wang, J. and Zhao, Y., *Environmental Technology*, *43*(22), 3355-3365, 2022.

Seasonal geochemical, isotopic and microbial circulation in the area of a closed pyrite mine in Wieściszowice (Sudetes, Poland)

[1]Wojciech Drzewicki, [1]Henryk Marszałek, [2]Dorota Górniak,[1]Marta Jakubiak, [1]Mariusz Jędrysek

[1]*Institute of Geological Sciences, Wrocław University, M. Borna Sq 9, 50-204 Wrocław, Poland*

[2]*University of Warmia and Mazury in Olsztyn, Oczapowskiego 1A, 10-957 Olsztyn, Poland*

In the area of the pyrite mine in Wieściszowice (Rudawy Janowickie, Western Sudetes), which has been closed since 1925, there are strong changes in the quality of waters with a clear hydrogeochemical anomaly, mainly with increased concentrations of sulphates, iron and aluminum [1,2,3]. In order to recognize the geochemical, isotopic and microbiological processes taking place in one of the three so-called Colorful Lakes, an analysis of temporal and spatial changes in selected chemical indicators, isotopic and microbiological composition of waters was carried out.

During three periods (in April, July and December 2022), water samples were collected both, from the surface and the bottom zone of the reservoir, as well as from streams recharging and draining the lake. Cores of bottom sediments were also collected to a depth of about 15 cm. In the spring and winter season, ice samples were additionally collected from the surface of the lake. Basic physicochemical parameters, ionic, isotopic and microbiological composition were determined in the waters. In the isotopic studies, the analysis of $\delta^{18}O$ and $\delta^{2}H$ in the water molecule and the isotopic composition of sulphate sulfur were also determined. Bottom sediment cores were divided into 2 cm intervals and then the sulfur speciation were extracted for both oxidized (sulfate ion) and reduced (elemental sulfur, monosulphides, polysulphides) forms. The obtained speciations were determined in terms of sulfur concentrations and isotopic composition.

Prokaryotic cells from a 2-liter sample volume were deposited under sterile conditions using the vacuum method on PAS membrane filters with a porosity of 0.2 µm. After DNA isolation, sequencing was performed on the Illumina MiSeq 2x300 bp platform, appropriate amplicon libraries of 16S RNA V3-V4 variable regions were created for this purpose. The obtained data were subjected to bioinformatics processing using the Qiime2 software and the Pathona dokdo package.

The measurements of basic physicochemical parameters showed that the electrolytic conductivity values ranged from 0.68 to 5.2 mS/cm, pH from 2.53 to 3.36, and redox potential from 390 to 566 mV. Iron and manganese concentrations varied depending on the sampling period. In April, the content of these metals in water samples ranged from 66 to 197 mg/L for iron and from 0.9 to 4.0 mg/L for manganese. In samples taken in July the concentrations of iron and manganese were changed from 86 to 500 mg/L and from 1.9 to 4.7 mg/L, respectively, while in December from 19 to 270 mg/L for iron and from 0.6 to 3.7 mg/L for manganese.

Analysis of the isotopic composition of oxygen and hydrogen in water samples showed significant differences depending on the sampling period (Fig. 1). The isotopic composition of $\delta^{18}O$ ranged from -16.91‰ to -7.33‰, and for $\delta^{2}H$ from -78.18‰ to -

53.51‰. The lowest values for both oxygen and hydrogen were shown in the spring sampling (April) and the highest in the summer season (July 2022). The main recharge of the reservoir comes from the adit located in the upper part of the lake. In the April 2022 sampling, there was little variation in the isotopic composition of oxygen and hydrogen in the water column. The values of δ^{18}O and δ^2H are close to the value of the sample taken from the adit. Due to the small depth of the reservoir (up to 2.5 m), the water in the lake was mixed in the winter and then covered with a layer of snow and ice, which persisted until April. In July, a significant shift of δ^2H and δ^{18}O towards positive values was demonstrated. This is due to the recharge of water significantly enriched in heavier oxygen and hydrogen to the reservoir. Evaporation was taking place in the lake itself. The difference in the isotopic composition of oxygen and hydrogen in the samples from the surface and bottom part of the lake was δ^2H=10‰ and δ^{18}O=2‰, respectively. The surface evaporation process lost its importance with depth. In winter, the recharge of the reservoir from the adit was very small. The isotopic composition of oxygen and hydrogen was at a similar level as in July. The waters in the lake were well mixed and covered with a several-centimeter layer of ice. The analysis of sulphate sulfur concentrations from water showed significant seasonal differences in the depth profile of the lake. SO_4^{2-} concentrations ranged from 1026 mg/L to 5579 mg/L. A high concentration of sulphate ion reaching 7186 mg/L was found in the outflow from the adit. Diversification of SO_4^{2-} concentrations in water was found in all samples, much higher in the bottom zone. The isotopic composition of $\delta^{34}S(H_2O)$ was positive and ranged from 2.17‰ to 3.17‰.

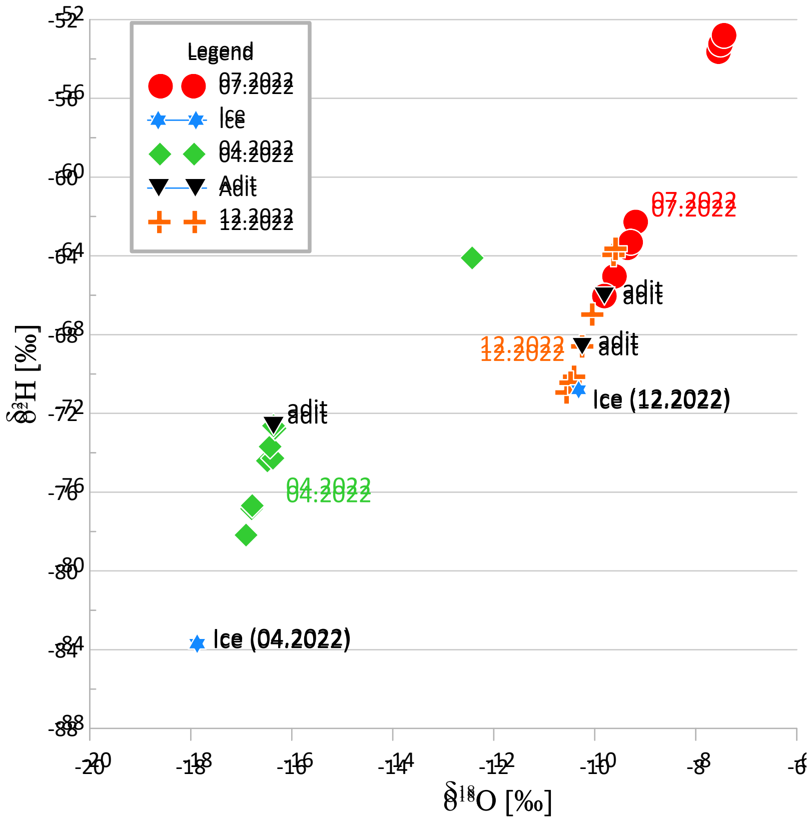

Figure 1. Isotopic composition of δ^2H and δ^{18}O in lake water samples

Microbiological studies using next-generation sequencing (NGS) on the Illumina MiSeq platform showed a predominance of acidophilic Proteobacteria in the reservoir microbiocenosis, which accounted for 48% of all detected transcripts. The most abundant were γ-Proteobacteria 33% and among them bacteria belonging to the genera Burgholderia (24%) and Xantomonas (3.6%). α-Proteobacteria accounted for 14.5%, with Acidibacteria (9%) and Acidobacteria (7%) dominating. The occurrence of acidophilic archaeons belonging to the two classes Thermoplasmata and Micrarchaeia was characteristic. These archaeons are widespread in anaerobic environments rich in sulfur, nitrogen and carbon dioxide compounds. Thermoplasmata is a widespread and ecologically important class of archaeons belonging to the phylum Euryarchaeota. They are acidophilic Archaea that thrive at optimal pH below 2. In their metabolism, they are involved in sulfur reduction, iron reduction, hydrogen metabolism and arsenic detoxification pathways, indicating potential in sulfur, iron, hydrogen and arsenic transformation. Micrarchaeia, on the other hand, include small acidophilic archaea, which in natural environments interact physically with some members of the Thermoplasmatales to form so-called multitrophic microbial assemblages. Examples of such relationships are systems composed of anaerobic methane oxidizing archaeons and sulfate-reducing bacteria (AOM, annoxic methane oxidation) or syntrophic SLIME (subsurface lithoautotrophic microbial ecosystem) assemblages composed of methanogens, acetogens and sulfate-reducing bacteria. Noteworthy is the presence of ultra-small bacteria belonging to Patescibacteria (7.3%) classified as obligate fermentation symbionts and Eremiobacterota (2%) an ecologically versatile cluster with the potential to thrive in a range of "extreme" environmental conditions found in sulfate-iron spring waters and characterized by facultative acidophilicity with a preference for peptides and amino acids as nutrient sources. All microorganisms identified by NGS were unculturable. The data obtained suggest that the metabolic properties of microbial communities in anaerobic ferrous environments support a coupled biogeochemical cycle of Fe, S and C.

Referemces

[1] Chudy K., Worsa-Kozak M., Wójcik A., Wolkersdorfer C., Drzewicki W., Konsencjusz D., Szyszka D. (2021). Chemical variations in mine water of abandoned pyrite mines exemplified by the Colorful Lakes in Wieściszowice, Sudetes Mountains, Poland**.** Journal of Hydrology, Regional Studies 38:10097

[2] Costa M.R., Marszałek H., da Silva E.F., Mickiewicz A., Wąsik M., Candeias C. (2021). Temporal fluctuations in water contamination from abandoned pyrite Wieściszowice mine (Western Sudetes, Poland)._Environmental Geochemistry and Health, 43, 3115–3132

[3] Marszałek H., Wąsik M., (2022). Hydrogeochemical anomaly in waters of the piryte deposit area in Wieściszowice (Western Sudetes, SW Poland). In: Seiler K.P, Wohnlich S. (eds); New approaches characterizing groundwater flow. Balkema.

Radiocarbon level in thevegetation and atmosphere of Râmnicu Vâlcea, Romania

Făurescu I., Varlam C., Făurescu D., Vagner I., Bogdan D, Costinel D.
National Research and Development Institute for Cryogenic and Isotopic Technologies – ICSI Râmicu Vâlcea, Romania

The paper presents C-14 variation in the vegetation and atmosphere of Ramnicu-Valcea Romania. The sampling location was the National Research and Development Institute for Cryogenic and Isotopic Technologies – ICSI Rm. Valcea, placed about 10 km south of Ramnicu Valcea city (Romania), in the Govora industrial area. This location has some particularities. A first particularity to take into account is the fact that the institute is located in an important industrial area. The institute operates a nuclear installation, namely "Experimental Pilot for Separation of Tritium and Deuterium" (PESTD), a semi-industrial installation designed for the detritiation of heavy water moderator of CANDU reactors. Until now, PESTD's normal operation was with heavy water and tritiated water below the exemption level approved by Romanian legislation. Foreseen experiments will be done with tritiated heavy water moderator from Cernavoda NPP (CANDU reactor technology). It is well known that heavy water reactors emit significant amounts of tritiated water and ^{14}C. The ^{14}C is a by-product resulting primarily from neutron activation of ^{17}O from heavy water molecules. The ^{14}C enters the natural environment as CO_2 and is found in water, air, soil, and sediments and from here to plants and animals [1]. Considering the fact that one of the important releases of PESTD is gaseous radioactive effluents, the baseline of atmospheric ^{14}C was a must for the environmental program. Another particularity is that the Govora industrial area operates a 315MW coal-fired thermoelectric power plant. Due to the Suess effect, a relative decrease of the ^{14}C activity on a local scale is expected as a result of the dilution of the carbon isotopic mixture by fossil carbon. A radiocarbon background level (250 Bq/kg of carbon) was established by international regulatory bodies [2]. Above this background level, other than the normal production of ^{14}C by cosmic radiation will be considered pollution.

In order to determine radiocarbon activity air samples were collected monthly by active absorption of CO_2 into sodium hydroxide (NaOH) with a Raschig tube (figure 1). In parallel with the air sampling, the CO_2 concentration was monitored using a gas analyzer type LICOR LI-850. Also were collected monthly evergreen vegetation (Thuja occidentalis L.) samples. Radiocarbon measurements were performed using the direct absorption method [3]. This consists in measuring ^{14}C contained in a known quantity of carbon, as carbon dioxide, obtained from a sample, standard or background material, counted in an ultra-low level liquid scintillation counter Quantulus 1220. The samples were counted using the following parameters: 1000 min counting time (10 × 100 min/cycle), counting efficiency at the best factor of merit was around 65% with a background around 2.2 cpm (counts per minute).

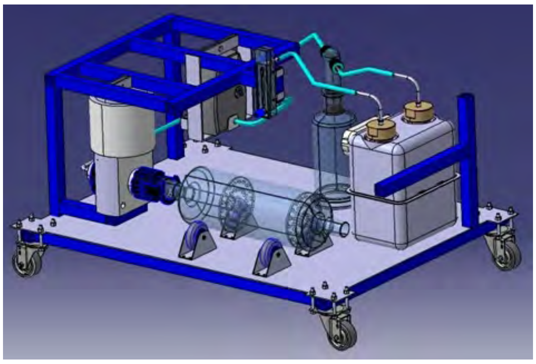

Figure 1: 3D view of CO_2 active absorption apparatus.

It can be observed that the specific activity of ^{14}C was similar for both types of samples investigated. The variations encountered generally within the limit of uncertainty associated with the activity of the ^{14}C concentration. The average specific activity of ^{14}C recorded has the following values: 0.233 ± 0.008 Bq/ C for Thuja occidentalis and 0.225 ± 0.008 Bq/gC for Raschig tube samples. From the analysis of this evolution, it can also be concluded that the minimums and maximums of ^{14}C activity encountered in the air are found also in the vegetation with a delay of several months, the time necessary for the transfer of radiocarbon from the air to the plant. The results have a clear decreasing trend, but due to local influence caused by the continuous production of fossil $CO_{2,}$ we cannot observe ^{14}C seasonal variations [4].

Acknowledgements

This work is financed by the Ministry of Research, Innovation and Digitization through Program 1 - Development of the national research and development system, Subprogram 1.2 - Institutional performance - Projects for financing excellence in R&D, Contract no. 19PFE/2021 and PN 23 15 03 01 part of Core Program ICSI Lab2Field.

References

[1] Libby, W.F. 1952. Radiocarbon dating, 2nd ed. The Chicago: University of Chicago Press. Manning, M., D. Lowe, W. Melhuish, R. Sparks, G. Wallace, C. Brenninkmeijer, and R. Mcgill.

[2] International Atomic Energy Agency [IAEA]. 2004. Management of waste containing tritium and carbon-14. Technical reports, nr 421. Vienna: IAEA. p 5–37. Available online at http://www-pub.iaea.org/MTCD/publications/PDF/TRS421_web.pdf.

[3] Varlam C, Stefanescu I, Varlam M, Popescu I, Faurescu I. 2007. Applying the direct absorption method and LSC for 14C concentration measurement in aqueous samples. Radiocarbon 49(2):281-289

[4] Marland, G., T.A. Boden, and R.J. Andres. 2006. Global, regional and national CO2 emissions. Trends: A compedium of data on global change. Carbon Dioxide Information Analysis Center, Oak Ridge National Laboratory, US Department of Energy, Oak Ridge, TN.

Hydrogeochemical study of the CO_2- rich mineral medical springs at Balatonfüred, Hungary

I. Fórizs[1], J. Deák[2], I. Dobos[3], Gy. Scheuer[3], Gy. Czuppon[1]
[1] *Institute for Geological and Geochemical Research, Research Centre for Astronomy and Earth Sciences, 1112 Budapest, Budaörsi út 45., Hungary*
[2] *GWIS Ltd., 8200 Veszprém, Hóvirág utca 9., Hungary*
[3] *retired*

Introduction

It is unknown when the use of the medical springs at Balatonfüred started, but archaeological findings indicate their likely utilization in the Roman times. Nowadays the main user is the State Heart Hospital, the history of which started at the beginning of the 18th century. The water of these medical springs is characterized by elevated TDS and temperature, and rich in carbon-dioxide, iron and trace elements comparing to the nearby karst springs.

Applied methods

During two campaigns in 2019 and 2022 water samples were taken for stable H and O isotope analysis in water, and stable C analysis in dissolved inorganic carbon (DIC) in five and six springs at Balatonfüred, Hungary. The stable isotope analyses were carried out at the Institute for Geological and Geochemical Research (CSFK), Budapest: H and O by LGR LWIA-24d laser liquid water isotope analyzer, and C by Thermo Finnigan delta V mass spectrometer. Main and trace element analyses were carried out in the laboratory of Bálint Analitika Ltd. in 2017.

Results

The stable water isotope data of the cool karst springs in the surrounding areas are on the Global Meteoric Water Line (GMWL, [1]), while those of medical springs are below the GMWL (Fig. 1) during both sampling campaign. The separation of the two sets are significant indicating their different genesis.

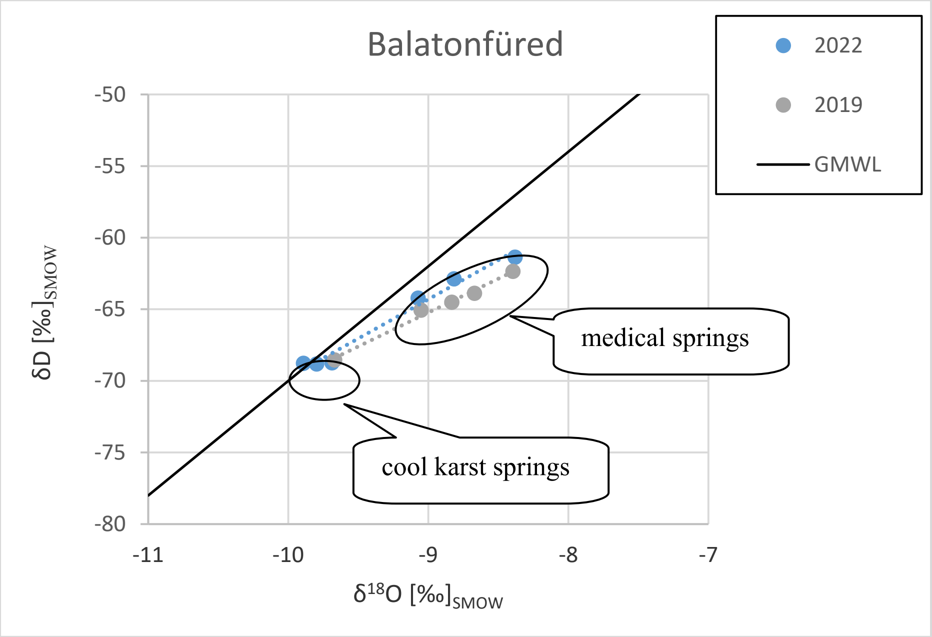

Figure: The δ-δ plot of the cool karst and medical springs in the Balatonfüred area.

The DIC concentration and the $\delta^{13}C_{DIC}$ values also differ for the two sets of springs. The medical springs contain much more DIC, mainly CO_2 than the cool karst springs. There is a difference in the temperature as well, the medical springs are 4 to 6 ^{o}C warmer than the cool karst springs. The chemistry also shows significant difference, e.g the TDS, Na^+, Cl^- and SO_4^{2-} values of the medical springs are much higher. The concentration of Fe and trace elements as B, Li, F, Br, Sr, Rn and Ba in the medical springs are 2-50 times higher than in the cool karstic springs.

Interpretation

The recharge area of both sets of springs is the higher elevation karst north of Balatonfüred (dolomite and limestone), but the medical springs contain ascending warm water component too, upwelling along tectonic fractures. The measured water chemistry and isotopic anomalies are the consequences of this mixing. Based on the water chemical and isotopic anomalies resulting from the mixing, it can be established that the upstream component has a high temperature and a high TDS, DIC and microelement content. The origin, mixing ratio and composition of the ascending component will be further investigated with new measurements and geochemical modeling.

In our presentation the conclusions drawn based on the stable isotope data are presented. We hypothesize that the ascending warm water is bringing up significant smount of carbon dioxide. The δ^{13}C value of the DIC of the warm water can be assessed as the intersection of the regression line on δ^{13}C vs. 1/DIC plot with the vertical axes at zero 1/DIC, which is cca. -3‰. This value is interpreted as of magmatic origin. Because the medical springs are under the GMWL, their upwelling warm water component must have δ^{18}O shifted to positive direction. There are such upwelling waters at several places in Hungary.

References

[1] Craig H, Science, N.Y, 1961 (133) pp. 1702-1703.

The use of isotopic approach (δ^{18}O-PO_4) to determine phosphorus origin in selected surface waters of the Vistula and Bug interfluve

Gebus-Czupyt B. [a], Chmiel S. [b], Kończak M. [b], Jacek Stienss [a], Huber M. [b], Mulczyk A. [a], Radzikowska M. [a], Stępniewski K. [b], Pliżga M. [b], Zielińska B.[b]

[a] *Institute of Geological Sciences, Polish Academy of Sciences, ul. Twarda 51/55, 00-818 Warszawa, Poland;*

[b] *Faculty of Earth Sciences and Spatial Management, Maria Curie-Sklodowska University, al. Kraśnicka 2cd, 20-718, Lublin, Poland*

Isotopic composition of oxygen in phosphates (δ^{18}O-PO_4), the most common form of P in lithosphere and hydrosphere, could be used as a tracer of phosphorus cycling between the biomass, soils, waters and sediments. Recently, the δ^{18}O-PO_4 analysis are widely used for identifying different phosphate sources and better understanding P cycling in marine and freshwater research (ie. [2], [5], [4], Gooddy et al., 2018). Phosphorus, like nitrogen, belongs to the crucial bioelements caused eutrophication, which is destructive for water quality and for ecological balance. Therefore studies that allow us to recognize the main sources of nutrients and their pathways in studied geo-ecosystem are very important and isotopic analysis can be crucial in this case.

Phosphorus has only one stable isotope (^{31}P), but in most of the compounds, like phosphates, P is strongly bound to oxygen, which allow us to measure oxygen isotopic composition of PO_4. Phosphates can be both natural and anthropogenic origin. The P sources could be point, such as sewage discharge sites and non-point, like soil leaching and agricultural run-off (McLaughlin et al., 2013). One of the important sources of phosphorus in surface waters may be also P leached from the P-rich bedrock, what is the subject of our research.

Our studies are focused on selected areas of the Vistula and Bug interfluve, in which were confirmed high orthophosphates concentration (av. 0.5 mg/dm^3) in water extracts from bedrocks collected on these area (the Maastrichtian and Tertiary formations, like opokas, margles, chalk, gaizes, sands), while for the nearest springs the PO_4 concentration was found on average 0.3 mg/dm^3.

The results of our studies shows a various ranges of δ^{18}O values in dissolved inorganic phosphate extracted from various sources (like spring waters, rivers, WWTP effluents, fertilizers, pollens or bedrocks) and indicate, that δ^{18}O-PO_4, with some limitations, could be useful tool to recognize phosphate sources and P cycling in studied area. Here we present and discuss the results of spatial and seasonal variabilities of the studied waters from the area of the Vistula and Bug interfluve.

Acknowledgement

These studies are founded by the Polish National Science Centre (grant No. UMO-2020/37/B/ST10/01994)

References

[1] Gooddy D, Bowes M, Lapworth D, Lamb A. Williams PJ. Newton R, Davies CL, Surridge B, Applied Geochemistry, 2018 (95) 139–146

[2] McLaughlin K, Kendall C, Silva S, Stuart-Williams H, Paytan A, Limnology and Oceanography: Methods, 2004 (2) 202–212,

[3] McLaughlin K, Young MB, Paytan A, Kendall C, AEA-TECDOC-1695, 2013, 93-110

[4] Paytan A, Roberts K, Watson S, Peek S, Chuang P-C, Defforey D, Kendall C, Science of the Total Environment, 2017 (579) 1356-1365

[5] Young MB, McLaughlin K, Kendall C, Stringfellow W, Rollog M, Elsbury K, Donald E, Paytan A, Environmental Science & Technology, 2009 (43) 5190–5196

Isotopic approaches in research on dedolomitization and speleogenesis processes in Rovte area (central Slovenia)

Gebus-Czupyt B.[1], Johnston V. E.[2], Otoničar B.[2], Tyc A.[3], Šarc F.[2],Ciesielczuk J.[3], Gaidzik K.[3]

[1] *Institute of Geological Sciences, Polish Academy of Sciences, Twarda 51/55, 00-818 Warszawa, Poland;*

[2] *Scientific Research Centre Of The Slovenian Academy Of Sciences And Arts, Karst Resarch Institute, Titov Trg 2, 6230 Postojna, Slovenia*

[3] *Institute of Earth Sciences, University of Silesia in Katowice, Będzińska 60, 41-200 Sosnowiec, Poland*

Although dedolomitization is a process often described in the literature on carbonate diagenesis or less often in hydrogeology, the direct relationship between dedolomitization and/or its products and speleogenesis is still not entirely clear. The project is conducting interdisciplinary research in the Rovte region (central Slovenia), where some basic phenomena related to speleogenesis in dedolomite have been discovered (e.g., Otoničar et al. 2013, 2016). The aim of the undertaken research is to describe new genetic (speleogenic) processes in the development of karst caves related to dedolomitization process, probably common in many environments where the regional groundwater flow is carried out through a complex of evaporite-carbonate rocks. This mechanism could be responsible for development of large-scale porosity and instability in carbonate rocks deep in the massifs, which will be associated with the flow of groundwater in karst reservoirs, the development of hydrocarbon deposits and geothermal reservoirs, and is also important for the initial stages of ore mineralization formation.

The main area of our study is the Rovte region, in which, according to the results of preliminary hydrogeochemical studies, the dissolution of calcium sulphates and dedolomitization are still ongoing processes (e.g., Philipp 2015, Otoničar et al. 2016). Due to this, this area is suitable for the study of direct relationships between the processes of dissolution of calcium sulfates, currently active dedolomitization and development of karst caves, and their products occurring in the form of sediments and minerals on the cave walls. Besides comprehensive mineralogical, petrographic, speleological, geomorphological and hydrogeochemical studies, extensive isotope analyzes of mineral phases and waters are carried out, supplementing the knowledge about the processes occurring in the research area and allowing to determine the origin of the studied compounds. In order to obtain the broadest possible spectrum of data, isotopic analyzes are carried out, among others carbonate fractions of the collected rocks, sulphate and sulphide minerals (gypsum, epsomite, pyrite) as well as waters and some components dissolved in them (as DIC and sulphates). The obtained results will be used to test various hypotheses regarding dedolomite-related speleogenesis.

The preliminary results of research undertaken in the Rovte region will be presented, including the results of comprehensive hydrogeochemical studies and isotopic analyzes of deep surrounding wells and multilateral studies of caves and surfaces obtained until this day. The results of the research undertaken in central Slovenia will contribute to a wider understanding of the processes occurring during speleogenesis and should also broaden the knowledge about the processes of formation of sulphide mineralizations in southern Poland.

Acknowledgements

These studies are founded by the Polish National Science Centre (grant No. UMO-2020/39/I/ST10/02357) and Slovenian Research Agency (No. N1-0226), within OPUS-20 (LAP).

References

Otoničar B, Tyc A, Osborne RLA, Bzowska G, Geološki Zbornik, 2013 (22) 113-115.

Otoničar B, Dublyansky Y, Osborne RAL, Tyc A, Philipp S, Proceedings of DeepKarst, 2016, 189-198.

Philipp S, Master thesis, Institute of Applied Geosciences, TU, 2015

Analyses of stable carbon ($\delta^{13}C$) and nitrogen ($\delta^{15}N$) isotope ratios from unburnt human remains from Świbie

Hałuszko A.[1], Pawełczyk S.[2], Pawełczyk F.[2] and Piotrowska N.[2]
[1]*Institute of Archaeology, Maria Curie-Skłodowska University, Pl. M. Curie-Skłodowskiej 5, 20-031 Lublin, Poland*
[2] *Institute of Physics – CSE, Silesian University of Technology, Konarskiego 22B, 44-100 Gliwice, Poland*

Reconstructing the palaeodiet of populations associated with the Lusatian Urnfields is an important part of the study of prehistoric communities. It is particularly important because of the limitations arising from the widespread use of cremation in this period, which precludes the determination of carbon ($\delta^{13}C$) and nitrogen ($\delta^{15}N$) stable isotope ratios in bone collagen.

The stable isotope ratios of carbon ($\delta^{13}C$) and nitrogen ($\delta^{15}N$) were analysed in bone samples selected from the 23 individuals recovered from inhumation burials in the bi-ritual cemetery of the Lusatian Urnfields in Świbie, Gliwice District. Samples from preserved fragments of long bone shafts and cranial bones, and in one case a fragment of the last lumbar vertebra, were selected for analysis. Due to the very poor state of preservations of the skeletons, it was impossible to carry out palaeodiet reconstruction studies for many of the individuals. No animal bones with diagnostic characteristics were preserved in the Świbie cemetery, so the trophic background was determined based on the published data for fauna from Neolithic and Late Bronze Age sites. All bone samples were mechanically cleaned. The obtained samples were then subjected to the standard collagen extraction procedure used in the Radiocarbon and Mass Spectrometry Laboratory, which is based on the modified Longin method.

For most of the individuals examined, some measurements of stable carbon and nitrogen isotopes were obtained despite their clear, macroscopically determined contamination with organic compounds. Most of the samples analysed showed a C/N ratio that met the quality criterion, which ranged between 2.9 and 3.6. Samples of two individuals, from graves 2 and 259, were contaminated, with subsamples for the individual from grave 2 well outside the range obtained for the others. The $\delta^{13}C$ values ranged from -21.22‰ to -17.63‰ (X = -18.86; S.D. = 0.825), while the $\delta^{15}N$ values ranged from 4.62‰ to 9.5‰ (X = 8.25; S.D. = 1.003), excluding the data for the contaminated samples.

The sample selected for an adult of undetermined sex, from grave 2, came from a pre-WWII excavation carried out around 1936. The contamination, shown by isotopic testing, most likely came from a preservative, which was probably isinglass (fish glue). It was most likely made from the swim bladders of freshwater fish. Most of the individuals examined to establish their palaeodiet were characterised by a high trophic level, indicating a balanced diet based on food of inland origin, with C3 plants and a high proportion of food of animal origin. The individual of undetermined sex and age at death from grave 79 was characterised by a plant-based diet. Individuals falling into the Infans I, Infans II and child age categories, due to their likely high milk consumption, were characterised by the highest $\delta^{15}N$ parameters, which are characteristic of a ‘pastoral diet’. The range of stable carbon ($\delta^{13}C$) and nitrogen ($\delta^{15}N$) isotope values obtained for the male individuals placed them at a slightly higher trophic level than the females, but these differences were not statistically significant (Mann-Whitney U test: for $\delta^{13}C$ p-value 0.88076; for $\delta^{15}N$ p-value 0.64552). Individuals of indeterminate sex and age at death displayed a wide range of carbon and nitrogen isotope values.

Performance of the Picarro CRDS water isotope analyzer for δ^2H tracer studies

M. E. G. Hofmann[1], J. Bhattacharya[2], J. Woźniak[1], J. Yan[2], P. Swinkels[1]
[1] Picarro B.V. Netherlands, Eindhoven, The Netherlands
[2] Picarro Inc. USA, Santa Clara, California

The Picarro water isotope analyzers (L2130-i/L2140-i) have become a standard technique to measure the natural abundance of δ^{18}O, δ^2H and ^{17}O-excess of water isotopes in climate, environment, and hydrological studies. In addition, some applications require to measure highly enriched δ^2H water isotope samples, e.g., when tracing water flows in hydrology. In this case, the ^{2}H/^{1}H ratio is used as a tracer when fluorescent tracers are not an option, e.g., when tracing drinking water.

Measuring highly enriched water samples with optical spectroscopy comes along with two challenges: (i) the memory effect, the carryover from small fractions of water from one sample to another, and (ii) the spectroscopic limits of the analyzer. Here, we address both challenges by characterizing the memory effect for highly enriched δ^2H samples considering the recently developed express mode that allows to reduce/remove the memory effect at a much faster rate compared to the standard mode [1, 2] and by reviewing the spectroscopic limits of the analyzer.

In this study, we tested the performance of the Picarro L2130-i water isotope analyzer for a set of samples with varying ^{2}H/^{1}H ratios of 0.1 to 2.0% (corresponding to δ^2H values of about 6,000 to 130,000‰). We found that (i) the analyzer shows an excellent linearity over a high δ^2H enrichment range (up to 130,000‰); (ii) the analyzer shows a negligible concentration dependence at high enrichment levels; (iii) the spectroscopic limits of the analyzer can be extended by reducing the injection volume (<1.8uL); (iv) the memory effect can be reduced significantly when using the express mode compared to the standard mode.

Our results show that the Picarro L2130-i water isotope analyzer is an adequate tool for measuring highly enriched δ^2H water samples, and we will discuss best practices when measuring these samples.

References

[1] Hofmann, M. E. G., Lin, Z., Woźniak, J., and Drori, K.: Improved throughput for δ18O and δD measurements of water with Cavity Ring-Down Spectroscopy, EGU General Assembly 2021, online, 19–30 Apr 2021, EGU21-14254, https://doi.org/10.5194/egusphere-egu21-14254, 2021.

[2] Landais, A., Minster, B., Zuhr, A., Hofmann, M., and Fourré, E.: Performances of express mode vs standard mode for δ18O, δD and 17O-excess with a Picarro analyzer, EGU General Assembly 2022, Vienna, Austria, 23–27 May 2022, EGU22-4278, https://doi.org/10.5194/egusphere-egu22-4278, 2022.

Potential of ^{18}O isotope signature for detecting adulteration of wine

Ionete R.E., Costinel D., Botoran O.R., Miricioiu M., Mathiu T.
National Research and Development Institute for Cryogenics and Isotopic Technologies - ICSI Rm. Valcea, Uzinei Street no. 4, 240050, Romania

Given that adulteration of wine is an ongoing issue, there is a need to develop appropriate analytical methods to gain a better understanding of the changes in wine's composition brought on by adulteration. When referring to "adulteration of wine", a series of unregulated or not allowed procedures are foreseen, such as (i) dilution with water, (ii) blending with wine of a lesser quality or denomination, (iii) addition of sugars or alcohol, or (iii) mislabelling. For instance, the EU's legislation forbids wine watering [1], while the USA (state of California) allows the minimal addition of water required to assist the natural fermentation of the wine [2, 3]. Also, the natural ethanol concentration of grape must or wine can be increased by adding sugar (beet, cane) or rectified must before or during fermentation in order to produce a higher-quality wine. This procedure is permitted to be used only in wine-growing regions and vintages that experience unfavorable weather conditions throughout the grape-ripening phase, which results in low grape sugar concentration, while in other areas the addition of sugar to wine is not allowed [3].

Tracing the wine's isotopic signature could be a useful tool in this regard since isotopic techniques rely on the fact that the same molecule displays different isotope contents (^{2}H/^{1}H, ^{18}O/^{16}O, ^{13}C/^{12}C) depending on its origin.

Compared to groundwater that roots absorb from the soil, grape water is always enriched in heavy isotopic forms due to the evapo-transpiration process in plants (vine) during grape ripening. This characteristic enables the detection of exogenous water in wine by determining the isotope ratios of oxygen-18 (18O) to oxygen-16 (16O), measured by isotope ratio mass spectrometry, and expressed as δ^{18}O value. Also, to determine the geographical origin of wine, several isotopic ratios have been proposed as indicators, including the ^{2}H/^{1}H, ^{18}O/^{16}O, and, to a lesser extent, ^{13}C/^{12}C ratios. This is because the specific location of the vineyard can influence the climatic conditions that the grapes experience during the ripening process, resulting in unique isotopic signatures in the wine.

In this context, it was aimed to investigate the effects on the final δ^{18}O value of the wine, due to the application of some potential wine production practices (permitted or not), such as the addition of technological water prior to grape fermentation, the addition of rectified concentrated must from a different geographical origin than the wine-originated must, and wine dilution. Therefore, three different experimental approaches have been considered: (i) addition of water in different percentages, ranging between 2 and 16%, to reduce must sugar pre-fermentation as a winemaking alcohol management; (ii) addition of rectified concentrated must (RCM), from 2 to 50g, at 200 ml of wine, as a wine sweetening procedure; and (iii) dilution of wine with waters (from 1 to 20%) with different isotopic signatures. The δ^{18}O values of water extracted from the samples, were measured by IRMS after equilibration.

As expected, at the first experiment, where water was added to the must, followed by the fermentation process, it was observed that the δ^{18}O value of the wine decreases as the dilution level increases (a decrease of around -1 ‰ of $\delta^{18}O$ at 8% water addition); there is a linear relationship between the amount of water supplied and the wine's $\delta^{18}O$ value. Furthermore, samples measured after distillation show a higher value of $\delta^{18}O$ when compared to samples measured prior to distillation or right after the addition of water. Although the addition of exogenous water alters the $\delta^{18}O$ value in controlled additions, it can be challenging to determine the precise amount of water added in real-control situations when the initial value of the must or grapes is unknown.

The second experiment examined the discrepancy between the wine's initial $\delta^{18}O$ value (white and red wine samples were used, with $\delta^{18}O_{water}$ of +3.08‰ and +0.39‰ respectively) and that attained after its sweetening with rectified concentrated must ($\delta^{18}O_{water}$ of +6.52‰). A linear increase of $\delta^{18}O_{water}$ was observed with the increase in the added amount of RCM. As in the first experiment, there was an increase in the $\delta^{18}O$water measured after versus before the distillation.

In the third experiment, two water samples with significantly different concentrations were used to dilute the wine. The trend in $\delta^{18}O$ variation was as in the first experiment. The decrease in $\delta^{18}O$ value was significantly higher for dilution with a water more depleted in oxygen-18.

Even if the experiments demonstrated a clear tendency for change in the $\delta^{18}O_{water}$ of the adulterated sample compared to the original one, in a real control process these differences are insignificant (deviation less than 1‰), especially when different winemaking technological practices are invoked (e.g., the addition of technological water below 10%, sweetening with rectified must from another geographical origin).

Keywords: oxygen 18, wine, origin

Acknowledgement

This work has been financed by the Ministry of Research, Innovation and Digitization through Program 1 - Development of the national research and development system, Subprogram 1.2 - Institutional performance - Projects for financing excellence in R&D, Contract no. 19PFE/2021, and NUCLEU Program, grant number PN 23150301 "*Implementation of integrated isotopic-chemical-nuclear analytical methodologies for authentication the traditional Romanian food products*".

References

[1] Versari A., Laurie V.F., Ricci A., Laghi L., Parpinello G.P. (2014). Progress in authentication, typification and traceability of grapes and wines by chemometric approaches. *Food Research International*, *60*, 2-18.

[2] Galpin V.C. (2006). A comparison of legislation about wine-making additives and processes. *Cape Wine Master Diploma Assignment*.

[3] Dordevic N., Camin F., Marianella R.M., Postma G.J., Buydens L.M., Wehrens R. (2013). Detecting the addition of sugar and water to wine. *Australian Journal of Grape and Wine Research*, *19*(3), 324-330.

CO_2 and CH_4 fluxes from different meadows

Marta Jakubiak[1], Adriana Trojanowska- Olichwer[1], Natalia Krzyśków[1], Mariusz Jędrysek[1], Zygmunt Kącki[2], Mateusz Meserszmit[2], Grzegorz Swacha[2]
[1]*University of Wroclaw, Pl. Uniwersytecki 1, 50-137 Wroclaw, Poland*
[2]*Botanical Garden, University of Wroclaw, Henryka Sienkieiwcza Str.23, 50-335 Wrocław, Poland*

Grassland accumulate carbon through an imbalance between plant uptake of atmospheric CO_2 by photosynthesis and the release of CO_2 to the atmosphere from respiration (the emission of CO_2 from vegetation – autotrophic and soil – heterotrophic respiration) (Acosta et al., 2017). Ecosystem respiration (Reco) plays an important role in estimating the global carbon balance of terrestrial ecosystems, however, the value of respiration is required to correctly assess the gross primary production (GPP) of such ecosystems.

The subject of this study was to determine the size of emitted fluxes of CO_2 and CH_4 gases from selected meadows. CO_2 flux measurements were carried out using a closed dynamic chamber system. Daily field surveys took place in September 2021 at two locations, Grębszyce and Boleścin villages. Direct analyses of gas concentrations were made with the PICARRO G2201-i gas analyzer, and directly at the same time, measurements of temperature, humidity, photosynthetically active radiation (PAR) and atmospheric pressure were carried out. The obtained results show daily changes in the fluxes of emitted gases. For the studied meadows, the average value of ecosystem respiration was -0.24 g m^{-2} h^{-1} for fresh meadows (*Arrhenatherion*) in Grębszyce, and 0.25 g m^{-2} h^{-1} for wet meadows (*Calthion*) in Boleścin (Krzyśków, 2021).

These studies were made in the framework of the project "Biogas potential of grassland biomass from lowland part of Lower Silesia BIOPOL-GAZ-EDU - stage I" realized by the Botanical Garden of the University of Wrocław.

Acknowledgements

Studies co-financed by the Provincial Fund for Environmental Protection and Water Management in Wrocław.

References

[1] Krzyśków N., Emisja CO_2 i CH_4 z wybranych łąk. *Uniwersytet Wrocławski* (2021), 1-60.

[2] Acosta M., Juszczak R., Chojnicki B., Pavelka M., Havránková K., Lesny J., Krupková L., Urbaniak M., Machačová K., Olejnik J. *CO_2 Fluxes from Different Vegetation Communities on a Peatland Ecosystem,* Wetlands, 2017, (37), 423 – 435.

Carbon isotopic variations in the CO_2-CO-CH_4 system during hard-coal stepwise heating

Jędrysek M.-O., Pleśniak Ł., Drzewicki W., Lis G., Moskwa K.
Institute of Geological Sciences, University of Wroclaw, 50-137 Wroclaw, Poland

Gas mixture obtained by means of stepwise heating of hard coal has been analyzed with respect to $^{13}C/^{12}C$ isotopic ratios. The goal was to observe differences in carbon isotopic ratios (Δ) or potential carbon isotopic fractionation (α) in the CO_2-CO-CH_4 system, due to desorption or generation of gases, respectively. The experiment has been carried out in off-line system according two strategies: 1) low-temperature using gas tight stainless-steel cylinder, with hard-coal core closed with a negligible amount of the main atmosphere – the core was step-wisely heated from a room temperature up to 90°C, and 30 gas-samples have been obtained (Fig 1); 2) high-temperature using quartz tubes (with hard coal) under initial vacuum – the stepwise heating was from 250 to 500°C and 6 gas-samples have been obtained. All gases were analyzed by means of GC/IRMS.

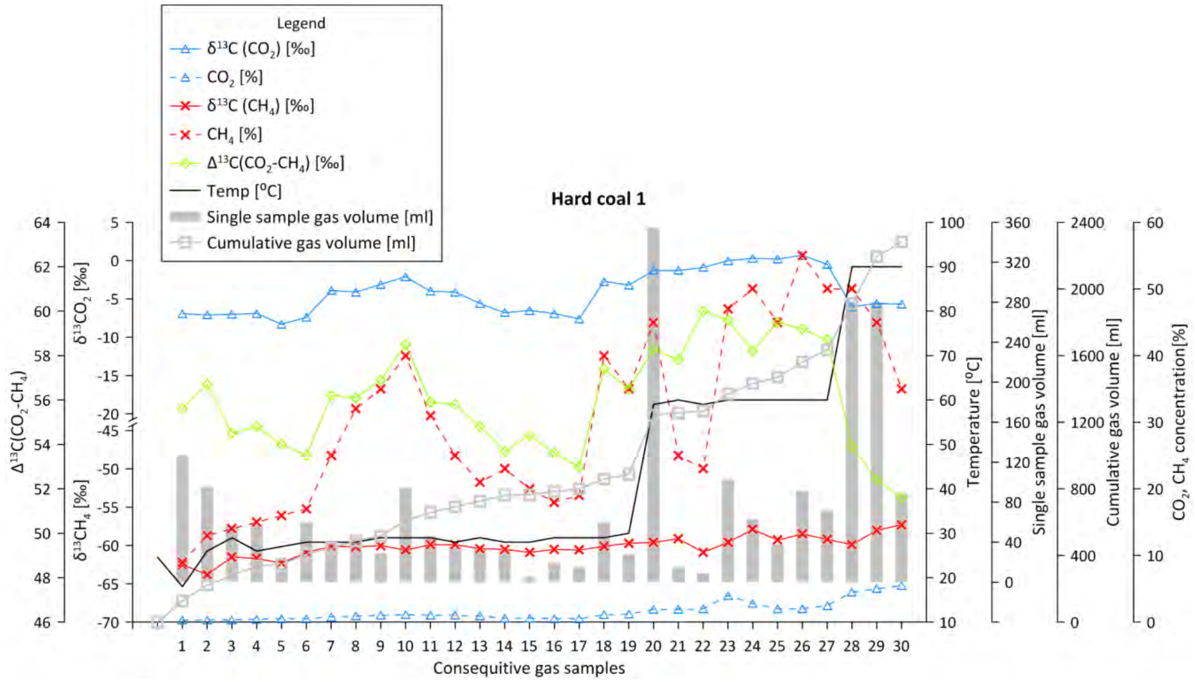

Fig. 1. Low temperature desorption of C-bearing gases from hard coal.

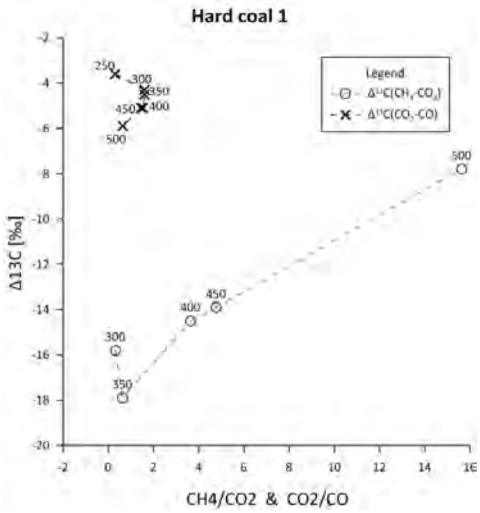

Fig. 2. High-temperature step-wisely evolved of C-bearing gases from hard coal.

Gas mixtures obtained were composed dominantly of N_2, O_2 at lower temperatures and increasing concentrations of carbon monoxide, carbon dioxide and methane at higher temperatures (Fig. 1, 2).

We conclude that at lower temperatures, up to about 350°C the gas was evolved mostly due to desorption from the coal, with small participation of the “new” gases, while above that temperature a new CO_2, CO, and CH_4 were formed due to pyrolysis. The volume and rate of generation of gases, their concentrations and isotopic ratios will be discussed during presentation.

Carbon cycling between surface water, groundwater and thermal water interaction at Čateško polje, SE Slovenia: geochemical and isotope approach

Kanduč T., Novak R., Zuliani T.
Jožef Stefan Institute, Department of Environmental Sciences, Jamova cesta 39, 1000 Ljubljana

It is well-known that toxic trace elements can be introduced into water systems from both natural and anthropogenic sources. In environments with no anthropogenic activity, the concentration of most metals is low and derives from the weathering of rocks [1, 2]. To gain a more comprehensive understanding of the quality of water bodies means determining the WQI (Water Quality Index) by combining a variety of water quality parameters, including temperature, pH, dissolved oxygen, nitrate, and phosphates [3, 4]. Additionally, stable and radiogenic isotopes can also be utilized to track water sources and provide insights into major biogeochemical processes in surface-groundwater interactions and spatiotemporal variations in water [1].

In this study, carbon cycling and elemental composition during groundwater-surface water interactions in the lower reaches of River Sava were investigated to provide baseline data prior to the construction of a hydroelectric power plant (HPP) at Mokrice. Indeed, this is the first such systematic seasonal study of geochemical (chemical and isotopic) variables in the groundwater of the Čateško polje, SE Slovenia. The stable isotopic composition of carbon ($\delta^{13}C_{DIC}$) and radiogenic tracer $^{87}Sr/^{86}Sr$ were determined to trace geochemical processes. Here, the local geology (Figure 1) consists of Quaternary rocks composed mainly of sand and gravel [5].

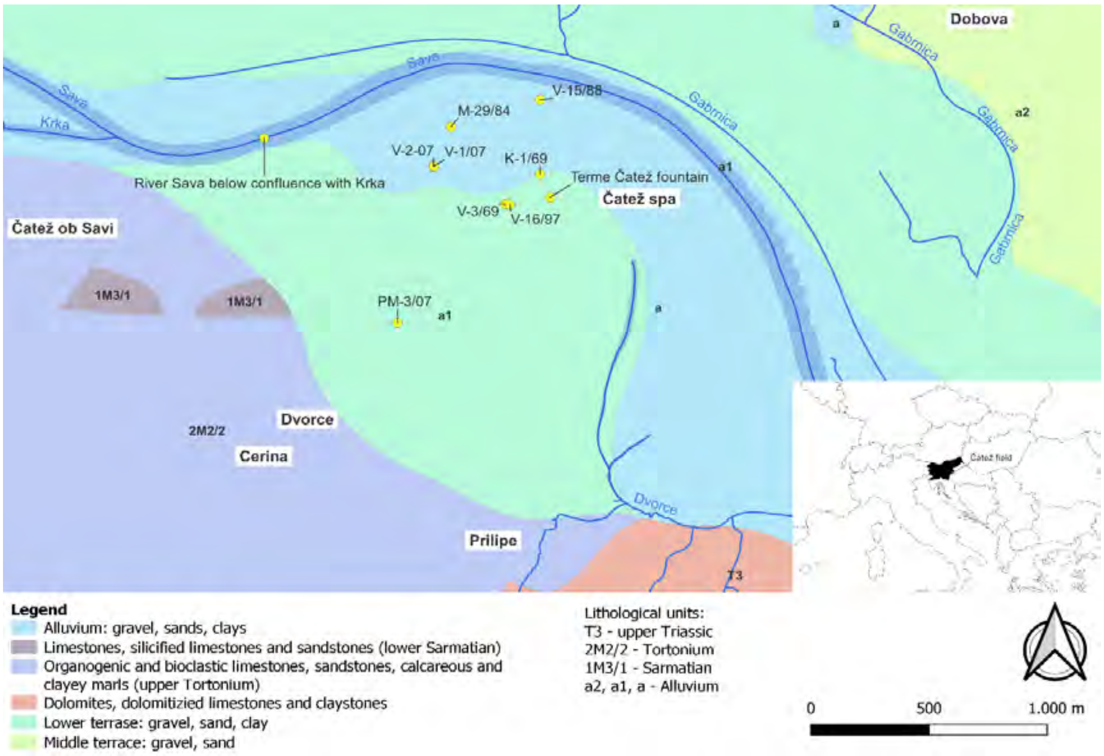

Figure 1: Sampling points (thermal waters: M-29/84, V-1/07, K-1/69, V-3/69, groundwater: PM-3/07, M-29/84, V-1/07, V-2/07, Terme Čatež fountain and River Sava below the confluence with Krka) and geological composition of the area.

Water samples (Figure 1) were collected from shallow piezometers (n = 2), deep piezometers (n = 2), the confluence of Sava and Krka rivers at Čatež (n = 1), from the thermal water (n = 4) and the Terme Čatež fountain (n = 1) in the Čateško polje. The elemental concentrations were determined using an inductively coupled plasma mass spectrometer (ICP-MS) (7900x Agilent Technologies, Tokyo, Japan). Based on total Sr concentrations, a known aliquot of the sample dried and the residue dissolved in 8 M HNO_3 and loaded onto the Sr selective resin (100-150 µm, TrisKem International, Bruz, France) for matrix removal. The $^{87}Sr/^{86}Sr$ ratio was then determined using a multi-collector ICP-MS (Nu II, Nu Plasma, Ametec, Wrexham, Great Britain). The total alkalinity was determined within 24 h of sample collection using the Gran titration method [6]. Continuous flow IRMS (Europa Scientific 20–20) with an ANCA-TG preparation module was used to measure $\delta^{13}C_{DIC}$. In addition, thermodynamic modelling was used to evaluate the pCO_2 and the saturation state of calcite ($SI_{calcite}$) and dolomite ($SI_{dolomite}$) using the PHREEQC speciation program [7].

The WQI was calculated as follows:

$$WQI = \sum[W_i \times (c_i/s_i)] \times 100 \tag{1}$$

Where W_i is the sum of the weightings of all parameters ($\sum wi = 42$); c_i is the concentration of each trace element in each water sample—here the average concentrations for both sampling seasons are considered (winter and summer seasons 2021), and s_i – represents the concentration listed in legislation [8]

All investigated water samples have distinct geochemical compositions indicating different geochemical processes in the water system. Water composition is related to geological composition, well depth, and distance from the river. Geochemical processes reveal redox reactions in the water system. The $\delta^{13}C_{DIC}$ seasonal range is from -13.8 to -12.2 ‰ in shallow wells, from -5.8 to -6.9 ‰ in thermal waters, from -7.8 to -5.7 ‰ in deep wells, from -11.1 to -9.9 ‰ in River Sava and from -11.8 to -11.3 ‰ in Terme Čatež fountain. $^{87}Sr/^{86}Sr$ ranges from 0.70858 to 0.70934.

The data indicate carbonate dissolution and plot along the carbonate weathering line. The exception is the deep well V-2/07, where the conductivity and total alkalinity indicate low mineralization. The soil CO_2 contribution is more expressed in river water, Terme Čatež fountain and shallow wells (PM-3/07), while more carbonate dissolution is expressed in deep wells (V-1/07) and thermal waters of Čateške spa. Only in well V-2/07 was the silicate fraction detected based on $^{87}Sr/^{86}Sr$ ratio.

The calculated WQI (Water Quality Index) [9] range 43.3 from to 232.9 and is as follows: V-1/07>Terme Čatež wells>M-29/84>PM-3/07>V-2/07>Terme Čatež fountain>River Sava after the confluence with Krka and indicates poor to good water quality. Results of PCA analysis, which are based on measured in-situ parameters (DO – dissolved oxygen, T, pH, conductivity), qualitative chemical analyses (Na, Mg, K, Ca, TA-total alkalinity, Li, B, Al, V, Cr, Mn, Fe, Co, Ni, Cu, Zn, As, Rb, Sr, Mo, Cd, Sb, Ba, Tl, Pb, U) and $\delta^{13}C_{DIC}$ reveal four different clusters.

In summary, constructing a hydrothermal power plant will likely influence the carbon cycle and biogeochemical processes in the affected water system, e.g., accelerate primary production, degradation of organic matter, and degassing of CO_2 from the river. Therefore, this local multi-parameter study of the Čateško polje is essential for future water management.

References

[1] Karlović I., Marković T., Kanduč T., Vreča P. 2022: Assessment of seasonal changes on the carbon cycle in the critical zone of a surface water (SW) – groundwater (GW) system. Water 2022, vol. 14, 21, 3372-1-3372_17. Doi: 10.3390/w14213372.

[2] Kanduč T., Grassa F., McIntosh J., Stibilj V., Ulrich-Supovec M., Supovec I, Jamnikar S. 2014: A geochemical and stable isotope investigation of groundwater/surface-water interactions in the Velenje Basin, Slovenia. Hydrogeology Journal, doi: 10.1007/s10040-014-1103-7.

[3] Hasan, A. B., Kabir, S., Selim R., Zaman N., Ahsan A., Rasmid M. 2013: Enrichment factor and geo-accumulation index of trace metals in sediments of the ship breaking area of Sitakund Upazilba (Bhatiory-Kumira). Chittagong Bangladrsh. Journal of geochemical exploration 125, 130-137. https://doi.org/10.1016/j.geoexplo2012.12.002.

[4] Xiao J., Jin Z., Wang J. 2014: Geochemistry of trace elements and water quality assessment of natural water within the Tarim River Basin in the extreme arid region, NW China. Journal of Geochemical Exploration 136: 118-126.

[5] Šikić, K., Bosch, O., Šimunić, A. 1972: Osnovna geološka karta SFRJ. 1:100.000. Tolmač lista Zagreb: L –33 – 53. Zagreb: Institut za geološka istraživanja (Tolmač lista Zagreb: L-33-53. Zagreb: Institute for geological research), 70 pp. (in Slovene).

[6] Clesceri, L.S., Greenberg, A.E., Eaton, A.D. 1998: American Public Health Association (APHA); American Water Works Association (AWWA); Water Environment Federation (WEF). Standard Methods for the Examination of Water and Wastewater, 20th ed.; American Public Health Organization: Washington, DC, USA.

[7] Parkhurst, D.L., Appelo, C.A., J 1999: User's guide to Phreeqc (Version 2) – a computer program for speciation, batch-reaction, one-dimensional transport, and inverse geochemical calculations. Water-resources investigations report 99-4259, Denver, Colorado, pp. 312.

[8] World Health Organization 2008: Guidelines for Drinking – Water Quality; World Health Organization: Geneva, Switzerland.

[9] Meng Q., Zhang J., Zhang Z., Wu T. 2016: Geochemistry of dissolved trace elements and heavy metals in the Dan River Drainage (China): distribution, sources, and water quality assessment, Environmental Science and pollution research 23: 8091-8103, doi 10.1007/s11356-016-6074-x.

Precise determination of uranium isotopes and their applications in geology

Gabriella Ilona Kiss[1, 2], Marjan Temovski[1], István Futó[1], László Palcsu[1]
[1]*Institute for Nuclear Research, Bem square 18/C, H-4026, Debrecen, Hungary*
[2]*University of Debrecen, Doctoral School of Physics, 4032 Debrecen, Egyetem tér 1.*

To understand better the hydrological and geochemical processes of our environment, the analysis of the isotopic composition of uranium is an excellent tool. For this goal, the multicollector ICP MS facility of our isotope laboratory is an applicable instrument based on its analytical efficiency.

The mass spectrometer is equipped with an SEM and 9 Faraday cups, from which 8 can be positioned by the tuning software in order to make sure that the ion beams to be measured could be fully detectable. Using of the secondary electron multiplier is required in case of measuring isotopes with very low intensities, such as ^{230}Th when dating carbonate samples.

The δ^{234}U value derived from the isotope ratios of ^{234}U and ^{238}U provides information on the transport and flow conditions in groundwater. In rocks older than a few million years, the two isotopes should be in secular equilibrium (i.e. the activity ratios are the same), but in natural waters different values can be measured. The alpha decay of ^{238}U damages the crystal lattice, so the resulting ^{234}U isotope, sitting in a defective lattice site, is prone to leaching from the rock and thus to relative enrichment in water [1-3]. The effect, expressed in permil, can be up to thousands of ‰ large, so its measurement is relatively simple, although not trivial because of the five orders of magnitude between the appearance of the ^{238}U and ^{234}U. Our previous measurements have been validated by determining the δ^{234}U value of ocean water samples, which is known to be +147 ‰ [4]. In addition, water samples from Hungary, Serbia, Romania and Ethiopia have been analysed.

Beside studying groundwater, uranium isotopes can be used also for palaeoclimatological research goals. In this field, the results can provide chronological framework for cave carbonate formations (i.e., speleothems) and combined with other geochemical properties, an insight into changes of environmental factors (e.g. temperature, precipitation, vegetation). During the formation of the speleothems, uranyl ions, which are highly soluble in the dripping groundwater, are incorporated into the carbonate structure. Their decomposition results in the formation of the ^{230}Th isotope. The age can be calculated from the ^{230}Th/^{238}U ratio [5,6]. For sample preparation, we use a triple spike containing two uranium isotopes (^{233}U, ^{236}U) and one thorium isotope (^{229}Th). The composition of the spike solution was further refined by measuring speleothem samples of "infinite" age (>2 million years) (here the secular equilibrium between the isotopes ^{238}U, ^{234}U and ^{230}Th is already re-established). The extent of mass discrimination is inferred from the intensity ratio of the measured ^{235}U-^{238}U ion currents in the sample, which is valid not only for uranium but also for thorium. Our previous studies have been carried out on speleothem samples from Hungary, Ecuador, Macedonia and Slovakia.

In some cases, however, differences in the ^{235}U/^{238}U ratio, taken as constant, can be measured. Throughout the Earth's history, climatic changes at the boundaries of the time scale have resulted in very small variations in the ratio of ^{238}U to ^{235}U isotopes. The variation is between 1 and 2 permil [7,8], and to determine it accurately (~0.05 ‰), the highest possible sensitivity and precision must be set under the same measurement conditions. To obtain accurate results, a double spike is used in the preparation, containing isotopes ^{233}U and ^{236}U, but also contributing to the measured values of the samples with a minimal amount of ^{235}U and ^{238}U isotopes, which must be corrected. By properly adjusting the detectors of the instrument, measuring each sample several times and using the Standard-Sample Bracketing method to measure a standard solution with the same concentration between the samples, the values of a limestone formation $\delta^{238}U$ in Hungary were determined with high accuracy. In order to validate our preparation and measurement protocol, we prepared and measured a few ocean water samples. Here we used the same approach not only for the chemical point of view, but also during the spiking procedure, and the measurement. Our results for the ocean $\delta^{238}U$ value were in an excellent agreement with the previously published data from the literature ($\delta^{238}U_{ocean}$ = -0.39 ± 0.05 ‰ [9, 10]).

References

[1] Camacho, A., Devesa, R., Vallés, I., Serrano, I., Soler, J., Blázquez, S., Ortega, X., Matia, L., Journal of Environmental Radioactivity, 2010, 101(12), 1048-1054.

[2] Tissot, F.L., Chen, C., Go, B.M., Naziemiec, M., Healy, G., Bekker, A., Swart, P.K., Dauphas, N., Geochimica et Cosmochimica Acta, 2018 (242), 233-265.

[3] Cizdziel, J., Farmer, D., Hodge, V., Lindley, K., Stetzenbach, K., Science of the Total Environment, 2005, 50(1-3), 248-260.

[4] Andersen, M.B., Stirling, C.H., Zimmermann, B., Halliday, A.N., Geochemistry, Geophysics, Geosystems, 2010, 11(12).

[5] Cheng, H., Adkins, J., Edwards, R.L., Boyle, E.A., Geochimica et Cosmochimica Acta, 2000, 64(14), 2401-2416.

[6] Cheng, H., Edwards, R.L., Shen, C.C., Polyak, V.J., Asmerom, Y., Woodhead, J., Hellstrom, J., Wang, Y., Kong, X., Spötl, C., Wang, X., Alexander Jr, E.C., Earth and Planetary Science Letters, 2013 (371), 82-91.

[7] Jost, A.B., Bachan, A., van De Schootbrugge, B., Lau, K.V., Weaver, K.L., Maher, K., Payne, J. L., Geochemistry, Geophysics, Geosystems, 2017, 18(8), 3093-3108.

[8] Tissot, F. L., Dauphas, N., Geochimica et Cosmochimica Acta, 2015 (167) p. 113-143.

[9] Andersen, M.B., Stirling, C.H., Weyer, S., Reviews in Mineralogy and Geochemistry 2017, 82 (1), 799–850.

[10] Clarkson, M.O., Lenton, T.M., Andersen, M.B., Bagard, M-L., Dickson, A.J., Vance, D., Nature Communications, 2021 (12), 399.

Insights into the ecology of planktonic crustaceans: what can we learn using stable isotopes?

Wojciech Krztoń[1], Edward Walusiak[1], Iwona Gołaś[2], Keith Hobson[3], Petar Žutinić[4], Marija Gligora Udovič[4] , Antonija Kulaš[4] , Judita Koreivienė[5] , Jur̄atė Karosienė[5] , Beata Gebus-Czupyt[6], Anita Galir Balkić[7] , Filip Stević[7] , Tanja Žuna Pfeiffer[7] , Dubravka Špoljarić Maronić[7], Elżbieta Wilk-Woźniak[1]

[1]*Institute of Nature Conservation Polish Academy of Sciences, Kraków, Poland*

[2]*Department of Water Protection Engineering and Environmental Microbiology, Institute of Engineering and Environmental Protection, Faculty of Geoengineering, University of Warmia and Mazury in Olsztyn*

[3]*Department of Biology, University of Western Ontario, London, Ontario, Canada*

[4] *Department of Biology, Faculty of Science, University of Zagreb, Zagreb, Croatia*

[5]*Nature Research Centre, Vilnius,Lithuania*

[6]*Institute of Geological Sciences Polish Academy of Sciences, Warsaw, Poland*

[7]*Department of Biology, Josip Juraj Strossmayer University of Osijek, Osijek, Croatia*

Freshwater ecosystems, despite covering only 0.8% of the Earth's surface, provide habitat for about 6% of species. Complex freshwater food webs consist of diverse species assemblages and their structure strongly depends on trophic links between phytoplankton (primary producers) and zooplankton (consumers). Energy flow in freshwaters relies on planktonic crustaceans – large bodied algal grazers and an important food for fish. Understanding energy flow pathways and conduits between planktonic crustaceans and primary producers is crucial to perceive ecosystem perturbations, especially in the face of global changes that will result in more frequent, intense and toxic cyanobacterial blooms.

Application of stable isotope-based approach in plankton ecology studies is advantageous compared to classically used methods which are based, for instance, on species and specimen counting. Here we used stable isotopes of carbon ($\delta^{13}C$) and nitrogen ($\delta^{15}N$) to study freshwater food webs with an emphasis on ecosystems with cyanobacterial blooms occurring annually.

We found that niches derived from isotopic biplots for selected groups of planktonic crustaceans were narrowest in the spring (13.8 – 21.5‰^{2}) and increased in breadth in summer (15.7 – 25‰^{2}) and fall (24.2 – 41.8‰^{2}), when cyanobacterial blooms were present. We found that lower values of $\delta^{13}C$ were related to highest chlorophyll *a* and phycocyanin concentration. This indicates use of algae/cyanobacteria-originating carbon by planktonic crustaceans during the highly productive season. On the other hand, we found that lowest $\delta^{13}C$ values in crustacean tissues were related to high densities of betaproteobacteria highlighting the role of this group of bacterioplankton in incorporating methane-originating carbon into the food web.

We analysed samples of planktonic crustaceans from three lakes located across latitudinal gradient in Europe: Lake Sakadaš (Croatia, Southern Europe), Tyniec oxbow lake (Poland, Central Europe) and Lake Gineitiškės (Lithuania, Northern Europe). Values of $\delta^{13}C$ of planktonic crustaceans were segregated among lakes. Lowest values of $\delta^{13}C$ which were found in lake Sakadaš (Croatia) indicate the relevant role of methane-originating carbon in that food web. Moreover, we found that the crustacean C:N ratio (a proxy for fatty acids and lipid content) was negatively correlated with $\delta^{15}N$ indicating that animals occupying highest trophic levels were depleted in lipid content compared to those situated closer to the primary producers. This effect was significant in all of the studied lakes, however it was strongest in Lake Sakadaš.

Is stable isotope analysis useful for determining of the origin smuggled turtles?

Kukla J. [1], Jandová K. [1], Trubač J. [2], Rajmonová E. [1], Kufnerová J. [1]
[1]*Faculty of Science, Institute for Environmental Studies, Charles University, Prague, Czech Republic*
[2]*Faculty of Science, Institute of Geochemistry, Mineralogy and Mineral Resources, Charles University, Prague, Czech Republic*

European species of tortoises of the genus Testudo (*T. hermanni*, *T. graeca, T. marginata*) are very popular pets. Therefore, they have also become the object of illegal trade, where even current statistics of seized live specimens list hundreds of individuals who are illegally trafficked each year. Legal trade is allowed in the EU with proven captive-bred specimens. Declaring smuggled turtles as bred in captivity is one of the most often used misdeclarations that proves poorly to the accused. One of the promising methods to distinguish wild caught from captive bred specimen is stable isotope analysis. With its help, it is possible to better estimate the geographical origin of animals. Carapace protein keratin is an ideal material for stable isotope analysis. Sampling from the edge of the carapace is not considered to be an invasive method, so it can be easily applied to live specimens without any harm. In our study, we analyse the basic set of stable isotopes within the collection of dozens of shells of European tortoises. Our material comes from the CITES rescue canter, where the specimens were placed after their seizure.

For the stable isotope analysis, we used central part of the scute (juvenile) and the most outer (adult), relevant to age of the animal. We found significant difference between species and significant difference between juvenile and adult scute of one animal.

Cloud formation in different scales and their impact on water isotope signature

László E[1], Palcsu L[1], Leelőssy Á[2]
[1]*Isotope Climatology and Environmental Research Centre (ICER), Institute for Nuclear Research, Bem tér 18/C, H-4026, Debrecen, Hungary.*
[2]*Department of Meteorology, Eötvös Loránd University, 1117 Pázmány Péter sétány 1/A., Budapest, Hungary*

The formation of stratiform and convective precipitation differs significantly in space and time, due to differences in vertical air movements and microphysical processes that regulate rain formation. Stratiform clouds are characterized by large horizontal extent with weak vertical movement, while convective clouds are characterized by large vertical extent with strong updrafts. These different rain formation mechanisms and cloud physical processes also appear in the amount of precipitation, which can be better understood by examining the weather parameters.[1,2] The variable ratio of stratiform and convective rain types can differ significantly in space and time at different stations, which is significantly influenced by the temperature field, soil conditions and geographical location. In this research, we reviewed the SYNOP reports using synoptic stations with different geographical and climatic conditions. Seasonal and long-term changes can be observed in the extracted time series, which affects the precipitation isotope ratios.

The variation in the isotopic ratios of precipitation depends on many factors during cloud formation. With this study, it was possible to observe that the content of stable isotope and tritium is strongly connected to the temporal distribution of precipitation types in the midlatitudes, especially in continental areas. The rainfall intensity significantly determines the regulation of precipitation isotopic composition, suggesting that long-term precipitation isotope time series reflect changes in mesoscale convective system (MCS) intensity.

Acknowledgement

The research leading to this paper was supported by the János Bolyai Research Scholarship of the Hungarian Academy of Sciences, and also supported by the ÚNKP-22-5 New National Excellence Program of the Ministry for Innovation and Technology from the source of the National Research, Development and Innovation Fund.

References

[1] László, E., Palcsu, L., Leelőssy, Á., 2020. Estimation of the solar-induced natural variability of the tritium concentration of precipitation in the Northern and Southern Hemisphere. ATMOSPHERIC ENVIRONMENT, 233 117605.

[2] Palcsu, L., Morgenstern, U., Sültenfuss, J., Koltai, G., László, E., Temovski, M., … Jull, A.. 2018. Modulation of Cosmogenic Tritium in Meteoric Precipitation by the 11-year Cycle of Solar Magnetic Field Activity. SCIENTIFIC REPORTS 8, 1, 12813

Mitigation of the diagenesis risk in biological apatite δ^{18}O interpretation

Christophe Lécuyer[1], Jean-Pierre Flandrois[2]
[1]LGL-TPE, CNRS UMR5276, ENSL, Univ Lyon, Univ Lyon 1, Institut Universitaire de France, 43 bd du 11 Novembre 1918, 69622 Villeurbanne, France.
[2]LBBE, CNRS UMR5558, Univ Lyon, Univ Lyon 1, 43 bd du 11 Novembre 1918, 69622 Villeurbanne, France.

The assessment of the potential blurring effect of diagenetic processes represents the greatest challenge for geochemists whose purpose is to reconstruct environmental parameters based on isotopic proxies. Numerous studies performed on phosphatic remains from terrestrial and marine sedimentary deposits have shown post-depositional isotopic modifications due to exchange reactions with surrounding waters. If diagenesis may be diagnosed through several lines of evidence such as mineralogical or chemical modifications of the pristine *in vivo* apatite after burial in soils and sediments, diagenesis does not prove that bioapatite phosphate exchanged or not oxygen isotopes with aqueous fluids. Therefore, we propose a new method of detection of diagenetic alteration of bioapatites based on a statistical approach designed to analyze sample collections. It means that phosphatic remains belonged to animals living during a short time interval and within an environment characterized by steady air or water temperature and the δ^{18}O of ambient water. We show that the distribution of bioapatite δ^{18}O follows a normal distribution resulting from the combination of independent factors such as those related to the genetics, environment and analytical measurements. In the case of oxygen isotope exchange between the bioapatite and various amounts of circulating aqueous fluids, our numerical simulations reveal that the distributions of bioapatite δ^{18}O are asymmetric with shapes depending on the temperature of reaction and the composition of the reacting aqueous fluid. This new statistical tool based on mass balance equations and Monte Carlo simulations is considered valuable to mitigate the diagenesis risk in the interpretation of biological apatite δ^{18}O as paleoecological and paleoclimatic proxies.

N_2O isotopocules and mineral N isotopes in tracing N cycling in soil and waters

Lewicka-Szczebak D.
Institute of Geological Sciences, University of Wrocław, ul. Cybulskiego 30, 50-205 Wrocław, Poland

The complex nitrogen cycling in the environment associated with diverse microbial N transformations is crucial in the interplay of agriculture and environmental issues. Nitrogen, as important nutrient for plants, is added to arable soils as fertilizer, however is not only assimilated by plants, but also transformed by soil microorganisms and released to the atmosphere in gaseous forms or leached to groundwaters. These cause not only a loss of more than a half of the added nitrogen but also severe environmental problems, *i.e.*, groundwater pollution and greenhouse gas emissions. Mitigation of these problems is difficult since the understanding of the complex nitrogen transformation processes in soils is still limited, *e.g.*, N_2 emission, not measurable due to high atmospheric background, is still a big unknown and precludes closure of the N balance.

The critical knowledge gaps in the nitrogen cycle can be possibly approached by isotopic studies of different N compounds. Isotope signatures can be used not only to detect particular N transformations but also to quantify unknown N fluxes. Stable isotope analyses provide an unique tool for getting insight into particular biochemical processes, which can be distinguished by different isotope fractionation factors. Quite innovative and perspective tool are the isotopomer analyses of N_2O, which comprises not only nitrogen and oxygen isotope values, but also the site specific N analysis, which differentiates the isotope enrichment on different N positions in the linear N_2O molecule. Hence, with isotope analysis of N_2O molecule, we obtain three isotope signatures, which are governed by the N_2O production pathways as well as by N_2O reduction. These results are rich in information, but also challenging in their interpretation. Recently, we developed a new modelling tool for interpretation of these three-dimentional N_2O isotope results [1]. This tool enables assessment of contribution of various N_2O production pathways as well as estimation of the N_2O fraction reduced to N_2, hence may help in quantification of the main missing compound in the N balance. This isotope calculation software, allowing for isotope **FRA**ctionation and **M**ixing **E**valuation (**FRAME**), is available as an easy-to-use interface and can be applied also for other isotope studies, where quantification of isotope mixing and/or fractionation processes is needed [2].

N_2O isotopomer analyses combined with isotope analyses of mineral nitrogen compounds in soils and waters, including ammonium, nitrate and nitrite, can provide a very detailed and complex insight into the ongoing processes. Nitrite isotope analyses in soils is a novel approach [3], which may open new interpretation perspectives, since it is an intermediate product of nearly all known N transformations. The linkage between mineral N transformations and gaseous emissions may help in unravelling important knowledge gaps.

References

[1] Lewicka-Szczebak D., Lewicki M. P., Well R., *Biogeosciences* 17, 5513-5537, 2020.

[2] Lewicki M., Lewicka-Szczebak D., Skrzypek G., *Plos one* 17 (11), e0277204, 2022.

[3] Lewicka-Szczebak, D., Jansen-Willems, A., Müller, C., Dyckmans, J, Well, R, *Scientific reports* 11, 5008, 2021.

Isotope FRActionation and Mixing Evaluation (FRAME) with a new modelling tool applying the Monte Carlo approach

Lewicka-Szczebak D.[1], Lewicki M.[2], Skrzypek G.[3]
[1] *Institute of Geological Sciences, University of Wrocław, ul. Cybulskiego 30, 50-205 Wrocław, Poland*
[2] *Institute of Nuclear Physics, Polish Academy of Science, Kraków, Poland*
[3] *West Australian Biogeochemistry Centre, The University of Western Australia, Perth, Australia*

The available stable isotope mixing models allow advanced quantification of mixing proportions but usually do not account for the stable isotope fractionation of the product. Here we present the newly developed model using Markov Chain Monte Carlo approach: isotope **FRA**ctionation and **M**ixing **E**valuation (**FRAME**), with a user-friendly graphical interface that can simultaneously determine mixing proportions and progress of the fractionating process [1]. The isotope fractionation may be defined by the user for specific requirements of the particular isotope system, e.g., open or closed system fractionation. The model can integrate up to three stable isotope signatures of each compound. This modelling approach has been designed and already validated for identifying N_2O production pathways and quantifying N_2O reduction progress in soil incubation experiments [2]. However, it can be applied to other isotope systems where both isotope mixing and fractionation may coexist.

In this presentation, we show the model performance based on three different case studies: (i) the soil-derived N_2O isotope studies, (ii) the river nitrate isotope budget and (iii) calculating evaporation from water isotopic signatures. For (i) the model includes three isotope parameters ($\delta^{18}O$, $\delta^{15}N$, and SP – site preference – the difference in $\delta^{15}N$ value between central and peripheral position of the linear N_2O molecule) to determine the contribution of four N_2O production pathways and the progress of N_2O reduction to N_2. For (ii) the model includes two isotope parameters ($\delta^{18}O$, $\delta^{15}N$) to determine fractions of three nitrate sources and the progress of nitrate fractionation associated with denitrification. For (iii) the model includes two isotope parameters ($\delta^{18}O$, $\delta^{2}H$) and takes into account only fractionation due to water evaporation to determine the evaporation to input ratio.

The model is potentially applicable across various study fields that employ isotope analysis. The open mathematical design allows for the implementation of additional processes that alternate the characteristics of the final mixture and can be applied to a broad range of mixing and fractionation models.

References

[1] Lewicki M., Lewicka-Szczebak D., Skrzypek G., Plos one 17 (11), e0277204, 2022.

[2] Lewicka-Szczebak D., Lewicki M. P., Well R., Biogeosciences 17, 5513-5537, 2020.

Drip water monitoring in a shallow karst cave (Jama v Dovčku, SE Slovenia): O, H and C stable isotopes as input parameters for climate reconstruction

Lojen S., Zuliani T., Vreča P., Kanduč T.
Jožef Stefan Institute, 1000 Ljubljana, Slovenia

Tičar J., Lipar M., Anton Melik
Geographical Institute, Research Centre of Slovenian Academy of Science and Arts, 1000 Ljubljana, Slovenia

Rusjan S.
Faculty of Civil and Geodetic Engineering, University of Ljubljana, 1000 Ljubljana, Slovenia

When isotopic and geochemical proxies are to be used for the interpretation of paleoclimate from speleothems, adequate cave monitoring of drip water and cave climate parameters must be conducted. Continuous long-term monitoring for at least a decade is recommended[1], however, in most cases this is not feasible. We report on a two-year (2021-2022) monthly monitoring of temperature, cave air CO_2 concentration and isotope composition, O and H isotope composition of precipitation and drip water, dissolved inorganic carbon (DIC) and basic hydrochemical parameters at 15 drips located at sites with a roof thickness between 0.9 and 49.1 m. The aim of the study was to assess how accurately the ambient isotopic and geochemical signals are transmitted from the surface through the vadose zone and to what extent the isotopes of O and C in stalagmites reflect the external environmental conditions. The spatial variability of mean travel times time (MTT) of groundwater feeding speleothems in the cave was determined[2,3], and the potential prior calcite precipitation (PCP) at individual drips that may obscure the environmental δ^{13}C signal of the carbonate precipitating from dripwater was estimated. The PCP represents the calcite precipitation before the drip water reaches the stalagmite, caused by the equilibration of groundwater with variable pCO_2 conditions in the conduits[4].

The studied cave is located in southeast Slovenia (45°49'27.5''N, 15°25'48.8''E) in an area composed of a patchy mix of dolomite and limestone. The surface is covered with a mixed forest, the climate is mild oceanic to continental (Köppen-Geiger type Cfb/Dfb). The entrance of the cave is at 458 m a.s.l., the length 316 m and the maximum depth about 54 m.

Elemental analysis of drip water showed that most sites lay along the carbonate dissolution line ($2[HCO_3^-] = [Mg^{2+} + Ca^{2+}]$), with only a few exceptions above it, indicating a contribution of silicate weathering to the dissolved load. The Mg/Ca ratio of drip water reflects the heterogeneity of lithology; depending on the location, the mean Mg/Ca ratio of drip water ranged from 0.21 to 1.4 (absolute range from 0.13 to 2.3). Values of Mg/Ca ratios above 1 may be partly related to the dissolution of Mg from silicates, but a relative depletion of drip water in Ca caused by the PCP occurring during water-rock interactions along individual groundwater flow paths associated with hydrological routing is a much more plausible explanation. The PCP is typically indicated by a strong positive correlation between Mg/Ca and Mg/Sr ratios of drip water, as well as strong positive correlations between [Me^{2+}] and 1/[Ca^{2+}]. We found that the PCP occurred preferentially along the conduits with low drip rates, which dried out several times during the year, while it was rather unlikely at continuously dripping conduits with high drip rates. Intensive cyclic PCP results in lower alkalinities and higher δ^{13}C-values of DIC caused by degassing.

The measured CO_2 concentration in cave air varied between 700 and 9400 ppm, with high values during the warmer part of the year; the cave is poorly ventilated, apart from short periods in the spring and autumn when a stratification of the atmosphere can be observed. Calculations based on δ^{13}C values of DIC (-15.5 to -4.8 ‰) and cave air CO_2 (-24.2 to -11.5 ‰) show that the concentration and isotope composition of atmospheric CO_2 in the cave are at or close to the equilibrium with the concentration and isotope composition of DIC.

The comparison of the isotopic composition of oxygen in precipitation and in the drip water showed variable degrees of homogenisation. The amplitude of δ^{18}O values of precipitation in the observation period was about 5.1 ‰, while individual drips showed amplitudes of 0.14 to 1.05 ‰, corresponding to MTT of drip water from approx. 1.6 to 3.7 years. No consistent correlation existed between the MTT and roof thickness, which is typical for heterogeneous karst aquifers. Large differences in MTT even in drips located within a few metres of each other indicate that different stalagmites may record climate variability at annual to decadal scales.

Acknowledgements

This study was funded by the Slovenian Research Agency, project J1-2748.

References

[1] Riechelman DFC, Riechelmann S, Schröder-Ritzrau A, Chemical Geology 2022 (590), 120704999.

[2] Rodgers S, Soulsby C, Waldon S, Tetzlaff D, Hydrology and Earth System Sciences 2005 (9), 139-155.

[3] Rusjan S, Sapač K, Petrič M, Lojen S, Bezak N, Journal of Hydrology 2019 (577), 123956.

[4] Fairchild IJ, Borsato A, Frisia S, Hawkesworth CJ, Huang Y, McDermott F, Spiro B, Chemical Geology 2000 (166), 255-269.

A quarter century of laser-based water isotope instrumentation

Markus Miltner, Jerome Chappellaz, Marc Chenevier, Roberto Grilli, Hans-Jürg Jost, Samir Kassi, Amaelle Landais, Janek Landsberg, Harro Meijer, Jerome Morville, Daniele Romanini, Andreas Zahn, and Erik Kerstel
Université Grenoble Alpes, Laboratory for Interdisciplinary Physics, 38000 Grenoble, France

In this talk I will review the early developments of laser-based water isotope infrared spectrometry, starting with the Krypton-ion pumped, color-center laser instrument we built during the second half of the 1990's at the Center for Isotope Research at the University of Groningen. Other early instruments using multiple-pass gas cells followed, and will briefly pass the review before describing in more detail the current spectrometers based on the technique of Cavity Enhanced Absorption Spectroscopy (CEAS) [Romanini 2014].

These developments were made possible when (1) near-infrared diode lasers became commercially available as a result of laser developments for the telecommunications industry, and (2) the potential of high-quality factor optical cavities was realized for the ultra-sensitive detection of gaseous species. A further advance was made with the invention of the technique of Optical Feedback Cavity Enhanced Absorption Spectroscopy (OFCEAS), which solved the problem of coupling the spectrally relatively wide, free-running laser emission (order of 10 MHz) into a very narrow cavity transmission mode (order of kHz) [Romanini 2003, Morville 2014]

A brief description of the optical technique of stable isotope ratio infrared spectrometry and its experimental implementations will be presented [Kerstel 2004], before discussing a selection of applications, ranging from biomedical energy expenditure measurements, to ecology, to ice-core research and atmospheric water studies. Two projects will be described in more detail.

The first is the adaptation of an OFCEAS spectrometer to the physical limitations of the SUBGLACIOR ice-core drilling probe for exploring the past climate. The probe was designed to provide in-situ real-time measurements of deuterium isotopic variations (δD) and methane (CH_4) concentrations down to 3500 m of depth within a single Antarctic season. The main goal of this project was to provide simultaneous and real-time vertical profiles of two key climate signatures for evaluating if a target site is suitable to drill probe ice cores as old as 1.5 million years, and to reconstruct past temperatures and climate changes. The spectrometer was successfully deployed during the 2016/2017 Antarctic summer, although the drill encountered problems.

The second project, currently underway, concerns the development of atmospheric water isotope spectrometers to be flown on a commercial aircraft. IAGOS (In-service Aircraft for a Global Observing System) is a European Research Infrastructure that uses regular passenger aircraft to carry scientific instrumentation to sample the atmospheric composition up to 12 km altitude. In IAGOS-CARIBIC (Civil Aircraft for the Regular Investigation of the Atmosphere Based on an Instrument Container), a container equipped with 20 scientific instruments is installed on a modified Airbus A350 by Lufthansa during several consecutive long-haul flights from Europe to many destinations worldwide. With roughly

12 campaigns per year, this flying laboratory provides data with high spatial and temporal resolution of about 100 trace gases, aerosols and cloud parameters, and this over several years/decades. Thereby it allows the validation of climate models and satellite observations.

Water is arguably the most important molecule in our atmosphere: The large enthalpy change associated with its evaporation and condensation, makes that water contributes significantly to the energy distribution over the planet in the form of latent heat. Furthermore, in the form of water vapor and clouds, water is responsible for about 75% of the Earth's greenhouse effect. This contribution is partly caused by feedback effects driven by the non-condensable greenhouse agents, foremost CO_2. These highly complex feedback effects are the reason that clouds are the major unknown in today's climate models. Since all these processes involving water are isotope dependent, water isotope ratios are ideal tracers to help quantify and disentangle these feedbacks. Water isotope ratios reflect the evaporation and condensation history of an air parcel and thus enable the identification of different air masses and the following of their mixing. Moreover, isotope measurements are excellent means to validate the growing number of isotope-enabled climate models.

For these reasons we are developing the next generation water isotope instruments for the CARIBIC instrument container. The OFCEAS technique has previously shown to be able to make isotope ratio measurements on atmospheric water vapor at very low water concentrations, as encountered at high altitudes [Landsberg 2014]. In fact, we adapt two OFCEAS spectrometers to the specific needs of airplane integration, one that measures the isotope ratio of the total water content, and one that measures the vapor phase only. The separate sampling is assured by the forward and sideward orientation of the air inlets and will help in interpreting the data. Here, we present the laboratory performance of this new instrument.

References

E. Kerstel. 2004. "Isotope Ratio Infrared Spectrometry." In *Handbook of Stable Isotope Analytical Techniques*, edited by P. A. De Groot, 1:759–87. Elsevier.

J. Landsberg, D. Romanini, E. Kerstel. 2014. "Very High Finesse Optical-Feedback Cavity-Enhanced Absorption Spectrometer for Low Concentration Water Vapor Isotope Analyses." *Optics Letters* 39 (7): 1795–98.

J. Morville, D. Romanini, E. Kerstel. 2014. "Cavity Enhanced Absorption Spectroscopy with Optical Feedback." In *Cavity-Enhanced Spectroscopy and Sensing*, 179:163–209. Springer Series in Optical Sciences.

D. Romanini et al.: Patents FR2830617 and WO03031949 (2003)

D. Romanini, I. Ventrillard, G. Méjean, J. Morville, E. Kerstel. 2014. "Introduction to Cavity Enhanced Absorption Spectroscopy." In *Cavity-Enhanced Spectroscopy and Sensing*, 179:1–60. Springer Series in Optical Sciences.

Unraveling mountain belts through U-Pb and Lu-Hf dating of detrital zircon and ^{40}Ar/^{39}Ar white mica: the Eastern Alps as an example

Franz Neubauer (1), Ruihong Chang (1, 2), Yunpeng Dong (3), Johann Genser (1), Yongjiang Liu (4)

(1) Dept. of Environment and Biodiversity, Paris-Lodron University of Salzburg, Hellbrunnerstr. 34, A-5020 Salzburg, Austria

(2) Dept. of Earth Sciences, University of Hongkong. China

(3) State Key Laboratory of Continental Dynamics, Department of Geology, Northwest University, Northern Taibai Str. 229, Xi'an 710069, China

(4) Key Lab of Submarine Geoscience and Prospecting Techniques, College of Marine Geosciences, Ocean University of China, Qingdao 266100, China

Radiogenic isotopes of detrital minerals from various clastic rocks of mountain belts can be used to reveal tectonic and sedimentary processes, which are otherwise difficult to detect. Here, we discuss three isotopic systems on detrital zircon (U-Pb and Lu-Hf) and detrital white mica (^{40}Ar/^{39}Ar, a variant of the K-Ar system). These minerals are widely used because of the high chemical and mechanical stability and their common occurrence in many magmatic, metamorphic and sedimentary rocks. During a thermal overprint, zircon is also resistant against temperature (>650 °C in the U-Pb system and even higher in the Lu-Hf system) implying that it records high-temperature processes. White mica usually records cooling through c. 400-450 °C: Consequently, the Lu-Hf zircon system is used as tracer of initial magma separation from the (depleted) mantle, the U-Pb zircon system records various stages of orogenies, ^{40}Ar/^{39}Ar white mica cooling through the Ar retention temperature.

In order to assess the significance of U-Pb zircon and ^{40}Ar/^{39}Ar mica age dating techniques in provenance studies we applied these methods on recent river sands (Mur and Salzach rivers) of Eastern Alps, where the hinterland is well constrained in terms of its tectonothermal evolution. The Eastern Alps include two Alpine suture zones: (1) the Early Cretaceous suture (ca. 100–95 Ma) within the Austroalpine basement unit with abundant eclogites reflecting subduction of continental crust; (2) the Eocene to Oligocene Penninic suture reflecting the closure of the Piemont-Ligurian closure, Paleogene tectonism (50 – 30 Ma) and Paleogene overriding of the Penninic orogenic wedge by the already cool Austroalpine nappe stack with its Cretaceous tectonism.

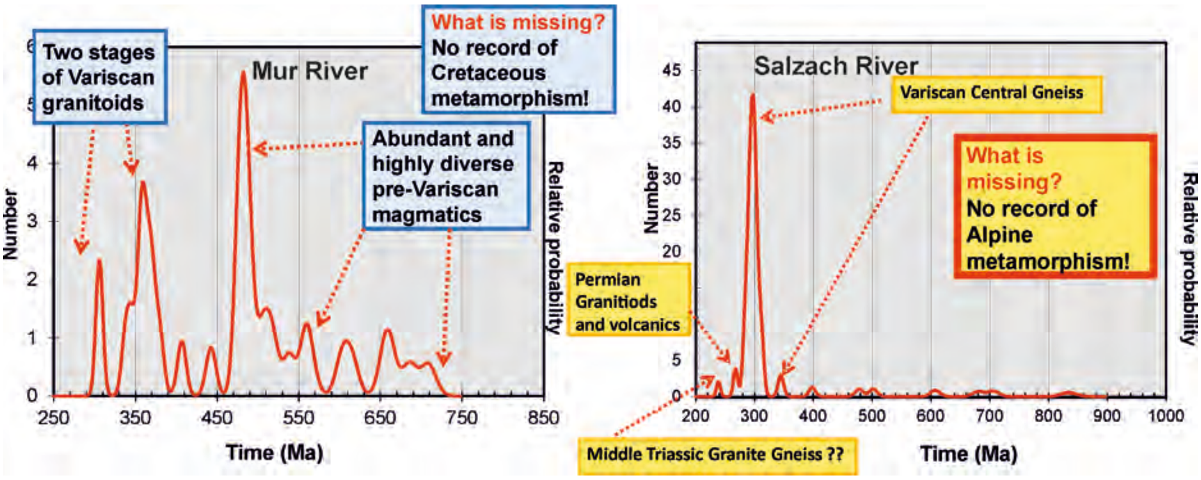

Figure 1. Comparison of detrital U-Pb zircon ages of two major rivers in Eastern Alps.

The principal results of our study are as follows (Figure 1): (1) The U-Pb zircon ages do not record any sign of Alpine tectonism and, therefore, no record of the last orogenic events and metamorphism can be found as no Alpine-aged granites are exposed in the hinterland of these two rivers, which cross the Alpine sutures. In short, when there is no granite in the hinterland, no significant amount of detrital zircon in clastic rocks can be found. Consequently U-Pb zircon studies can miss the record of collisional orogenies. (2) In contrast, ^{40}Ar/^{39}Ar white mica ages well record the last orogeny and metamorphism but show limitations in the record of the pre-orogenic history. Further limitations of the method are mainly due to the grain size selected: the age of metamorphism within low-grade metamorphic terrains is commonly not recorded. Both systems, U-Pb zircon and ^{40}Ar/^{39}Ar white mica, yield different information in provenance studies and should be used in combination.

The lag time is the time between the cooling within deep in the crust and deposition in a sediment (Figure 2). It records, therefore the time interval from cooling through the appropriate retention temperature, exhumation, erosion and transport until deposition. This interval is is dominated by slow exhumation, whereas other processes are fast. Figure 2 shows the successful application of ^{40}Ar/^{39}Ar white mica ages of various Mesozoic and Cenozoic formations in Eastern Alps, when plotted against the stratigraphic (depositional) age. The data show that Variscan and Cretaceous-aged, eo-Alpine metamorphic terrains dominate. However, otherwise nearly undetected processes can be revealed, too, e.g., rifting processes between 270 and 240 Ma, and 200 and 180 Ma (Figure 2).

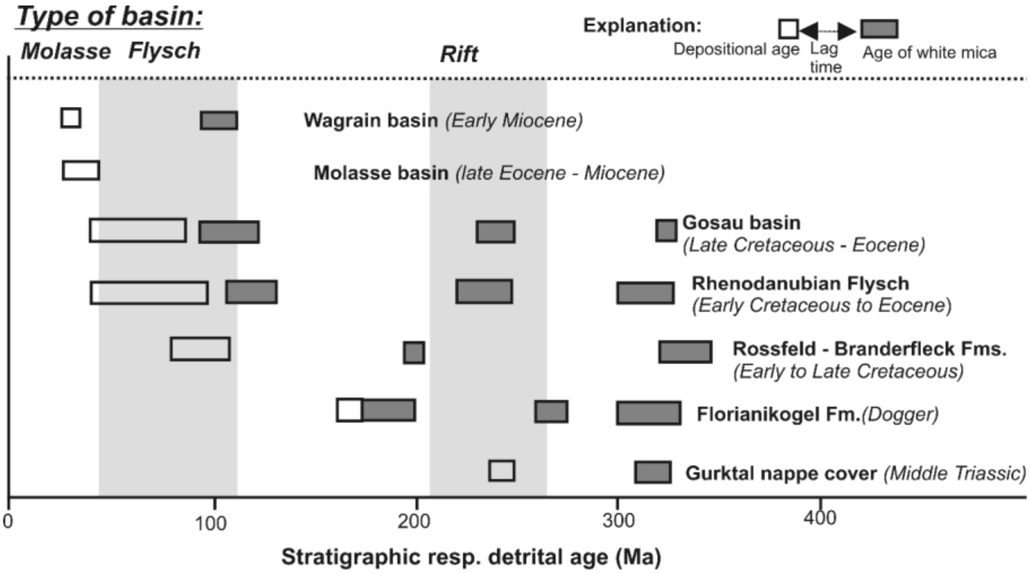

Figure 2. Simplified diagram showing the distribution of detrital white mica ages in Mesozoic and Cenozoic basins of Eastern Alps during the Alpine cycle (from [1]).

Extensive U-Pb dating and Lu-Hf isotopic tracing of zircons combined with U-Pb dating was applied to three key basement areas of the eastern Austroalpine basement, including the (i) Wechsel Gneiss and Waldbach Complexes, and Wechsel Phyllite Unit, (ii) Saualpe-Koralpe-Pohorje, and (iii) Schladming-Seckau areas [2]. We determine the Wechsel Gneiss Complex to be a continental magmatic arc formed during 500–560 Ma in the proximity to a continental block with a ‘memory’ of Late Archean to Early Proterozoic continental crust. The Wechsel Gneiss Complex has Hf model ages of 2.1 to 2.2 Ga and 2.5 to 2.8 Ga that indicate a close relationship to Neoarchean to Early Proterozoic cratons in northern Gondwana, with depleted mantle Hf model ages as old as 3.5 Ga. The Wechsel Phyllite Unit structurally overlying the Wechsel Gneiss Complex has partly different sources, including juvenile crust formed at ca. 530 Ma. In contrast, the Waldbach Complex constantly added new crustal material during the 490–470 Ma period and bears considerably more positive ε_{Hf}(t) values than the underlying Wechsel Gneiss Complex and gives relatively young, depleted mantle model ages of 700 to 500 Ma. The Waldbach Complex is, therefore, interpreted to be part of a magmatic arc that formed during closure of the Prototethys and was metamorphosed during Variscan orogenic events at ca. 350–330 Ma. The Schladming-Seckau and Wechsel Complexes represent a Cambro-Ordovician magmatic arc system formed by Prototethys subduction processes with the associated Late Neoproterozoic to Early Ordovician ophiolitic Speik complex having formed in its back-arc basin or as Prototethyan lithosphere [1, 3].

The Plankogel Complex and structurally overlying micaschist and amphibolite units represent accreted ocean, ocean island, and continent-derived materials, interpreted to be an accretionary complex formed during the Permo-Triassic closure of the Paleotethys. Many granites with Permian ages (e.g., porphyric granite called Grobgneiss and other granite gneisses and associated pegmatites) were likely formed in an extensional environment that culminated in the opening of the Middle-Late Triassic Meliata oceanic rift. These granites formed by partial remelting of crust with mainly Middle Proterozoic Hf model ages [2]. Taken all these data together, we find that the Austroalpine basement is heterogeneously composed and includes complexes of different ages, different tectonic evolutionary histories and different remolten sources representing different locations before final accretion [3]. The composite of pre-Alpine complexes in the Austroalpine mega-unit likely assembled not earlier than Late Permian or Early/Middle Triassic.

Comparison of data from Western Alps with the studied Austroalpine units show the much higher proportion of juvenile crust in the Austroalpine units east of the Tauern window, and the high rate of recycling in Western Alps (Figure 3) [2].

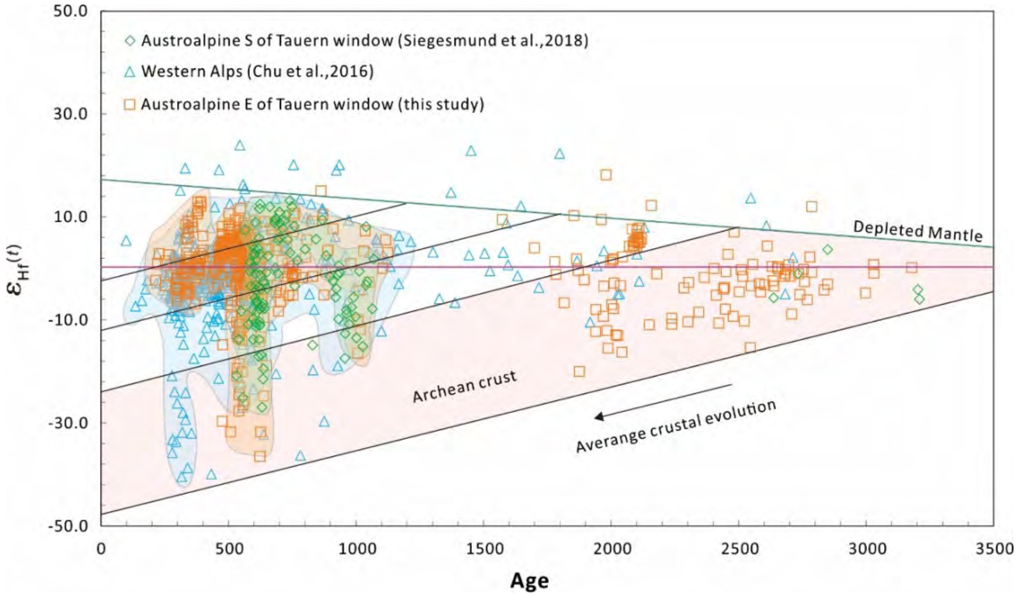

Figure 3. Plot of εHf(t) vs. U-Pb age for comparison of major Alpine basement units.

References

[1] Neubauer, F., Friedl, G., Genser, J., Handler, R. Mader, D., Schneider, D., Austrian Journal of Earth Sciences 2007 (100), p. 8–23.

[2] Chang, R.H., Neubauer, F., Liu, Y.-J., Yuan, S.-H., Genser, J., Huang, Q.W., Q.-B., Yu, S.-Y., Earth-Science Reviews 2021 (221), art. no. 103772.

[3] Neubauer, F., Liu, Y.-J., Dong, Y.P., Chang, R.-H., Genser, J., Yuan, S.-H., Earth-Science Reviews 2022 (226), art. no. 103923.

Hydrological Contribution of Fog to Atmospheric Deposition in the Czech Republic

Oyewole T.G. [1], Hunova I. [1,2], Jandova K. [1], Kukla J. [1], Tesar M. [3]
[1]*Charles University, Faculty of Science, Institute for Environmental Studies, Benatska 2, 128 01, Praha 2, Czech Republic*
[2] *Czech Hydrometeorological Institute, Na Sabatce 17, 143 06 Praha 4, Czech Republic*
[3] *Czech Academy of Science, Institute of Hydrodynamics, Pod Patankou 30/5, 160 00 Praha 6, Czech Republic*

Process of atmospheric deposition has both advantages and disadvantages for the environment. It is an important source of nutrients but could also transport pollutants from the atmosphere to ecosystems. It is easier to measure wet deposition which is in the form of falling precipitation (rain and snow), whereas it is much more difficult to measure occult deposition (fog and rime) and thus it is mostly unaccounted for. With growing interest in atmospheric deposition in the field of environmental science, stable isotopes of water (δ^{2}H and δ^{18}O) have been stipulated to be capable of revealing information about the physical processes that lead to formation and transport of hydrometeors.

The aim of this study is to: (i) compare the stable isotopes δ^{2}H and δ^{18}O of rain, throughfall and fog collected in the Czech Republic, and (ii) to use a simple mixing model to estimate the fog hydrological contribution to atmospheric deposition.

In this study, we employed the use of stable isotopes analysis in the samples of rain, throughfall and fog that were collected in three sites namely in the Šumava, Krkonoše and Jizerské hory Mts. in April 2019 – November 2020. To test if the fog, rain and throughfall samples differ, the nonparametric Wilcoxon and Kruskal-Wallis statistical tests were performed. Furthermore, we tried to calculate the contributions of fog and rain to throughfall using the simple linear mixing model equation.

The results from the statitistical tests for both the δ^{2}H and δ^{18}O data for fog vs rain, throughfall vs rain and fog vs throughfall showed that the significance level of 0.05 was only established for ð^{2}H fog vs throughfall which substantiated that the samples of fog and throughfall were relatively different. From the calculations done using the mixing method, the percentage of fog from throughfall was in the range of -0.25% and 2.72% for δ^{2}H and -0.13% and 7.17% for δ^{18}O.

In total, there were 36 samples with all 3 components (rain, throughfall and fog) in 11 sampling periods in which fog, rain and throughfall all have 12 samples each. Our results indicated that the δ^{2}H and δ^{18}O values for fog ranged between -15.6% and -64.3%, and -0.3% and -9.9, respectively; δ^{2}H and δ^{18}O values for rain ranged between -20.9% and -90.6 and -0.6% to 12.9 respectively; while the δ^{2}H and δ^{18}O values for throughfall ranged between -28.6% and -80.2% and -1.0% to -11.8%, respectively.

When compared to a previous study [1], there was much higher differences in the δ^{2}H and δ^{18}O values of fog, rain and throughfall. This differences can however be likened to the time of sample collection, weather conditions during sample collections of both projects as the sampling methods and sites remained the same. The percentage of fog from through fall from this study when compared to the previous study also showed a significant difference as more samples showed realistic percentages in this study compared to only a few samples showing realistic percentages in the previous results.

Acknowledgements

The samples of fog, rain and throughfall were collected from established sites located in selected mountains forested areas ((the Šumava, Krkonoše and Jizerské hory Mts.) in the Czech Republic within the ongoing TAČR project SS 02030031 ARAMIS granted to the Czech Hydrometeorological Institute.

References

[1] Hunova I, Hanuskova D, Jandova K, Tesar M, Kveton J, Kukla J, European Journal of Environmental Sciences 2020 (10), 89–97.

Climatic signal in oxygen and hydrogen stable isotope ratios of tree rings - case study for Suwałki region

Pawełczyk S., Pazdur A.
Institute of Physics – CSE, Silesian University of Technology, Konarskiego 22B, 44-100 Gliwice, Poland

Water is essential for the life of plants and the process of photosynthesis. Epstein et al. (1977) [1] were the first to notice the possibility of utilizing the studies on stable isotope ratios in precipitation [2] to look at the isotopes of oxygen and hydrogen, archived in annual rings. Numerous research studies have confirmed that the isotopic composition of annual rings ($\delta^{18}O$ and $\delta^{2}H$) can be considered to be a valuable source of information in the reconstructions of the isotopic composition of water, which was used by the plant in life processes, i.e. groundwater coming from precipitation. The isotopic composition of atmospheric precipitation is diversified spatially and temporally. This is related to the isotopic fractionation accompanying the processes of evaporation from the ocean and the condensation during the transport of water vapour. It can be said that the isotopic composition of the waters contained in the soil generally reflects the weighted average of the precipitation for the studied area [3]. In the case of the studies devoted to the annual rings, the isotopic characteristics of precipitation, expressed by $\delta^{18}O$ and $\delta^{2}H$, is modified during a number of complex processes, dependent on environmental conditions, leading to the formation of wood. It should be noted that the fractionation coefficients are different for oxygen and hydrogen, but the same fractionation model can be used for the studies of both isotopes [4]. There is no clear fractionation during the collection of groundwater through the root system. Significant fractionation can be observed in the chemical reactions occurring in the leaves. Therefore, $\delta^{18}O$ and $\delta^{2}H$ in plant tissues reflect: (1) the variability of the isotopic composition of the water source, (2) the enrichment of water in heavier isotopes in a leaf, caused by transpiration, and (3) biochemical fractionation during the synthesis of organic matter [5, 6]. Both water and carbon dioxide provide oxygen atoms for the carbohydrates metabolism conducted by plants. However, the oxygen derived from CO_2 is completely exchanged with water before carbohydrate synthesis [7].

Investigations of stable isotopic C, H, and O composition in □-cellulose extracted from tree rings of pines (*Pinus sylvestris* L.) growing in the ecologically clean Suwalki Region, North Eastern part of Poland, were undertaken. Presented isotope records cover the period of 1931-2003. Values of $\delta^{18}O$ and $\delta^{2}H$ measured in the tree ring α-cellulose were compared to meteorological data (temperature, insolation, relative humidity, and precipitation). Values of $\delta^{18}O$ and $\delta^{2}H$ in tree ring cellulose respond to current year temperature, insolation, relative humidity, and precipitation.

The strongest correlation was found between $\delta^{2}H$ and temperature for the period June-August (r=0.60). Relations between isotopic and meteorological data demonstrate that precipitation influences the stable isotopic oxygen and hydrogen ratios to a lower extend than the humidity. The intensity and duration of summer storm events can determine this effect.

The temporal stability of climate signals was analysed in this research by means of the moving correlation function for moving intervals with a 25-year window.

References

[1] Epstein S, Thomson P. Yapp CJ, Science (198), 1977 p. 1209-1215,

[2] Dansgaard SW, Tellus B (16), 1964 p. 436-468,

[3] Różanski K, Arguas-Arguas L, Gonfiantini R, 1993. Isotopic patterns in modern global precipitation. W: Climate Change in Continental Isotopic Records, Geophys. Monogr. Ser., vol. 78, edited by P. K. Swart et al., AGU, Washington, p.1 – 36,

[4] McCarroll D, Loader NJ, Quaternary Science Reviews (23), 2004 p.771-801,

[5] Ferrio JP, Resco V. Williams DG, Serrano L, Voltas J, Investigación Agraria: Sistemas y Recursos Forestales (14), 2005 p. 371-382.

[6] Roden JS, Lin G, Ehleringer JR, Geochimica et Cosmochimica Acta (642), 2000 p.21-35.

[7] DeNiro MJ, Epstein S, *Science* (204), 1979 p.51-53.

Mass spectrometric studies of the formation of negative ions from SO_2 and their application in the analysis of stable sulfur isotopes.

Andrzej Pelc, Karolina Marciszuk
Maria Curie-Skłodowska University, Institute of Physics, Divison of Biophysic, Mass Spectrometry Laboratory, Pl. M. Curie-Skłodowskiej 1, 20-031 Lublin, Poland

Sulfur dioxide (SO_2) is one of the most harmful gases polluting the atmosphere. This gas enters it mainly as a by-product of burning fossil fuels. It is estimated that the increase in coal consumption observed in recent years causes an increase in SO_2 emissions by about 5% per year. SO_2 is also generated in natural geothermal and biogenic processes, e.g. during volcanic eruptions, hence the knowledge of the origin of SO_2 (and basically sulfur) is of great importance in explaining geological, biological or environmental processes.

In distinguishing the sources of sulfur, it is extremely helpful to analyze the composition of stable sulfur isotopes in a sample. Sulfur has 4 stable isotopes, namely ^{32}S, ^{33}S, ^{34}S and ^{36}S. In the commonly used methods of isotope analysis, sulfur from the studied sample is converted to gaseous form - SO_2. The resulting SO_2 is then analyzed by positive ion mass spectrometry (MS).

In our MS research, we used the thermal surface ionisation method of forming negative ions from SO_2. Ions are generated by the contact of molecules with a hot metal surface. As a result of this process, the SO_2 molecule can dissociate into S^-, SO^-, and O^-. Interestingly, other ions with mass-to-charge ratios of 64, 96 and 128 were also observed. In the presentation, the results of the conducted research, their interpretation and reference to isotope studies will be presented.

References

[1] Karolina Marciszuk, Tomasz Pieńkos, Patryk Gontarz, Andrzej Pelc, „Negative Ion Formation by Thermal Surface Ionization of Sulfur Dioxide", ChemPhysChem 2020, 21, 1695 –1702

[2] K. Marciszuk, A. Pelc, "The mass-spectrometric studies of negative ion formation from SO_2 and its application to the sulfur stable isotope analysis" in Vacuum Technique and Technology, Editor: E. Czerwosz, Oficyna Wydawnicza Politechniki Wrocławskiej , Wrocław 2021, 97-105

Isotope effects accompanying δ^2H, δ^{18}O and δ^{17}O analyses of brines using cavity ring-down laser spectroscopy: insights from dedicated laboratory experiments

A. Pierchala, M. Dulinski, K. Rozanski, Z. Gorczyca, R. Czub, M. Marzec
AGH University of Krakow, Faculty of Physics and Applied Computer Science,
al. Mickiewicza 30, 30-059 Krakow, Poland

Deuterium and oxygen-18 isotope composition of water molecules in concentrated saline solutions (brines) has been employed as a powerful tool in deciphering the origin and evolution of formation fluids encountered in deep sedimentary basins and fluids associated with exploration and exploitation of oil and gas reserves. Moreover, ^{2}H and ^{18}O isotopes were widely used as tracers in quantifying water balances of lakes, including high-salinity systems, as well as deciphering the origin of water appearances in salt mines. Typically, ^{2}H/^{1}H and ^{18}O/^{16}O isotope ratios were measured in such studies using Isotope Ratio Mass Spectrometry (IRMS) technique combined with often troublesome and time-consuming sample preparation procedures and usage of appropriate correction factors. With the advent of laser spectroscopic methods of water isotope analyses there is a need to determine if, and to which extent, concentrated saline solutions can be analysed directly using this methodology.

We present here the results of dedicated laboratory experiments aimed at quantifying isotope effects associated with direct δ^2H, δ^{18}O and δ^{17}O analyses of single- and double-salt solutions prepared with water of known isotope composition, as a function of their molality. The isotope analyses were conducted with the aid of Picarro L2140-*i* CRDS spectrometer. Three single-salt solutions (NaCl, $CaCl_2$ and $MgSO_4$) and two double-salt (NaCl-$CaCl_2$ and NaCl-$MgSO_4$) mixtures were prepared and analysed, for molalities ranging from ca. 0.5 mol/kg H_2O up to saturation conditions. NaCl and $CaCl_2$ solutions revealed small negative offsets $\Delta\delta$ ($\Delta\delta = \delta_m - \delta_o$, where δ_m stand for the measured δ value of the analysed sample and δ_o signify the isotopic composition of deionised water used for preparation of the solutions), independent on the molality of the solution and comparable with the measurement uncertainties. In contrast, $MgSO_4$ and $MgCl_2$ solutions showed roughly one order of magnitude higher offsets, gradually increasing with growing molality of the solution. Isotope offsets for double-salt mixtures mirror the effects observed for single-salt solutions; the NaCl-$CaCl_2$ mixture revealed roughly constant offsets of similar magnitude to those observed for single NaCl and $CaCl_2$ solutions, whereas NaCl-$MgSO_4$ mixtures revealed gradually increasing offsets, reaching significantly higher values than those observed for single $MgSO_4$ solution.

The above-outlined isotope offsets are linked to the processes occurring during injection of the analysed salt solutions to the vaporizer unit of the CRDS spectrometer. Fast evaporation of the injected water sample leads to super-saturation and crystallization of salts occurring predominantly in the salt liner of the vaporizer. Precipitating salts retain certain amount of the analysed water, thus leading to the observed isotope effects.

Acknowledgements

The presented work was supported by the National Science Centre (research grant No. 2021/43/B/ST10/00599) and through the subsidy from the Ministry of Science and Higher Education (project no. 16.16.220.842 B02).

AMS spectrometry in the ^{14}C and Mass Spectrometry Laboratory in Gliwice, Poland

Natalia Piotrowska, Alicja Ustrzycka, Adam Michczyński, Fatima Pawełczyk
Silesian University of Technology, Institute Of Physics - CSE, Division of Geochronology and Environmental Isotopes, Konarskiego22B, 44-100 Gliwice, Poland

The Laboratory of ^{14}C and Mass Spectrometry operates in the Institute of Physics - Science and Didactic Centre of the Silesian University of Technology. The infrastructure of the Laboratory is used primarily by the staff of the Department of Geochronology and Environmental Isotopic Research. The ^{14}C and Mass Spectrometry Laboratory has been working with scientists in the natural sciences, archaeology and history for more than 50 years. It is a unique research laboratory where both radiocarbon dating by various techniques, light stable isotope compositional analyses of carbon, nitrogen, oxygen and hydrogen of a variety of materials, as well as dendrochronological analyses can be performed. In recent years, the ^{14}C and Mass Spectrometry Laboratory has performed approximately 400 radiocarbon analyses and a similar number of isotopic analyses annually, for the purposes of internal research, national and international research projects and commissioned scientific-research work.

The ^{14}C and Mass Spectrometry Laboratory has been developing a methodology for preparing samples for radiocarbon measurements by accelerator mass spectrometry (AMS) since 1999. The AMS technique has many advantages, of which, in contrast to radiometric techniques, the most significant are:

- low required sample mass of the order of 1 mg of carbon or less;
- short measurement time, in the order of minutes per sample;
- the high performance of the measuring instrument;
- the possibility of obtaining high-precision measurement results.

The consequence of the above features is the possibility of analysing thousands of samples per year with a single instrument and obtaining results with relatively small statistical uncertainties (0.3%). An additional effect of the use of lower sample masses is the reduced consumption of chemicals necessary for the preparation process, thus minimising the negative impact on the environment.

Measurements of ^{14}C concentrations in graphite targets prepared in the Laboratory were carried out in external laboratories equipped with an AMS spectrometer. Thanks to the implementation of the 'CEMIZ Isotopic Methods Centre' project, subsidised by European funds (ERDF), a modern AMS spectrometer of the MICADAS – MIni CArbon DAting System [1], manufactured by the Swiss company IonPlus, was installed in 2022. This enabled performing all required ^{14}C AMS analyses on site in Gliwice.

The size of the instrument is relatively small (3.2m x 2.6m) and, thanks to the use of permanent magnets and air cooling, typical power consumption does not exceed 2.5 kW. The components of the AMS MICADAS spectrometer and their basic parameters are:

- caesium multi-cathode (40 samples) ion source and ion beam forming electrodes;
- 90° magnet injection system, B=415 mT;
- tandem accelerator with 200 kV nominal voltage, vacuum insulated;
- 90° analysing magnet, B=968 mT;

- drift chamber with Faraday cups for measurement of ^{12}C, ^{13}C and ^{13}CH currents;
- 90° electrostatic analyser;
- ^{14}C detector - ionisation chamber filled with isobutane.

During operation from September 2022 April 2023, ^{14}C concentration analysis have been performed for approximately 500 graphites, including ca. 80 radiocarbon concentration standards (NIST Oxalic Acid II), 60 graphites produced from background material (coal, phthalic anhydride) and 45 graphites from IAEA reference materials. The overall performance of the MICADAS was deduced from results treated as a quality control samples, to check the repeatability and associated routine accuracy. The data reduction was carried out using the BATS software [2]. The results showed the routinely achievable age limit is 45-46 kaBP, based on coal, anthracite and phthalic anhydrite background materials. The typical Ox2 precision is 0.25-0.30%, which corresponds to determined age uncertainties of maximum 30 years for “young” samples and reaching 50 years for Younger-Dryas-aged samples.

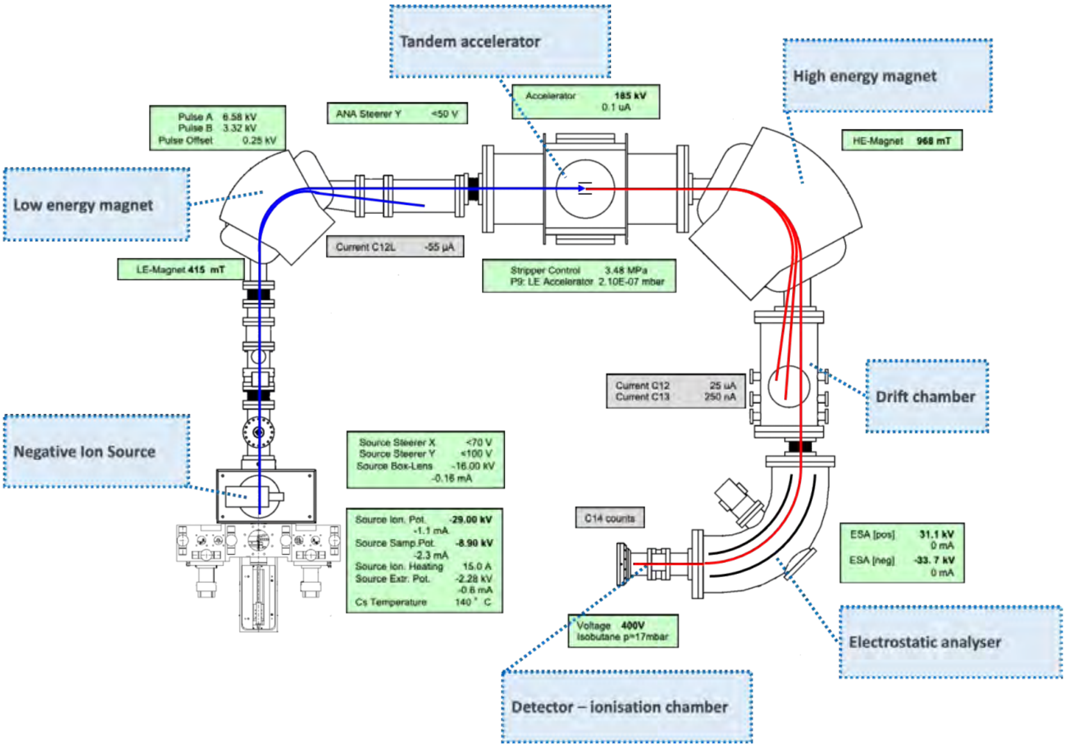

Figure 1. MICADAS device layout and typical values for radiocarbon measurements (Ionplus AG, Switzerland, version: 2017/02/10; modified).

References:

[1] Synal, H. A., Stocker, M., & Suter, M. (2007). MICADAS: A new compact radiocarbon AMS system. *Nuclear Instruments and Methods in Physics Research Section B: Beam Interactions with Materials and Atoms*, 259(1), 7–13.

[2] Wacker, L., Christl, M., Synal, H.-A. (2010). BATS: A new tool for AMS data reduction. *Nuclear Instruments and Methods in Physics Research Section B: Beam Interactions with Materials and Atoms*, 268(7–8), 976–979.

Carbon Isotope Ratios of Phenethylamine and Phenylacetylglutamine and their Applicability to Doping Controls

Piper T, Krombholz S, Thevis M
Institute of Biochemistry – Center for Preventive Doping Research, German Sport University Cologne, Am Sportpark Muengersdorf 6, 50933, Cologne, Germany

Phenethylamine (PEA) is a naturally occurring trace amine that acts as a modulator in the central nervous system. It is widely sold as a dietary supplement and advertised for its mood enhancing effects and should support weight loss. It is prohibited in sports and itemized as a stimulant on the Prohibited List issued by the World Anti-Doping Agency (WADA).

After oral administration of PEA, its urinary concentration is found only slightly elevated while metabolites of PEA show a significant increase.[1,2] Besides 2-(2-hydroxyphenyl)acetamide sulfate, especially phenylacetylglutamine (PAG) was found at significantly elevated urinary concentrations after the administration.[2] Due to large inter- and intra-individual variations in urinary concentrations of all metabolites, establishing a concentration or concentration ratio-based threshold remained complicated to unambiguously identify post-administration samples.[2]

In accordance with the approach employed in detecting testosterone misuse, the applicability of isotope ratio mass spectrometry to differentiate between endogenously elevated concentrations and PEA administrations was investigated. A method encompassing solid-phase extraction combined with acetylation and high-performance liquid chromatography (HPLC)-based clean-up was developed and validated for PEA. The more abundant metabolite PAG was purified by a direct injection approach on the HPLC and could be analysed without the need for derivatization. Both methods were validated considering applicable WADA regulations.

A reference population was investigated to establish population-based thresholds considering the carbon isotope ratios (CIR) found at natural abundance for PAG. The derived threshold was tested for its applicability by re-analysis of numerous post-administration samples encompassing single- and multi-dose trials.[2]

References

[1] Sigmund G, Dib J, Tretzel L, Piper T, Bosse C, Schänzer W, Thevis M, Drug Test Anal, 2015 (7) 1057-1062.

[2] Krombholz S, Thomas A, Piper T, Lagojda A, Kühne D, Thevis M, Biomedical Chromatography, 2021, e5274

Variability of gases concentration and carbon stable isotopic composition of methane and carbon dioxide in an exploited hard coal mine

Pleśniak Ł.[1], Woźniak W. [1], Wierzbicki M. [2], Jędrysek M.-O[1].
[1] *University of Wroclaw, Uniwersytecki sq. 1, 50-137 Wroclaw, Poland*
[2] *Central Measurement and Research Laboratory, Rybnicka str. 6, 44-335 Jastrzębie Zdroj, Poland*

The combination of traditional research methods of gases occurring in hard coal deposits with the study of the carbon isotopic composition of methane and carbon dioxide, makes it possible to accurately determine the genesis of gases occurring in coal deposits. Thanks to this, it is possible to identify primary and secondary biological processes in the deposit (1,2) that affect the chemical and isotopic composition of gases at the site of mining.

The described analyses were carried out on gas samples that were separated from fragmented coal fragments procured during the drilling of C-1 and C-1a slipways in a selected HCM (Hard Coal Mine), which is located in Poland. The age of the coals is defined as Lower Pennsylvania (3). Carbon stable isotope ratios were performed using a Thermo Scientific Delta V Advantage mass spectrometer coupled with a Trace GC 1300 gas chromatograph, on the QPlot column. The results of the research were analysed in terms of the possible genesis of gas formation, as well as potential primary and secondary biogenic processes occurring in the deposit.

The obtained results of the carbon stable isotopic composition in gases in hard coal seams indicate the occurrence of $\delta^{13}C$ in methane ranged from-41,5 ‰ to -24,3 ‰ and $\delta^{13}C$ in carbon dioxide ranged from -5,4 ‰ to +15,9 ‰. In comparison with other works dealing with this subject, important in the context of the genesis of gas, are the results obtained in the zone from 300 meters to 550 meters of length of the C-1 slipway and from 200 to 410 meters of length of C-1a slipway. In this zones, obtained results of geochemical parameters of the gas indicate the presence of thermogenic methane and do not show signs of microbiological activity that could have a significant impact on the change in the geochemical parameters of the analyzed gases, because the range of $\delta^{13}C$ is in the range from -30 ‰ to -40 ‰ for the methane and from +5 ‰ to +15 ‰ for the carbon dioxide. Carbon stable isotopic composition of carbon dioxide indicates the potential generation of gas from underlying carbonates due to metamorphic processes (4), which allows us to assume that this gas escaped from the place of genesis to the studied formation through a system of cracks and faults of a tectonic nature.

The results for HCM indicate quite unique values of the carbon stable isotope composition in methane and in the carbon dioxide (5,6,7).The enrichment of the the isotope ^{13}C in methane is visible in zone from 50 to 150 meters in slipway C-1 and in zone around 100 meters in slipway C-1a. This could be explained by a potential bacterial oxidation of methane and carbon dioxide production which is depleted of the isotope ^{13}C. Apart from that the concentration of methane in these zones is lower than in others which may confirm the thesis about possible bacterial oxidation of methane (8).

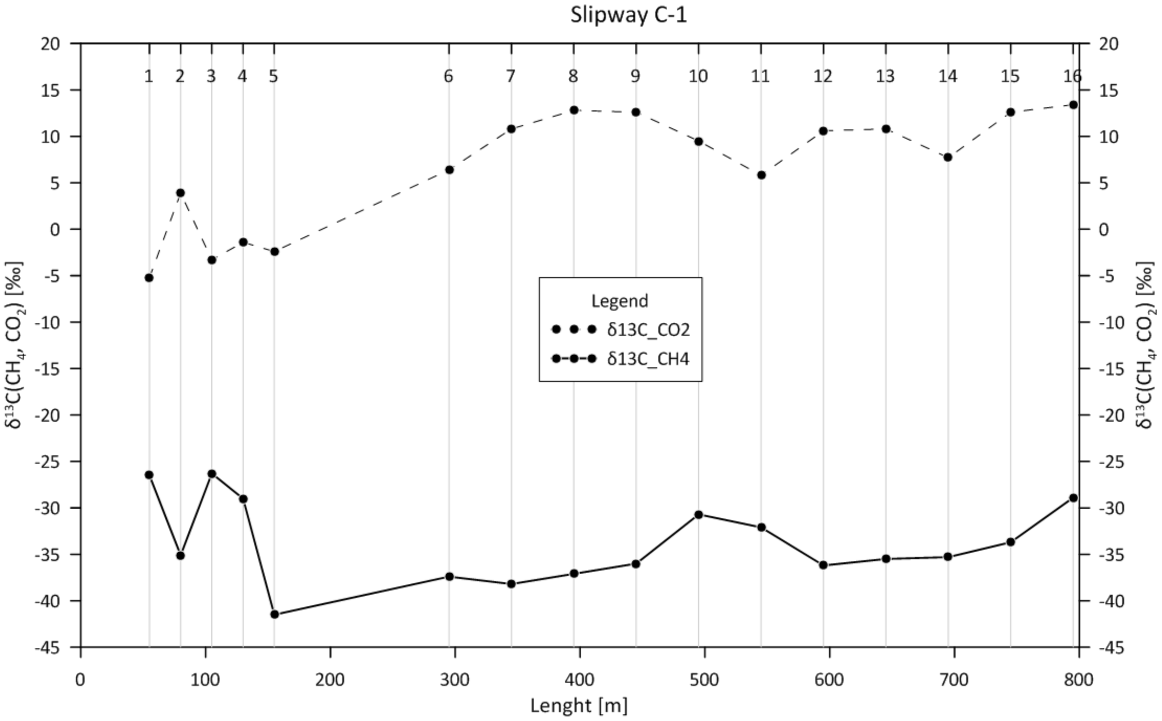

Figure 1. Variability of δ^{13}C in methane and carbon dioxide in a slipway C-1.

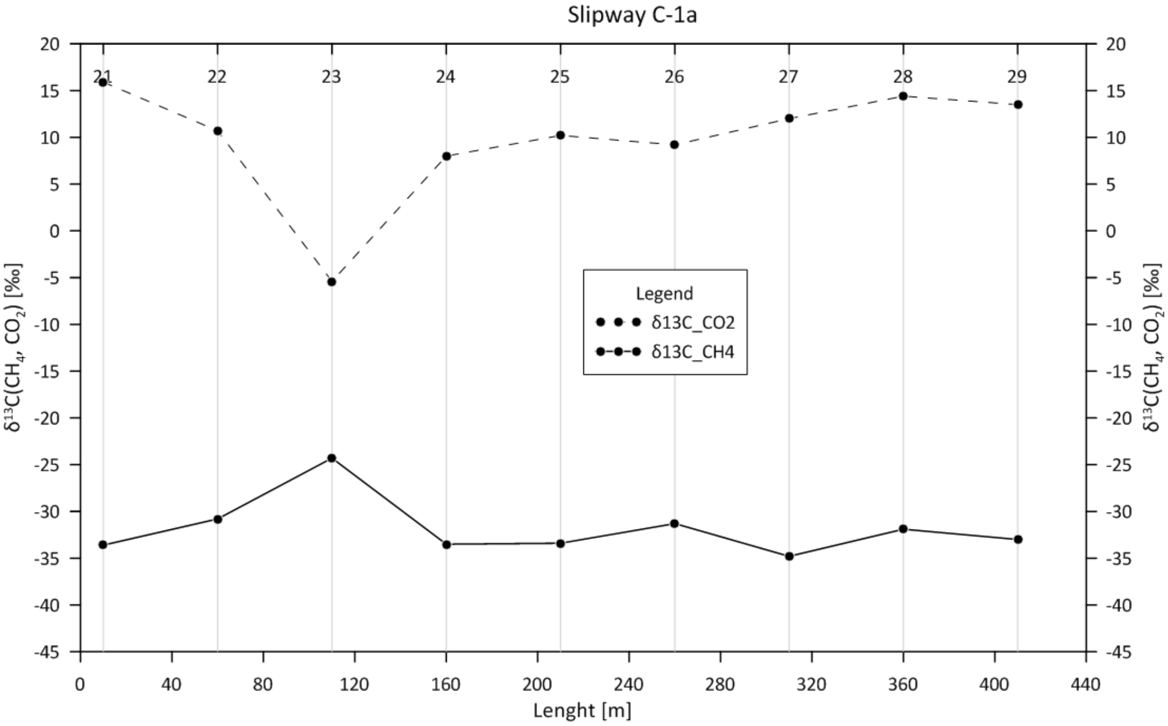

Figure 2. Variability of δ^{13}C in methane and carbon dioxide in a slipway C-1a.

References

[1] Milkov V., „New Approaches to Distinguish Shale-sourced and Coal-sourced Gases In Petroleum Systems." Org. Geochem., v. 158, 2021, https://doi.org/10.1016/j.orggeochem.2021.104271

[2] Milkov V., Etiope G., „Revised Genetic Diagrams for Natural Gases Based On a Global Dataset of >20,000 Samples." Org. Geochem, v. 125 ,. pp. 109-120, 2018, https://doi.org/10.1016/j.orggeochem.2018.09.002.

[3] Jureczka J., Szewczyk A., Ślusarczyk-Krawiec E. , Ogrodowczyk W., „Atlas geologiczno-złożowy polskiej i czeskiej części Górnośląskiego Zagłębia Węglowego w skali 1:200 000”, 2005, Polish Geological Institute.

[4] Ciężkowski W., Duliński W., Józefko I., Kiełczawa B., Liber-Madziarz E., Witczak S., Zuber A., Żak S., „Występowanie, dokumentowanie i eksploatacja endogenicznego dwutlenku węgla w Polsce”, 2002, WTN Print, Warsaw.

[5] Kotarba M. J., „Composition and origin of coalbed gases in the Upper Silesian and Lublin basins, Poland”, Org. Geochem., Volume 32, Issue 1, 2001, Pages 163-180, https://doi.org/10.1016/S0146-6380(00)00134-0.

[6] Kotarba M. J., Pluta I. , „Origin of natural waters and gases within the Upper Carboniferous coal-bearing and autochthonous Miocene strata in South-Western part of the Upper Silesian Coal Basin, Poland”, Appl. Geochem., Volume 24, Issue 5, 2009, Pages 876-889, https://doi.org/10.1016/j.apgeochem.2009.01.013.

[7] Kotarba M. J., Sumino H., Nagao K., „Origin of hydrocarbon and noble gases, carbon dioxide and molecular nitrogen in Devonian, Pennsylvanian and Miocene strata of the Polish Lublin and Ukrainian Lviv basins, southern part of the Upper Silesian Coal Basin and western part of the Carpathian Foredeep (Poland)”, Appl. Geochem., Volume 108, 2019, https://doi.org/10.1016/j.apgeochem.2019.104371.

[8] Whiticar M. J., „Carbon and hydrogen isotope systematics of bacterial formation and oxidation of methane”, Chem. Geo., Volume 161, Issues 1–3, 1999, Pages 291-314, https://doi.org/10.1016/S0009-2541(99)00092-3.

Laser Ablation IRMS analyses of δ^{13}C in solid and liquid food

Pușcaș C.M.[1], Stremțan C.C.[2], Armstrong G.[3], and Green D.[2]
1 Terra Analitic SRL, Str. Tudor Vladimirescu nr. 32, 510095 Alba Iulia, Romania
2 Teledyne Photon Machines, 384 Gallatin Park Drive, Bozeman, MT 59715, USA
3 Sercon Limited, Unit 3B Crewe Trade Park, Gateway, Crewe, Cheshire CW1 6JT, UK

The modern consumer no longer focuses solely on food safety and affordability, instead becoming increasingly aware of food origin and source traceability, to the point where spending habits are often shifted based on provenance. A reliable and cost-effective solution for tracing ingredients is offered by either elemental or stable isotope geochemistry. The methods are well defined and applied by food industry and regulators alike. For discrete elemental analysis, laser ablation (LA) is often the standard sample introduction technique used for the instrumental setup. It offers speed, high sample throughput with minimal sample preparation and is also economical when considering consumables and operating costs. For stable isotope analyses, the elemental analyzer (EA) has been the standard sample introduction method for solid samples. A few pioneer labs have adopted the laser as sample introduction peripheral for IRMS analyses and having thoroughly evaluated the method, we believe that LA IRMS should become the go-to method for stable isotope ratio measurements.

We present two sets of examples; one is a series of sugars/sweeteners made from a variety of plants (sugar cane, sugar beet, corn, birch, coco palm, etc.), the second a set of vegetable oils extracted from various plans as well (corn, sunflower, palm, rice, grape seed, etc.) analyzed via LA IRMS. The analytical setup is composed of a Teledyne Photon Machines LSX 213 G2+ 213 nm wavelength laser ablation system connected to a Sercon HS2022 IRMS via a CryoPrep sample preparation module. A specially designed LA IRMS sample chamber was used (isoScell Δ100, from Terra Analitic). For the sugar samples, split samples were also analyzed via traditional EA IRMS (Sercon), for inter-instrument comparison. Cellulose (IAEA CH6) was used as reference in both instruments.

Our data shows that LA IRMS can reliably replace EA IRMS for accurate and precise determination of δ^{13}C in most solid, organic matrices, while offering the significant advantage of drastically reduced sample preparation and reduced overall analytical costs. Replicate analysis when sample amount is limited is not often possible by EA but given the minuscule amount of sample removed through ablation, this is a viable option with LA (if the sample is homogenous or homogenized).

An additional advantage of LA vs. EA IRMS? A single sugar crystal (beet) is enough for more than ten ablations and the δ^{13}C standard deviation in our tests was 0.03‰. One other clear advantage? We found that liquid samples are just as straightforward to analyze!

Laser ablation IRMS – the minimally destructive alternative for in-situ δ^{13}C analyses of solid or liquid matrices

Pușcaș C.M.[1], Stremțan C.C.[2], Armstrong G.[3], Sahlstedt, E.[4], and Green D.[2]
1 Terra Analitic SRL, Str. Tudor Vladimirescu nr. 32, 510095 Alba Iulia, Romania
2 Teledyne Photon Machines, 384 Gallatin Park Drive, Bozeman, MT 59715, USA
3 Sercon Limited, Unit 3B Crewe Trade Park, Gateway, Crewe, Cheshire CW1 6JT, UK
4 Natural Resources Institute Finland, Latokartanonkaari 9 00790, Helsinki, Finland

For decades elemental analyzers (EA) have been the go-to sample introduction instrument for IRMS analyses of solid materials. Sample preparation is often labor intensive and time consuming. Sample recovery is impossible in case of instrument malfunction, i.e., no repeat analysis when sample amount is restricted. It might be time for the obvious alternative to EA to become mainstream. The one that offers minimal to no sample preparation, allows for minimally invasive and repeat measurements even on minute sample amounts, even in situ sequential sampling. LA IRMS (laser ablation hyphened with an isotope ratio mass spectrometer) is a thrilling alternative to EA IRMS and opens a world of possibilities!

We evaluated LA IRMS on a variety of organic materials such as pollen, wood [1], bone collagen [2], whole bone, tooth, chitin (hair -human and animal, fingernail, and sheep horn), plant derived sugars and sweeteners, vegetable oils, bee honey and wax [3], airborne particulate matter, whole blood, and many more. For some of these we also present EA data, to show method equivalency.

Depending on the matrix, we carried out these tests using two instrumental set-ups. The front end was either an LSX 213 G2+ 213 nm wavelength laser ablation system or a Fusions CO2 laser (both Teledyne Photon Machines, Bozeman MT, USA). The back end in all testing was an HS2022 IRMS via a CryoFlex sample preparation module (both Sercon, Crewe, UK). An isoScell Δ100 (Terra Analitic, Alba Iulia, Romania) sample chamber, specifically designed for LA IRMS, was utilized for all analyses. The EA IRMS used for inter-instrument comparison is also Sercon. Optimally tuned, this setup allows for blank levels as low as 6E-10 (ca. 2% of sample-peak size).

Establishing the optimal laser parameters is a two-step process; the first one is fine tuning the laser energy to ensure the sample is ablated efficiently. The next step requires finding the optimal spot size and ablation time necessary for producing sufficient aerosol to be converted into CO2 in the combustion furnace. For all the matrices we tested with our current setup, this process translated into two or three measurements, meaning 15 – 30 minutes for optimizing the matrix-dependent laser parameters.

Samples for which spatial resolution is crucial (e.g., wood, hair, fingernail, tooth) can be ablated sequentially at intervals of down to 20 μm (matrix and laser-type dependent). As each ablation removes a minute amount of sample, replicate analysis will not be an issue for homogenous matrices.

We also show that with LA matrix-matching the reference material to the unknown sample might be unnecessary, an important aspect both financially and for ease of use.

References

[1] https://sercon-instruments.com/wp-content/uploads/LAIRMS-Tree-Rings.pdf
[2] https://sercon-instruments.com/wp-content/uploads/App-Note-040-Bone-Collagen-LAIRMS.pdf
[3] https://sercon-instruments.com/wp-content/uploads/Application-note-41-Pollen-Bees-Wax-and-Honey-Measurements.pdf

Oxygen-17 in isotope hydrology: is it worth to measure it?

Rozanski, K.
AGH University of Krakow, Faculty of Physics and Applied Computer Science, al. Mickiewicza 30, 30-059 Krakow, Poland

Recent advances in laser spectroscopy resulted in construction of commercial laser instruments capable of simultaneous analyses of ^{2}H, ^{18}O and ^{17}O contents in water, with measurement uncertainties comparable (δ^{18}O, δ^{17}O), or surpassing (δ^{2}H) those routinely achieved by off-line and on-line sample preparation methods, combined with the isotope-ratio mass spectrometry techniques. This prompted renewed interest in the heavy isotopologue of water ($^{1}H_2{}^{17}O$) as an additional tracer in hydrology. Isotope hydrology, which is now more than sixty years old, relied so far on two heavy water isotopologues: $^{1}H^{2}H^{16}O$ and $^{1}H_2{}^{18}O$.

Deuterium and oxygen-18 turned out to be powerful tools in addressing numerous problems in hydrology, such as identifying the origin of different groundwater types including groundwater recharged under different climatic regimes, quantifying groundwater mixing across various temporal and spatial scales, interactions between surface water and groundwater systems, and quantifying water budgets of lakes and surface water reservoirs, just to name few.

The presentation will start with touching upon some technical aspects of ^{2}H, ^{18}O and ^{17}O assay in water using laser technology and will continue with reviewing rapidly accumulating knowledge and data on the behavior of $^{1}H_2{}^{17}O$ isotopologue in the hydrological cycle. First, the five-year record of triple-isotope composition of daily precipitation at two contrasting sites in southern Poland will be presented. Then, three specific examples of using triple-isotope composition of water in solving practical problems in hydrology will be discussed: (i) mixing of different groundwater types, (ii) quantifying water budgets of lakes, and (iii) isotope monitoring of water appearances in salt mines for safety purposes. The presentation will conclude with an overview of triple-isotope composition of different groundwater systems in Poland.

A comprehensive study of the climatic changes in the South Asian region during the Latest Pleistocene till the present, based on planktonic foraminiferal δ^{18}O and δ^{13}C with special reference to the monsoonal rainfall

Sarkar Ashish
Jheel Road, Sweetland, Kolkata, India

The southwest monsoon system covers the areas inhabited by nearly half of the global population. As far as the crop cultivation to sustain the lives are concerned, in the absence or paucity of the irrigation system, the southwest monsoon system appears to be the lifeline of this huge global popolation residing in the Southeast Asian, South Asian, Southwest Asian, and the Central African regions. In order to understand the monsoonal variability, and the forecasting of it in these regions, a time series through changing paleoclimate needs to be studied.

The present paper attempts to have a look at some of the published and unpublished data by the author to understand the climate system induced southwest summer monsoon operating in the Indian subcontinent during the Latest Pleistocene till the Present based on the planktonic foraminiferal δ^{18}O and δ^{13}C. Depending on the fluctuations in planktonic foraminiferal population dynamics, and the stabale oxygen and carbon isotopic signatures derived from the select species of planktonic foraminiferal calcite, viz., *Globorotalia menardii*, *Globigerinoides sacculifer*, *Globigirinoides ruber*, Guha and Sarkar (1990), Sarkar and Guha (1993, 1997a, 1997b), Sarkar *et al* (1996), Sarkar *et al* (2000), Agnihotri et al (2003), Sarkar (2009, 2011), Sarkar and Ogle (2015), deciphered the climatic changes during the Late Pleistocene to the near present.

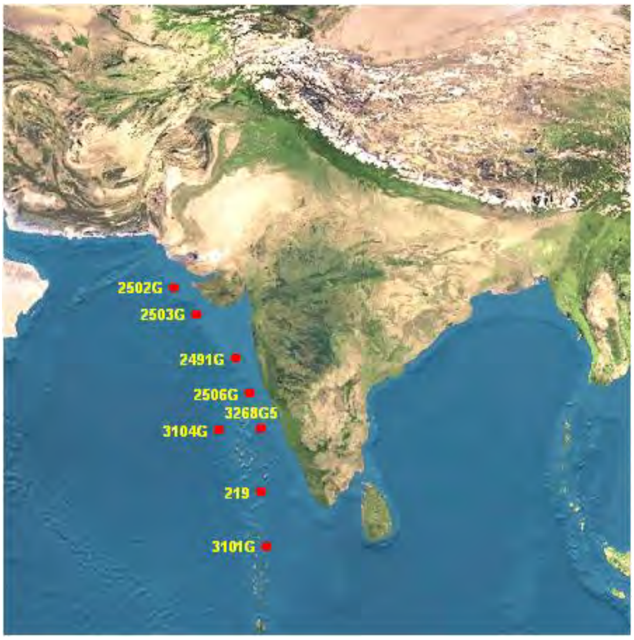

Figure 1. Location of the sediment cores studied. The cores are located at different water depths, with diverse proximity to the land, and have varied water mass conditions.

Various climatic events eg., Last Interglacial Maxima, Last Glacial Maxima, 8.2 ka global cooling event etc., were depicted by the climatic events recorded in these studies from the Arabian Sea, which corroborate earlier observations and also validate the interpretations. At the end of the last glaciation and with the initiation of the Holocene, as the sea attained its present level, the 'modern monsoon' was established. Most of the workers on monsoon treat this term (monsoon) synonymous to the rainfall, which is not true. Indian monsoon has two distinctly different monsoon systems with annual reversals, one, the southwest (summer) monsoon blowing towards the Himalayas, and the northeast (winter) monsoon blowing seaward. While summer monsoon carries water vapour, causes rainfall in general, the winter monsoon being mostly vapourless, does not produce rainfall, except in parts of Tamilnadu. As the summer precipitation depends on many factors, summer monsoon merely carrying water vapour does not cause a definite amount of rainfall, and hence, the monsoon and the rainfall should not be used interchangeably.

The studies (*op cit*) from all the sea sediment cores retrieved from few hundreds to more than a couple of thousands meters water depth with varied geographical locations and with diverse water mass conditions, depict that changes in foraminiferal $\delta^{18}O$ can not be generalised to interpret the contemporary environmental conditions. The sediment core in close proximity to the land off the Mangalore, India depict, the Indian summer rainfall had been increasing steadily till about 2000 years BP since the initiation of Holocene. This is supported by more and more depletion in $\delta^{18}O$ of the planktonic foraminiferal calcite, with a few enrichments in its course, most conspicuous being around 4000 – 4500 years BP. The enrichment may be correlated with the downfall of the Great Harappan Civilisation. On the other hand, the changes in the intensity of monsoonal rainfall can not be judged from the sediment cores located quite a distance from the land mass, as the rainfall induced surface run-off gets mixed with the sea water, thereby loosing the 'signature' before reaching the distant locations. In order to determine the high resolution monsoonal rainfall from the planktonic foraminifearl $\delta^{18}O$, a sediment core needs to be raised from a suitable location with ample freshwater influx, rapid sediment accumulation rate, and having abundant planktonic foraminiferal population at that location. One such core from the Eastern Arabian Sea helped to conclude a decreasing trend of the summer monsoon since the last 200 years in the Indian subcontinent, with some extreme fluctuations.

References

[1] Guha A K and Sarkar Ashish; Jour. Pal. Soc. India; 1990 (35), 169-175.

[2] Sarkar Ashish and Guha A K; Journal Geol. Soc. India, 1993 (41), 397-416.

[3] Sarkar Ashish, Guha A K and Chakraborty S; Proc. Indian Acad. Sci. (Earth Planet. Sci.), 1996 (105), 119-129.

[4] Sarkar Ashish and Guha A K; Journal Geol. Soc. India, 1997a (49), 169-178.

[5] Sarkar Ashish and Guha A K; Indian Journal of Marine Sciences, 1997b (26), 84-87.

[6] Sarkar Ashish, Ramesh R, Somayajulu B L K, Agnihotri R, Jull A J T and Burr G S; Earth and Planetary Science Letters, 2000 (173), 209-218.

[7] Agnihotri R, Sarin M M., Somayajulu, B L K, Jull A J T, Burr G S, and Sarkar Ashish; Palaeogeogr. Palaeoclimatol. Palaeoecol., 2003 (197), 43-60. with a corrigendum in Palaeogeogr. Palaeoclimatol. Palaeoecol. 2004 (202), 353.

[8] Sarkar Ashish; International Conference on Geoscience for Global Development, Dhaka, Bangladesh, 2009, 132.
[9] Sarkar Ashish; European Geosciences Union (EGU) General Assembly, Vienna, Austria, 2011.
[10] Sarkar A, Ogle N; Procedia Earth and Planetary Science, 2015 (13), 138-141.

Validity of the precipitation minus evaporation (P – E) and/or evaporation minus precipitation (E – P) parameter in climate studies based on $\delta^{18}O$, with special reference to a case history from the Eastern Arabian Sea

Sarkar Sudipta
Jheel Road, Sweetland, Kolkata, India

The present paper aims to argue whether the parameter, precipitation minus evaporation (P – E) and/or evaporation minus precipitation (E – P) used in the climate studies are trustworthy? As human civilisation is getting increasingly affected by adverse climate changes, more and more researchers are getting engaged in search of the parameters controlling the environment in general, and past climate in particular. In search of the parameters influencing the climate, workers began using another parameter, precipitation minus evaporation and/or evaporation minus precipitation. Understanding of the past climate is the key to forecasting. The success of the forecasting of the climate change depends on the reliability of the time series, which in turn, depends on the robustness of the data. Data cannot be robust with flawed observations. Moreover, robustness of the observation depends on the complete environment around the location of observation. The present conceptual paper is based on the observations made on a work (Sarkar *et al*., 2000) while reviewing it after years.

Sarkar *et al.* (op cit.) in a very significant work, based on the $\delta^{18}O$ of planktonic foraminiferal calcite and surface sea water as well, deciphered the change in summer monsoonal rainfall in the Indian subcontinent during the Holocene. In their quest to decode the summer monsoonal fluctuations, they used a parameter evaporation minus precipitation (E – P). In order to study the regional pattern of climate in general, and specifically the summer monsoonal rainfall, they considered two sediment core locations with nearly 10º latitudinal separation in the Eastern Arabian Sea. While the northern core (2502G; 21º51.9' N, 67º59.3' E) comes from a water depth of 280m, with a sediment accumulation rate 100cm/ka; the southern core (3268G5; 12º31.8' N, 74º10' E) is situated at a water depth of 600m, with a sediment accumulation rate 8cm/ka. This means, while the total core length of 120cm at northern location covers a total time duration of 1336±39 calendar years, the total core length of 77.5cm at the southern location covers a total time duration of ~10 thousand calendar years (Somayajulu *et al*., 1999), which depicts, the southern core represents a total duration of ~7.5 times more than that of the total duration covered by the northern core.

On enquiry (personal communication with the author), about the strategy of choosing the locations, if any, it was found that while coastal areas adjacent to the northern location receives annual rainfall of less than 300mm, the same of southern location receives close to 3000mm (Parthasarathy, 1984). Nearly all the precipitation happens during the summer monsoon from June to September, when the planktonic foraminiferal population grows in abundance in a year thereby arresting ambient $\delta^{18}O$ in their tests. Sarkar *et al* (*op cit*) opined that while variation of $\delta^{18}O$ of planktonic foraminiferal calcite at the northern location is because of the scanty rainfall and evaportion, the variation in $\delta^{18}O$ of planktonic foraminiferal calcite at the southern location is because of the combined effects of evaportion and precipitation. Hence, they subtraced the average of downcore $\delta^{18}O$ at the northern location from the $\delta^{18}O$ of each level at the southern location to note only the precipitation (E – P). In my opinion, this exercise is a redundant one, as subtracting/addiding a constant value from a data set, though shifts the curve to left or to the right, yet it doesn't change the nature of the curve anyway. Moreover, downcore averaging of $\delta^{18}O$ also does not appear logical.

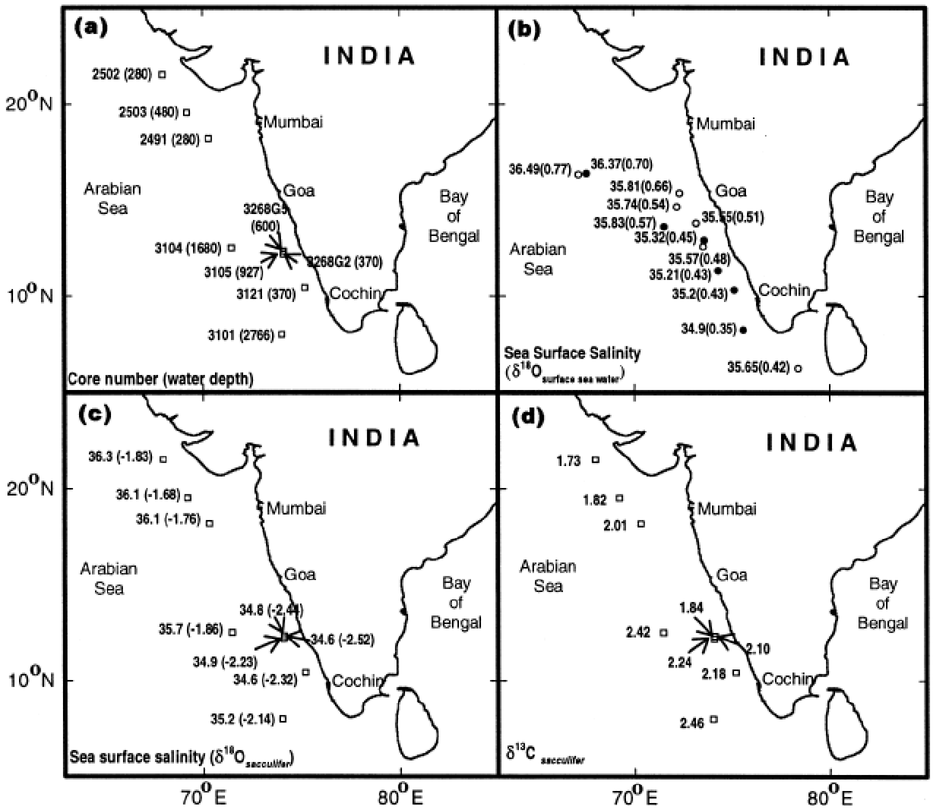

Figure 1: Maps illustrating (a) core locations with water depths in m; (b) sea surface salinity (‰) and the corresponding $\delta^{18}O$ of sea surface water (‰ relative to the V-SMOW) during the May-June (filled circle) and during the July (open circle); (c) sea surface salinity (‰) and the corresponding $\delta^{18}O_{Gs.\ sacculifer}$ (‰ relative to the V-PDB) from the core-top sediments in parentheses and (d) $\delta^{13}C_{Gs.\ sacculifer}$ (‰ relative to the V-PDB) of from the core-top sediments (After Sarkar *et al.*, 2000).

While working on the variability of salinity, evaporation, precipitation, freshwater budget (E – P), Sea Surface Salinity (SSS) and estimating the evaporation in various locations like, Karimata Strait, Java Sea and Banda Sea in Indonesian maritime continent (IMC) seas, Ratnawati *et al.* (2018) showed, variation of SSS dominated the half of the E – P variations, while the rest was explained by other factors; and interestingly, SSS variations were explained by the significant E – P, which was significantly influenced by the precipitation. They found, SSS in the IMC waters are significantly influenced by the zonal and meridional wind. Elbaum *et al.* (2022) during their work on the regional precipitation minus evaporation (P – E) in the Coupled Model Inter-comparison Project (CMIP) with 48 models, opined, while thermodynamic changes drive the multi-model mean hydrologic changes, dynamic changes cause uncertainty.

Regional wind pattern strongly influences the sea surface currents resulting in the changes in the composition of the sea water. Tchernia (1980) demonstrated the changes in the sea surface current patterns in the Arabian sea during the southwest and northeast monsoons, which shows remarkable interseasonal changes. India's instrumental record of rainfall is available from 1871. Since 1877 till 1974, 60% of the 25 observations show a positive correlation between the El-Nino years and the years of failure of the summer monsoonal rainfall in India (Sikka, 1980). This observation depicts influence of the regional ocean/sea circulation pattern (dynamic influence) on the monsoonal rainfall. Moreover, River Indus, mostly glacial melt water (δ^{18}O around –15‰) fed drains to the north of the northern location, which must have depleted the δ^{18}O of the water at this location. In a nutshell, subtracting the average downcore $\delta^{18}O_{northern\ location}$ from the $\delta^{18}O_{southern\ location}$ to get the E – P parameter ie., Δ^{18}O does not appear very much convincing.

Acknowledgement

Author thanks Dr. Ashish Sarkar for all the discussions, and for taking the criticisms very sportingly.

References

[1] Sarkar Ashish, Ramesh R, Somayajulu B L K, Agnihotri R, Jull A J T and Burr G S; Earth and Planetary Science Letters, 2000 (173), 209-218.

[2] Somayajulu B L K, Bhushan R, Sarkar Ashish, Burr G S, Jull A J T; The Science of the Total Environment, 1999 (237 & 238), 429-439.

[3] Parthasarathy B, Proc. Indian Acad. Sci. (Earth Planet. Sci.), 1984 (93) pp. 371-385.

[4] Ratnawati H I, Aldrian E, and Soepardjo A H; AIP Conference Proceedings (2023), 2018, https://doi.org/10.1063/1.5064249.

[5] Elbaum E, Garfinkel C I, Adam O, Morin E, Rostkier-Edelstein D, and Dayan U; Geophysical Research Letters, 2022 (Manuscript submitted, Nov.).

[6] Tchernia P, Descriptive Regional Oceanography, Oxford: Pergamon, 1980, 253 pp.

[7] Sikka D R; Proc. Indian Acad. Sci. (Earth Planet. Sci.), 1980 (89) pp. 179-195.

Multiproxy, systematic and advanced stable isotopes investigations of Scots pine growing in Silesian forests (Poland) – review of the last ten years research

Barbara Sensuła
The Silesian University of Technology, Institute of Physics – Center for Science and Education, Konarskiego 22B, Gliwice 44-100, Poland

The purpose of this paper is to describe findings from systematic, advanced and multiproxy isotopic studies of environmental changes in Silesian forests, conducted since 2011 at the Institute of Physics-CND of The Silesian University of Technology, allow for a comprehensive analysis of the impact of climate change and different human activity on the environmen [1-15].

The scientific backround to the isotopic studies was dendrochronological research conducted in 15 sampling sites [12,14], conducted in the first phase of BIOPOL project, which determined the representative area for farther isotopic and elemental analysis[1-11,13]. The resarch, conducted across Silesia and Opolskie vojewodships (100km^2), under inter alia BIOPOL and ISOPED projects, cover the period of time since the first decades of the 20th centure up to now [1-14].

Spectrometric studies assess the impact of climate change and industrial air pollution on changes in the width of pines annual tree-rings (wood, cellulose and glucose) and needles, and theirs isotopic composition.

Determination of carbon and oxygen isotopes in α-cellulose was carried out to assess differences in photosynthetic efficiency and stomatal conductivity from 1975 to 2012. Carbon and oxygen stable isotope compositions were measured at the Mass Spectrometry Laboratory of the Institute of Physics at the Silesian University of Technology, Poland, using continuous-flow isotope ratio mass spectrometry (ISOPRIME, GV Instruments, Manchester, UK). The detailed analysis of the carbon and oxygen isotopes fractionation has been discussed detailed [1-15].

Trees have been shown to be sensitive bio-indicators and archives of the changes (natural and anthropogenic) of the ecosystem in which trees have been growing. The main factors influencing the formation of wood in the pines were thermal conditions in the winter season and pluvial conditions in the previous autumn, and also in spring and summer in the year of tree ring formation. The impact of thermal and pluvial conditions in the year of tree ring formation has also been reflected in the isotopic composition of tree rings and water use efficiency[1-3]. Relationship between trees (isotopic composition of tree rings and needles) and fluctuations in air temperature, amount of precipitation, insolation, humidity, and level of CO_2 and other pollutants in the atmosphere and trees isotopic composition was evident [1-11]. However, temporal and spatial analysis of the results shown that trees reaction to the environmental changes across research area has been unhomogenic and local factors (such as type of the point-emitters source, distance to the road, and some local incidence in the past, etc.) might have the impact on trees growth and physiology. The studies have been also explored, for the first time, the interaction between pine growing provinces (isotopic composition and iWUE fluctuation) in Silesia and Opolskie and Standardized Precipitation-Evapotranspiration Index (SPEI) [1]. Based on the analyses of the isotopic composition, also the CO_2 emission component was estimated in selected areas.

The research was part of the ISOPĘD, ISOPĘD2 and BIOPOL project entitled: 'Trees as bioindicators of industrial air pollution during the implementation of the pro-environmental policy in the Silesia region', funded by the National Science Center and allocated on the basis of decision number DEC-2011/03/D/ST10/05251. This work was supported by the following contracts and grants: the Initiative of Excellence – Research University program implemented at the Silesian University of Technology, grant no.: 14/020/SDU-10-05-03 and 14/020/SDU-10-05-02.

References:

[1] Sensuła B, Wilczyński S, Plants, 2022(11:24), 1-20.
[2] Sensuła B, Wilczyński S, Water Air and Soil Pollution,2022 (233), no 143.
[3] Sensuła B. Contemporary problems of power engineering and environmental protection, 2021, 29-34.
[4] Sensuła B, Fagel N, Michczyński A, Radiocarbon, 2021(62:2), 713-726.
[5] Sensuła B, Michczyński A, Piotrowska N, Wilczyński S., Radiocarbon, 2018(60:4), 1041-1053.
[6] Sensuła B, Wilczyński S, Geochronometria, 2018 (45:1), 130-145.
[7] Sensuła B, Wilczyński S, Geochronometria, 2017(44:1), 240-255.
[8] Sensuła B, Wilczyński S, Monin L, Allan M, Pazdur A, Fagel N, Geochronometria, 2017(44:1), 226-239.
[9] Sensuła B, Water Air and Soil Pollution, 2016 (227) art. no. 106.
[10] Sensuła B, Wilczyński S, Piotrowska N, Sylwan, 2016(9), 730-740.
[11] Sensuła B. Water Air and Soil Pollution, 2016(227:2), art. no. 68.
[12] Sensuła B, Opała M, Wilczyński S, Pawełczyk S, Dendrochronologia, 2015(36), 1-12.
[13] Sensuła B, Water Air and Soil Pollution, 2015 (226:11), art. No. 362.
[14] Sensuła B, Wilczyński S, Opała M, Water Air and Soil Pollution, 2015 (226), art. no. 220.
[15] Sensuła B, Pazdur A, Geochronometria, 2013 (40:2), 145-152.

Similarities and contrasts in $\delta^{15}N$ in pine growing in Silesia

Barbara Sensuła
The Silesian University of Technology, Institute of Physics – Center for Science and Education, Konarskiego 22B, Gliwice 44-100, Poland

Nitrogen is the most abundant element in the atmosphere. The processes of internal cycling of nitrogen in trees have been reviewed and discussed by scientists [1]. The scientists confirm that the analysis of the nitrogen isotopes ($\delta^{15}N$) in tree rings is potentially useful for evaluating the temporal development of the nitrogen (N) deposition to forests and for studying the long-term effects of N accumulation in ecosystems.

The first results of nitrogen isotopes composition of annual Scots pine growing in industrial forests in Silesia (Poland) and in comparative site (100 km far away from industrial area) in the last century will be presented.

The significant decrease in $\delta^{15}N$ has been observed in sampling sites in industrial area in compare with comparative site in late 1980s till mid 1990s. Similar effect have been observed also in other forrest in Silesia (results not printed yet). In this moment it is difficult to explain this phenomenon, but the analisis of other isotopes (carbon and oxigen) confirm that there is a different physiological response (dynamics changes in the stomata conductances and photosynthesis rate) to environmental changes by plants in this period of times.

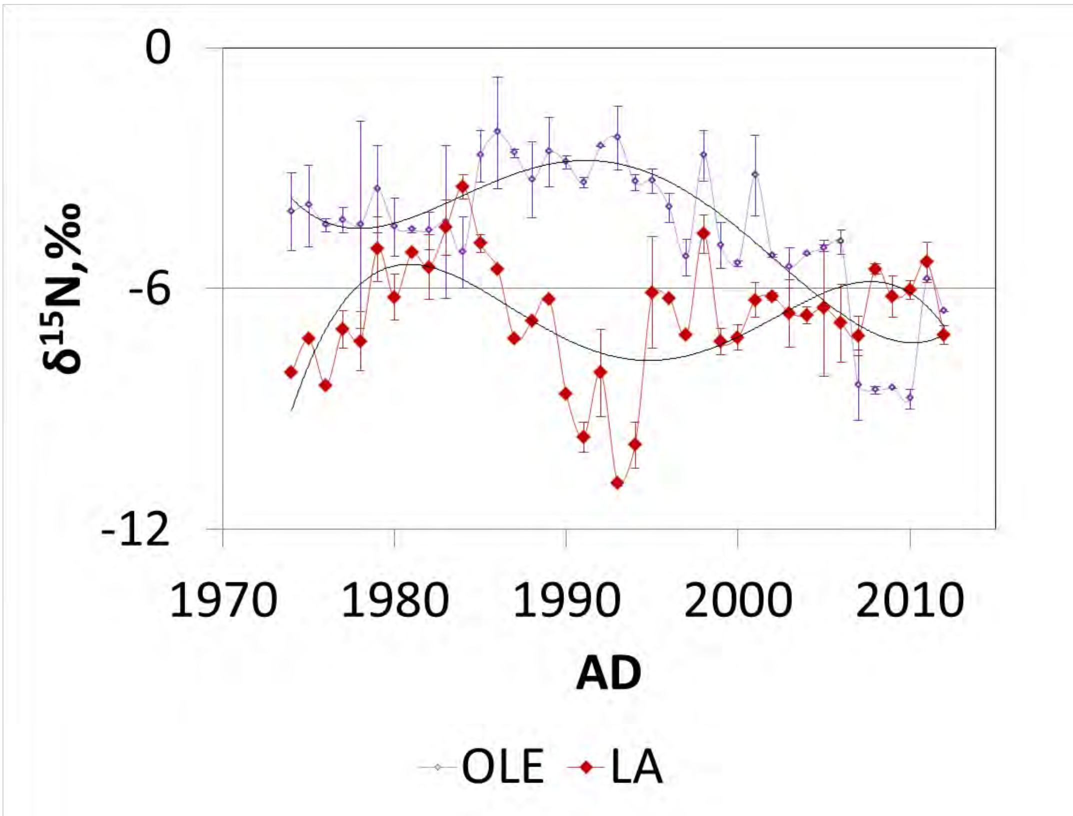

Figure 1. Nitrogen isotopis composition of annual tree rings of pines growing nearby heat and power plant (LA) and in comparative site (OLE) (results not printed yet). Black lines indicate smoothed average value.

Detailed analysis of $\delta^{15}N$ in tree-rings was done taken into account stomata conductivity and photosyntehsis rate conducted based on oxygen and carbon isotopes analysis of plants tissues. Some similarities and contrasts in ^{15}N has been observed in tree rings and in the leaves in selected area.

The purpose of this presentation is to describe and discuss findings from systematic, advanced isotopic studies of environmental changes in Silesian forests, conducted since 2011 at the Institute of Physics-CND of The Silesian University of Technology.

The scientific backround to the this study was dendrochronological and spectrometric research conducted in 15 sampling sites, conducted in the first phase of BIOPOL project, which determined the representative area for farther isotopic and elemental analysis. The resarch, conducted across Silesia and Opolskie vojewodships (100km^2), under inter alia BIOPOL and ISOPED projects, cover the period of time since the first decades of the 20th centure up to now.

The research was part of the ISOPĘD, ISOPĘD2 and BIOPOL project entitled: ‘Trees as bioindicators of industrial air pollution during the implementation of the pro-environmental policy in the Silesia region’, funded by the National Science Center and allocated on the basis of decision number DEC-2011/03/D/ST10/05251. This work was supported by the following contracts and grants: the Initiative of Excellence – Research University program implemented at the Silesian University of Technology, grant no.: 14/020/SDU-10-05-03 and 14/020/SDU-10-05-02.

References

[1] Rolf T. W. Siegwolf, J. Renée Brooks, John Roden, Matthias Saurer, 2022.Stable isotopes in Tree rings. https://doi.org/10.1007/978-3-030-92698-4

The impact of pluvial and thermal conditions on the pines growing in the forests of Silesia and Opole voivodeships

Barbara Sensuła[1], Slawomir Wilczyński[2]

1 The Silesian University of Technology, Institute of Physics – Center for Science and Education, Konarskiego 22B, Gliwice 44-100, Poland

2 The University of Agriculture in Krakow. Department of Forest Ecosystem Protection, Al. 29 Listopada 46, 31-425 Kraków, Poland

Dendrochronological methods together with mass spectrometry techniques have been used in the advanced research on pine growing in the industrial forests in Silesia (Poland) to analyse the response of the trees to stress connected with pluvial and thermal conditions and increase of CO_2 emission in the last century.

Dendrochronological analyzes cover a period of time from 1900–2012. The relationship between precipitation, temperature, and BAI was analyzed for the period of time between 1951 and 2012, while the relationship between precipitation, temperature, and drought index (SPEI), $\delta^{13}C$, and iWUE was analyzed for the period of time between 1975 and 2012 [1-5].

Scots pine trees at all sites systematically increased the basal area increment (BAI) and the intrinsic water use efficiency (iWUE) and decreased $\delta^{13}C$ in the last century[1]. Industrial pollution caused a small reduction in the wood growth of pines and an increase in the heterogeneity of annual growth responses of trees.

Detailed analysis-based bootstrap and moving correlation between climatic indices (temperature, precipitation, and Standardized Precipitation-Evapotranspiration Index) and pine parameters confirmed that this species is very sensitive to weather conditions, but its sensitivity can be masked by the impact of the pollution[1,4].

SPEI analysis confirmed that there could be a different scenario of the dynamic tree response to water stress. Three different scenarios of trees' reaction link to the reduction of stomata conductance or changes in photosynthesis rate as the response to climate changes in the last 40 years have been proposed [1].

The research was part of the ISOPĘD, ISOPĘD2 and BIOPOL project entitled: 'Trees as bioindicators of industrial air pollution during the implementation of the pro-environmental policy in the Silesia region', funded by the National Science Center and allocated on the basis of decision number DEC-2011/03/D/ST10/05251. This work was supported by the following contracts and grants: the Initiative of Excellence – Research University program implemented at the Silesian University of Technology, grant no.: 14/020/SDU-10-05-03 and 14/020/SDU-10-05-02.

References

[1] Sensuła B, Wilczyński S, Plants, 2022(11:24), 1-20.

[2] Sensuła B, Wilczyński S, Water Air and Soil Pollution, 2022 (233), no 143.

[3] Sensuła B, Ochrona środowiska i gospodarka odpadami – współczesne rozwiązania i perspektywy na przyszłość, 2022, 73-85.

[4] Sensuła B, Wilczyński S, Geochronometria, 2017(44:1), 240-255.

[5] Sensuła B, Water Air and Soil Pollution, 2016 (227: 2), art. no. 68.

Strontium isotopes in Finnish strawberries and agricultural soils

Siira J.[1,2], Beier C.[2], Jokinen S.[1], Karhu S.[3], Rantanen M.[4], Welling A.[1] and Lahtinen M.[1,5]
[1]*Finnish Food Authority, Mustialankatu 3, 00790 Helsinki, Finland*
[2]*University of Helsinki, Department of Geosciences and Geography, P.O. Box 64, 00014 Helsinki, Finland*
[3]*Natural Resources Institute of Finland (Luke), Horticulture Technologies PharmaCity, Itäinen Pitkäkatu 4 A, 20250 Turku, Finland*
[4]*Natural Resources Institute of Finland (Luke), Horticulture Technologies, Survontie 9, 40500 Jyväskylä, Finland*
[5]*University of Helsinki, Finnish Museum of Natural History, The Laboratory of Chronology, P.O. Box 64, 00014 Helsinki, Finland*

Discovering new and innovative approaches to detect food frauds is crucial to maintain food security, support the local production and develop novel tools for the food authorities in the European Union. Food frauds are a growing world-wide problem including both the forging of origin and consistency of food. *The development of strontium isotope method in identification of food forgeries* (SIKRUT) is a research project of the Finnish Food Authority funded by the Jane and Aatos Erkko Foundation. The project aims to develop a reliable method and baseline based on strontium isotopes (^{87}Sr/^{86}Sr) for identifying the frauds of food origin.

Strontium isotope ratios (^{87}Sr/^{86}Sr) provide a well-known tool for tracing the origin of different food materials based on the local ^{87}Sr/^{86}Sr variation in the bedrock and soil [1]. Previously the method has not been widely applied in Finland due to the lack of local baseline. Finland is geologically very heterogeneous but well mapped and studied area, which makes it an interesting target to study ^{87}Sr/^{86}Sr variation in agricultural environments. The method has been widely applied to different environmental and food matrices ranging from wine [2] to soils and tree leaves [3].

This study presents the ^{87}Sr/^{86}Sr ratios and elemental concentrations from 120 Finnish strawberry samples and 47 soil samples from strawberry fields. The study covers a large part of the cultivated agricultural areas of Finland and considers the effects of bedrock, soil, later glacial sedimentary formations, pH, liming, and irrigation on the variation of the ^{87}Sr/^{86}Sr ratios in agricultural environments. For the soil samples we use total alkali fusion extraction method [4]. Elemental concentrations are analysed from different matrices using a sector-field inductively coupled plasma mass spectrometer (ICP-SFMS) with methane addition [5], and ^{87}Sr/^{86}Sr ratios with a multi-collector inductively coupled plasma mass spectrometer (MC-ICP-MS) [6].

The first results of this study show that both rock and soil type are connected to the variation of the ^{87}Sr/^{86}Sr ratios of the strawberries. In addition, a considerable spatial correlation with the ^{87}Sr/^{86}Sr ratios of the strawberries and their geographical origin can be observed. Strawberries collected from western and eastern Finland show lower ^{87}Sr/^{86}Sr ratios than strawberries collected from southern Finland.

A comparison between the ^{87}Sr/^{86}Sr ratios of the strawberries, soils from the strawberry fields and the bedrock shows considerable differences between different proxies. Generally, the $^{87}Sr/^{86}Sr$ ratios of the strawberries are significantly lower than in the soils and the bedrock, and they do not show a clear linear correlation. Moreover, we found clear indications that irrigation practice (watering vs. no watering) and source (groundwater vs. surface water) affect the $^{87}Sr/^{86}Sr$ ratios of the strawberries and the soils which might explain the differences in the isotope ratios of different proxies from the same geospatial locations.

Here, we present the first preliminary $^{87}Sr/^{86}Sr$ baselines of Finland for agricultural products covering the majority of local agricultural production areas. In addition, the previously published $^{87}Sr/^{86}Sr$ data of Finnish agricultural soils [7] is complemented. This data will be used to create an isoscape, a map of bioavailable strontium, covering the majority of agricultural regions of Finland. The results may be used as baselines in different applications, like identifying the potential source of food, plant-based materials, and human and animal individuals. To conclude, the results of this research can be used to develop a method based on the $^{87}Sr/^{86}Sr$ to identify frauds of food origin in Finland, and potentially distinguish Finnish food products of those of foreign origin.

References

[1] Åberg G, Water Air Soil Pollut., 1995 (79), 309–322.
[2] Rapa M, Ferrante M, Rodushkin I, Paulukat C, Conti ME, Food Chem., 2023 (404) 134771.
[3] Pallavicini N et al., J Spectrosc, 2018 7408767.
[4] Ödman F et al., Appl. Geochem., 2006 (21), 2112–2134.
[5] Rodushkin I et al., J. Anal. At. Spectrom., 2005 (20), 1250–1255.
[6] Rodushkin I et al., J. Anal. At. Spectrom., 2016 (31), 220–233.
[7] Hoogewerff J et al., Sci. Total Environ., 2019 (672), 1033–1044.

Isotopic investigation of stratigraphic divisions in Triassic dolomites

Sulejewski M. and Pawlyta J.
OLD RED ul. Kozielska 12, 40-076, Katowice, Poland and AGH University of Science and Technology in Kraków, al. Mickiewicza 30, 30-059, Kraków, Poland

We investigated 100 meters from an 830-meter-long G8-bis core. The rocky material was acquired from borehole G8-bis located in southern Poland (in the vicinity of Jaworzno town). The coordinates of the borehole are 50°9'2.24"N, 19°19'27.52"E. We have sampled the whole Triassic interval of the G8-bis borehole (about 120 m of Triassic deposits) taking 89 samples (mostly Mg-limestone and dolomite). The studied section covered the Lower and Middle Triassic. The investigations focused on the carbon and oxygen isotopic composition of dolomite and magnesium calcite. In general, we found a good correlation between lithostratigraphic boundaries; cyclostratigraphic boundaries and carbon isotopic variability. To further confirm this, we used cluster analysis.

Organic matter origin and transformation in the freshwater sediments of dam reservoirs - insights from C and N stable isotope ratio

Adriana Trojanowska-Olichwer, Marta Jakubiak, Mariusz-Orion Jędrysek
Institute of Geological Sciences, University of Wrocław, Maks Born Square 9, 50-205 Wrocław, Poland

The sources of organic matter in sediments and its biogeochemical transformations may be identified using stable C and N isotope ratios (δ^{13}C and δ^{15}N) of organic matter (OM).

The research was conducted on the three eutrophic dam reservoirs located in Poland: Turawa, Sulejowski and Siemianówka. Organic content in the sediments was ranging from 0,45 to 24,16 %(average: 6,78%) in Turawa, 6,04 to 21,06 % (average: 6,04%) in Sulejowski and 0,95 fo 17,26 % (average: 7,67%) in Siemianówka.

The stable isotope ratio of carbon δ^{13}C(OM) and nitrogen δ^{15}N(OM) in sedimentary organic matter in Turawa were spatially diversified and was ranging from -29,66 ‰ to -25,88 ‰ and from 0,25 ‰ to 3,44 ‰, respectively. δ^{13}C(OM) either δ^{15}N(OM) did not show any significant correlation. However, it can be assumed that bacterial nitrogen turnover was important, as indicated by the correlation between total bacteria number and NO$_3^-$ concentration in the pore water (r=-0,74, p=0,008) as well as between NO$_3^-$ and NO$_2^-$ concentrations (r=0,67, p=0,023).

The δ^{13}C(OM) either δ^{15}N(OM) in Siemianówka reservoir varied between: -30,93‰ and -22,93‰ as well as -0,34‰ and 2,93‰, respectively. Statistically significant correlations between б^{13}C(OM) and total bacteria number (r=-0,70, p=0,003), as well as redox potential (r=0,78, p=0,000), have been recorded. Total bacteria number was also related to NH4+ concentration in pore water (r=0,79, p=0,000) and also NH$_4^+$ to redox potential (r=0,52, p=0,039). This indicates the importance of microbial processes and redox conditions in organic matter decomposition and nitrogen turnover in sediments.

The δ^{13}C(OM) either δ^{15}N(OM) in the Sulejowski reservoir were fluctuating between: -32,33‰ and -25,61 ‰ as well as -0,52 ‰ and 2,14 ‰, respectively.

Significant correlation between δ^{15}N(OM) and organic matter content (r=0,99, p=0,002) as well as δ^{13}C (r=0,55, p<0,005) were noted. The important role of organic matter decomposition in the nitrogen turnover is indicated by the correlation between δ^{15}N(OM) and NH$_4^+$ (r=0,99, p<0,05), OM and NH$_4^+$ (r=0,99, p=0,000), total bacteria number and NH$_4^+$ (-0,59, p<0,05), total bacteria number and NO$_2^-$ (r=0,49, p<0,05). Simultaneously, the relationship between NH$_4^+$ and NO$_3^-$ (r=0,49, p<0,05) as well as NO$_2^-$ (r=-0,75, p<0,05) was proved.

The swift in the б^{13}C(OM) in the organic matter of sediments due to the delivery of fresh cyanobacterial biomass was observed in the Sulejowski dam reservoir. Values of б^{13}C(OM) in May achieved an average of -20,60 ‰ (SD: 4,85), while in August, just after sedimentation of cyanobacterial scum, depleted to -27,33 ‰ (SD: 1,10).

New isotope approaches to reconstruct the diet and palaeoecology of fossil vertebrates

Thomas Tütken
Institut für Geowissenschaften, Univeristät Mainz, 55128 Mainz, Germany

Hard tissues such as bones and teeth are often the only fossil remains from vertebrates and their morphology, histology and chemistry are analysed to reconstruct the palaeobiology and feeding ecology. However, classical diet proxies such as tooth shape may yield ambiguous results or collagen-bound C and N isotopes can be biased by fossilisation processes. To overcome these challenges new deep-time diet proxies were recently developed that are independent of tooth shape and species but also resistant to diagenetic alteration enabling deep-time dietary reconstructions.

Non-traditional stable isotope systems such as enamel-bound N isotopes ($\delta^{15}N_{enamel}$)[1-3], Zn isotopes ($\delta^{66}Zn$)[4-7] and Ca isotopes ($\delta^{44/42}Ca$)[8-10] in enamel bioapatite represent a new deep-time diet toolbox that enables us to reconstruct the diet and trophic ecology of ancient and extinct vertebrates. This is possible because systematic isotope fractionations of around +2 to 4 ‰ ($\delta^{15}N_{enamel}$)[1], -0.6 ‰ ($\delta^{44/42}Ca$)[10] and -0.4 to -0.6 ‰ ($\delta^{66}Zn$)[4,5] occur with each trophic level along the food chain, which are related mainly to the type of diet (i.e., amount of protein, bone and meat consumption, respectively).

Tooth enamel is a taphonomically robust, highly mineralised (up to 96 wt%) phosphatic hard tissue quite resistant against diagenetic and isotopic alteration[5,8,9,11,12]. Incrementally growing enamel thus records time series of isotope compositions reflecting the isotopic properties of food and water ingested over months to years. This enables us to reconstruct the diet and trophic interaction of fossil vertebrates in ancient food webs and to infer ontogenetic or evolutionary diet shifts from animal- to plant-feeding. To validate these dietary proxies, controlled feeding experiments[1] but also analyses of modern wild animals[2,4,9] with well-known diets are key to establish a reference database for diet assignment in extinct species[13]. For this purpose, small mammals, birds and reptiles were fed with natural and custom-made diets containing meat, plants or insects and the isotope compositions of their soft and hard tissues were analysed.

Furthermore, these dietary isotope proxies ($\delta^{15}N_{enamel}$, $\delta^{44/42}Ca$, $\delta^{66}Zn$) have a long-term preservation potential in enamel, which was assessed experimentally[11,12] and empirically[5,6,8,9]. Furthermore, these dietary proxies can be analysed in combination on the same tooth to reconstruct the diet of ancient vertebrates in a more refined manner and their trophic level in fossil food webs. Case studies applying these different isotope systems to dinosaurs, megatooth sharks, Neanderthals and sympatric mammals with implications for their feeding habits will be presented. Both $\delta^{15}N_{enamel}$ and $\delta^{66}Zn$ data identify the extinct megatooth sharks *Otodus megalodon* as marine top predator[3,6] while Zn isotopes suggest a potential food competition with the Great white shark in the Pliocene, which may have contributed to the demise of the former[3]. Low $\delta^{66}Zn$ of a Neanderthal from Spain further corroborates a meat-rich Neanderthal diet[7]. Finally, $\delta^{44/42}Ca$ data for the extinct flightless

Paleogene ground bird *Gastornis*, traditionally viewed as a giant terror bird, demonstrate that it was in fact a herbivore similar to a *Moa*, and not a bone-crushing carnivore like T-Rex.

Overall, these non-traditional isotope systems are very promising tools to determine niche partitioning, the length of food chains and who was eating whom in modern and past food webs and by this shedding new light on faunal evolution and extinction. This toolbox is versatile and has a wide applicability outside palaeontology, including diet reconstructions in archaeology, anthropology and ecology.

References

[1]Leichliter, J.N., Lüdecke, T., Foreman, A.D., Duprey, N.N., Winkler, D.E., Kast, E.R., Vonhof, H., Sigman, D.M., Haug, G.H., Clauss, M., Tütken, T., Martínez-García, A., 2021. Nitrogen isotopes in tooth enamel record diet and trophic level enrichment: results from a controlled feeding experiment with rodents. Chemical Geology 536:120047

[2]Leichliter, J.N., Lüdecke, T., Foreman, A.D., Bourgon, N., Duprey, N., Vonhof, H., Sigman, D., Tütken, T., Martínez-García, A., 2023. Tooth enamel nitrogen isotope composition records trophic position: a tool for reconstructing food webs. Communications Biology 6, Article number: 373.

[3]Kast, E.R., Griffiths, M.L., Kim, S.L., Rao, Z.C., Shimada, K., Becker, M.A., Maisch, H.M., Eagle, R.A., Clarke, C.A., Neuman, A.N., Karnes, M.E., Lüdecke, T., Leichliter, J.N., Martínez-García, A., Akhtar, A.A., Wang, X.T., Haug, G.H., Sigman, D., 2022. Cenozoic megatooth sharks occupied extremely high trophic positions. Scienc Advances 8, eabl6529

[4]Jaouen, K., Beasley, M., Schoeninger, M., Hublin, J.-J., Richards, M.P., 2016. Zinc isotope ratios of bones and teeth as new dietary indicators: results from a modern food web (Koobi Fora, Kenya). Scientific Reports 6. Article number: 26281.

[5]Bourgon, N., Jaouen, K., Bacon, A.-M., Jochum, K.-P., Dufour, E., Duringer, P., Ponche, J.-L., Joannes-Boyeau, R., Boesch, Q., Antoine, P.-O., Hullot, M., Weis, U., Schulz-Kornas, E., Trost, M., Demeter, F., Patole-Edoumba, E., Shackelford, L., Dunn, T., Zachwieja, A., Duangthongchit, S., Sayavonkhamdy, T., Sichanthongtip, P., Sihanam, D., Souksavatdy, V., Hublin, J.-J., Tütken, T., 2020. Zinc isotopes in Late Pleistocene fossil teeth from a Southeast Asian cave setting preserve paleodietary information. Proceedings of the National Academy of Sciences U.S.A. 117, 4675-4681.

[6]McCormack, J., Griffiths, M.L., Shimada, K., Kim, S., Karnes, M., Maisch IV, H., Pederzani, S., Bourgon, N., Jaouen, K., Becker, M.A., Jöns, N., Sisma-Ventura, G., Straube, N., Pollerspöck, J., Hublin, J.J., Eagle, R.A., Tütken, T., 2022. Trophic position of *Otodus megalodon* and great white sharks through time revealed by zinc isotopes. Nature Communications 13:2980. https://doi.org/10.1038/s41467-022-30528-9.

[7]Jaouen, K., Villaba Mouco, V., Smith, G.M., Trost, M., Leichliter, J., Lüdecke, T., Méjean, P., Mandrou, S., Chmeleff, J., Guiserix, D., Bourgon, N., Blasco, F., Mendes Cardoso, J., Duquenoy, C., Moubtahij, Z., Salazar Garcia, D.C., Richards, M. and Tütken, T., Hublin, J.J., Utrilla, P., Montes, L., 2022. A Neandertal dietary conun-

drum: new insights provided by Zn isotopes at Gabasa, Spain. Proceedings of the National Academy of Sciences 119:e2109315119.

[8]Heuser, A., Tütken, T., Gussone, N., Galer, S.J.G., 2011. Calcium isotopes of fossil bones and teeth — diagenetic versus biogenic origin. Geochimica et Cosmochimica Acta 75, 3419-3433.

[9]Martin, J.E., Tacail, T., Cerling, T.E., Balter, V., 2018. Calcium isotopes in enamel of modern and Plio-Pleistocene East African mammals. Earth Planetary Science Letters 503, 227-235.

[10]Tacail, T., Le Houedec, S., Skulan, J.L., 2020. New frontiers in calcium stable isotope geochemistry: perspectives in present and past vertebrate biology. Chemical Geology 537, 119471.

[11]Weber, K., Weber, M., Menneken, M., Kral, A., Mertz-Kraus, R., Geisler-Wierwille, T., Vogel, J., Tütken, T., 2021. Diagenetic stability of non-traditional stable isotope systems (Ca, Sr, Mg, Zn) in tooth enamel – an in-vitro alteration experiment of biogenic apatite in isotopically enriched tracer solution. Chemical Geology 572:120196.

[12]Martínez-García, A., Jung, J., Ai, X.E., Sigman, D.M., Auderset, A., Duprey, N.N., Foreman, A., Fripiat, F., Leichliter, J., Lüdecke, T., Moretti, S., Wald, T., 2022. Laboratory assessment of the impact of chemical oxidation, mineral dissolution, and heating on the nitrogen isotopic composition of fossil-bound organic matter. Geochemistry, Geophysics, Geosystems, 23, e2022GC010396.

[13]Merceron, G., Tütken, T., Scott, R., 2023. Understanding dental proxies of ancient diets. Palaeogeography, Palaeoclimatology, Palaeoecology 621: 111589.

Carbonates isotopic response on physical and chemical condition of water for 50 Polish lakes

Ustrzycka A., Piotrowska N., Rousseau D.D., Kaczmarek K., Bonk A., Tylmann W., Filipiak J
Silesian University of Technology, Akademicka 2A, 44-100 Gliwice, Poland

Laminated lake sediments are a popular subject of climate change research because their biological, physical and chemical composition can reflects the biological, physical and chemical conditions that prevailed in the water column during the formation of this sediment [1, 2]. On the other hand all of the water parameters mentioned above are controlled by the lake catchment area and weather conditions (mainly temperature and precipitation) [3].

More and more often in research, not only qualitative but also quantitative reconstructions of temperature are desired. For quantitative reconstructions it is necessary to create a transfer function (paleothermometry). For isotopic measurements of calcium carbonate in lake sediments, it is a function that was created on the basis of the correlation of the isotopic composition of oxygen in the carbonate, in the layer formed in a specific year (determined, for example, by radiocarbon dating) and oxygen composition of water with the actual air temperature in the month/months when this carbonate was precipitated [4]. Therefore, it is crucial in this process to carry out monitoring to determine the months when carbonate precipitates in the lake.

We present analysis of carbon and oxygen composition of carbonates deposited in 2012 in 50 Polish lakes located between the eastern and western borders of Poland. Seasonal changes in chemical and physical parameters of water (temperature, pH, conductivity, concentration of Ca^{2+} and HCO_3^- ions) in those lakes were measured. We determined the seasonal changes of Langelier Saturation Index values in order to check when the physico-chemical conditions of the lake water are conducive to the carbonates precipitation.

To determine the temperature of which months have the greatest impact on the isotopic composition of carbonates, we searched for the relationship between $\delta^{13}C$ and $\delta^{18}O$ of $CaCO_3$ deposited in sediment traps and seasonal water parameters (temperature, pH, conductivity, carbonate ion concentration) and seasonal air temperatures.

Based on δD and $\delta^{18}O$ analyses in lake surface water of analyzed lakes we determined Local Evaporation Line and compared it with Global Meteoric Lokal Line to check the effect of the evaporation.

References

[1] Cohen AS, Paleolimnology. The history and evolution of lake systems. 2003

[2] Zolitschka B, Varved lake sediments, 2007, 3105

[3] Zolitschka B, Francus P, Ojala A, Schimmelmann A, Varves in lake sediments – a review, 2015, 1

[4] Różański K, Klisch MA,Wachniew P, Gorczyca Z, Goslar T, Edwards TWD, Shemesh, A, Oxygen-isotope geothermometers in lacustrine sediments: New insights through combined $\delta^{18}O$ analyses of aquatic cellulose, authigenic calcite and biogenic silica in Lake Gościaz, central Poland, 2010, 2957

Tritium and Radiocarbon in wines from Drăgășani Area, Vâlcea, Romania

Vagner I., Varlam C., Făurescu I., Bogdan D., Miricioiu M., Făurescu D.
National R&D Institute for Cryogenics and Isotopic Technologies, ICSI Râmnicu Valcea, 240050, Romania

Tritium and radiocarbon are ubiquitous radionuclides formed in the upper atmosphere by interaction of ^{14}N with neutrons generated by cosmic radiation. These nuclides equilibrate quickly in the atmosphere, reach the Earth's surface and are eventually incorporated by all plant and animal life, by food chain, through the metabolic proceses and photosynthetic activity. The concentration of radiocarbon in wines and spirits should be closely related to the mean atmospheric level during the growth period of the original plant, i. e. grapes [1, 2]. During the lifetime of the ^{14}C, an equilibrium concentration of around 225 mBq ^{14}C/g carbon is established in the Ramnicu Valcea area [3].

The situation is more complicated in the case of tritium, as its content in rain water depends on many conditions. Biomagnification of tritium is not a factor in food chain transfer. The lack of significant isotopic effects or biomagnification means that tritium transport and cycling in the environment can be predicted on the basis of the transport processes, hydrogen content, and chemical transformation of hydrogen and its compounds in the environment [4]. In the case of wines, it has been well established in the 1970s that the tritium content correlates well with the age of the wine as there is no more tritium exchange after the harvest, and the 12.3 year half-life is optimally suited for this type of age determination [2], being suggested that tritium analysis of wines from the pre-thermonuclear era might be suitable for dating wines. It is confirmed that wine tritium data reflect not only the long-term trend but also the seasonal variation. Wine tritium analysis can therefore be used for dating when long-term changes are greater than seasonal ones. Wine analysis is also promising as a means of revealing local abnormalities (local fallout, discharges) if their magnitude is sufficiently high and/or the event happens shortly before vintage. Such analysis can also be useful when information on the geographical extent and on the distribution of the event is insufficient [5]. Thus more recent work has reported a wide range of concentration values for tritium in wine samples, with values from 0.17 to 12.1 Bq/L, including organically bound tritium [6, 7].

Our work involved tritium and radiocarbon analysis in wines, including tritium analysis from free water, coupled with organically bound tritium and radiocarbon resulted from combustion of wine's ethanol.

In order to separate the aqueous phase of the wine samples, a fractional distillation was performed. These were prepared using automatic distillation control system (ADCS), with Cadiot columns. After fractional distillation of the wine samples, the aqueous fractions resulted have a high organic content, being also colored, depending on the color of the wine they come from. For this reason, we applied a purification method, in order to eliminate all the impurities which might interfere with LSC tritium measurement and, to preserve in the same time hydrogen isotopic content.The aplied purification method implied chemical treatment using Na_2O_2 and $KMnO_4$, followed by lyophilization.

The ethanol resulted from wines distillation, having a concentration around 92%, was subsequently subjected to a supplimentary purification, prior to combustion, involving its treatment with molecular sieve MS C 542 (Grace Davison). The after-treatment ethanol sample, having a concentration about 95%, was combusted in a Parr bomb type 1121. The combustion gass mixture resulted after combustion was purrified and bubbled for 20 minutes, in a inhouse scintillation cocktail [8], CO_2 resulted from sample combustion being detained as carbamate in the scintillation cocktail.

Figure 1: Liophylization installation for purification of water samples for tritium analysis.

The organically bound tritium from wine sample was determined by collecting the ethanol's combustion water directly from the bomb vessel, purification of the combustion water using the same method and installation as for the free water [9], see Figure 1.

The radiocarbon samples were measured using a low-background liquid scintillation spectrometer Quantulus 1220TM (PerkinElmer), the counting time for each sample and blank was 1000 min, and 100 min for the standards, divided in 10 cycles. For all experiments 20 mL of scintillation cocktail was used for each replicate prepared for measurement, and for each standard and background. The measuring vials used were 20 mL low-potassium glass vials (PerkinElmer). The background samples were prepared from combustion of fossil diesel. The value for the counting efficiencies was around 58%.

All tritium measurements were performed by the same low-background liquid scintillation spectrometer Quantulus 1220, using a low background liquid scintillation cocktail (Ultima Gold uLLT). Thus 8 g of water sample (purified water resulted from aqueous fraction of the wine) was mixed with 12 g of scintillation cocktail mentioned above in 20 ml polyethylene vials. Background samples and tritium standards were simultaneously prepared for each batch. Counting efficiency was determined by internal standard method according to SR EN ISO 9698:2019 [10] using as tritium standard tritiated water provided by PerkinElmer. Tritium free water used as background was deuterium depleted water obtained in our institute. Samples and backgrounds (tritium free water) were counted for 1,000 min per sample with a counting efficiency around 24% at the best figure of merit.

The tritium and radiocarbon concentration values measured in wine samples were in the range of the precipitation and air, respectively, for the Valcea area, namely around 1.5 Bq/L for tritium [11], and 225 mBq/g of carbon for radiocarbon [3].

Acknowledgements

This work is financed by the Ministry of Research, Innovation and Digitization through Program 1 - Development of the national research and development system, Subprogram 1.2 - Institutional performance - Projects for financing excellence in R&D, Contract no. 19PFE/2021 and PN 23 15 03 01 part of Core Program ICSI Lab2Field.

References

[1] Baxter MS, Walton A, Carbon-14 Concentrations in Recent Wines and Spirits, Journal of Food Science, Volume 36, 1971

[2] Scherer UW, Jacobi M, Castillo J, Fostel DH, Ultra-low-level Measurements of ^{3}H and ^{14}C in wines and champagne, Radiation Effects and Defects in Solids, Volume 164, 2009

[3] Faurescu I, Varlam C, Vagner I, Faurescu D, Bogdan D, Costinel D, Radiocarbon Level in the Atmosphere of Ramnicu Valcea, Romania, Radiocarbon, Volume 61(6), 2019

[4] Murphy CE, Tritium Transport and Cycling in the Environment, Health Physics, Volume 65(6), 1993

[5] Kozák K, Biró T, Reconstruction of environmental tritium levels from wine analysis. Health Physics, 46(1), 1984

[6] Surano KA, Hudson GB, Failor RA, Sims JM, Holland RC, MacLean SC, Garrison JC, Helium-3 Mass Spectrometry for Low-Level Tritium Analysis of Environmental Samples, Journal of Radioanalytical and Nuclear Chemistry, Volume 161(2), 1992

[7] Lawrence Livermore National Laboratory Annual Report 2001, UCRL-50027-01, avilable at https://aser.llnl.gov/report-archive/environmental-annual-2001

[8] Vagner I, Varlam C, faurescu D, Bogdan D, Faurescu I, Reproducibility of CO2 Absorption Method for Measurement of Radiocarbon Using a Parr Bomb and LSC, Radiocarbon, Volume 61(6), 2019

[9] Varlam C, Vagner I, Faurescu I, Faurescu D, Combustion Water Purification Techniques Influence on OBT Analysis using Liquid Scintillation Counting Method, Fusion Science and Technology, Volume 67, 2015

[10] Romanian National Standardization Body – ASRO. SR EN ISO 9698:2019. Calitatea apei. Tritiu. Metoda de încercare prin numărarea scintilațiilor în mediu lichid

[11] Varlam C, Duliu OG, Faurescu I, Vagner I, Faurescu D, Tritium time series in precipitation of Rm. Valcea, Romania, Isotopes in Environmental and Health Studies, Volume 52(4-5), 2016

Update of the Present Challenges of Environmental Tritium Measurement Using Liquid Scintillation Counting

Carmen Varlam, Irina Vagner, Ionuț Făurescu, Diana Bogdan, Denisa Făurescu
National R&D Institute for Cryogenics and Isotopic Technologies, ICSI Râmnicu Vâlcea, 240050, Romania

Tritium, the radioactive isotope of hydrogen, found as application its dual role as a tracer of hydrogen and carbon structures, making it as one of the most versatile radionuclide. It can provide basic isotopes information for isotopic hydrological investigations, and it can be used to verify and improve the atmospheric circulation models [1], to study the water interaction with the atmosphere and biosphere [2], to provide an isotopic baseline for authentication of food and drinks [3]. Concentration levels of tritium in the environment not influenced by nuclear activities ranges from 1-4 Bq/l of water for continental environment to 0.1 or 0.2 Bq/l in the marine environment [4]. The level of 1-2 Bq/l can be found in water vapour of the atmosphere or in biological matrices.

The tritium of the most of the samples is usually prepared in its aqueous form, whether it is gaseous form, liquid form, or assimilated in living organism as tissue free water tritium and organically bound tritium [5]. There are different types of tritium measurements, but for environmental tritium level only two, He-3 ingrowth (mass spectrometry of rare gases) and tritium enrichment followed by liquid scintillation counting (LSC), [6]. LSC is preferred method in the case of large number of samples (radioactivity monitoring program, precipitation, drinking water, underground water) due to the reasonable necessary time to provide the results.

The present challenges are affecting both liquid scintillation cocktail and liquid scintillation spectrometers. Nonylphenol Ethoxylates (NPE’s) are an important components of the majority of liquid scintillation cocktails available on the market. They are involved in forming homogeneous mixture of sample and liquid scintillation cocktail and, due to their aromatic nucleus, they are facilitating the transfer of the radioactive decay into the light. The European Commission announced the addition of NPE to Annex XIV, the list of chemicals subject to authorization under the EU Registration, Evaluation, Authorization and Restriction of Chemical substances (REACH) legislation [7]. The availability of the liquid scintillation cocktails will be adversely affected by the change in EU regulations preventing the use of NPE’s. Their price will be higher to include the necessary authorizations, but even so, the NPE’s production will be limited due to lower market demand.

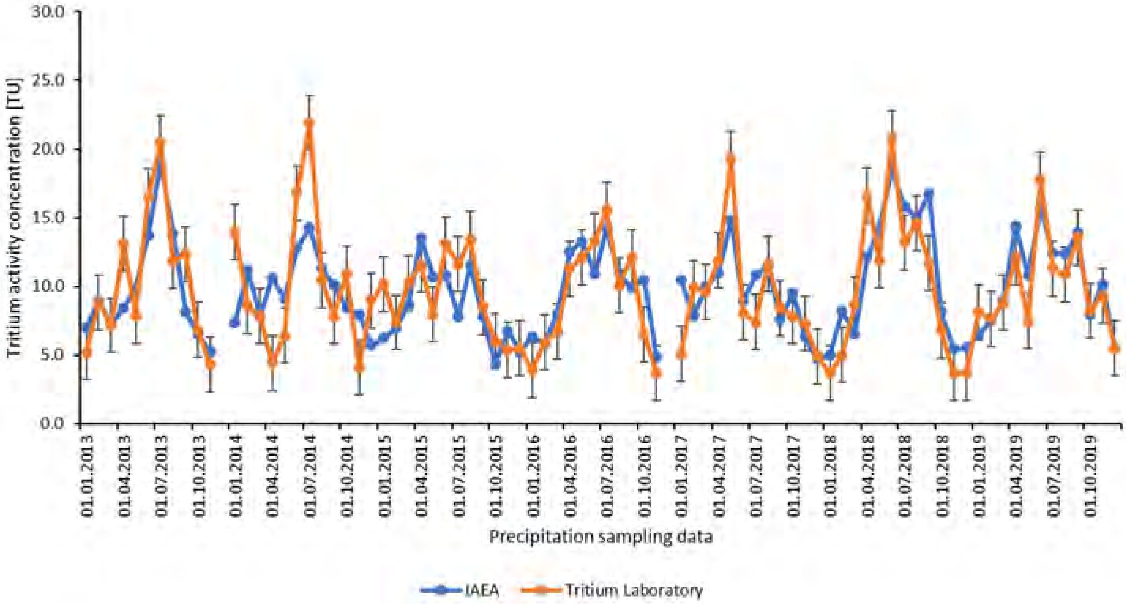

Figure 1. Monthly tritium activity concentration in precipitation during the 2013-2019 period measured by ICSI Tritium Laboratory and Hydrology Laboratory of IAEA

The environmental tritium level is usually low, Figure 1, and due to this characteristic, some type of liquid scintillation spectrometers used are dedicated to low-level measurement and they are able to detect approximately 1 Bq/l of tritium in water without electrolytic enrichment [8]. The routine procedure of tritium measurement in the environment uses liquid scintillation spectrometer Quantulus 1220. Despite the very good performances of this liquid scintillation spectrometer of environmental radioactivity monitoring, it has no longer been available on the market, and its provider decided that this type of spectrometer have reached the end of its serviceable lifecycle. The environmental radioactivity monitoring laboratories need to consider a new generation of liquid scintillation spectrometers available on the market. The ALOKA LB7 spectrometer, with its 0.3 Bq/L limits of detection for tritium [9], seems to be appropriate for the environmental applicaton. Another option is the Quantulus GCT 6220 spectrometer, which uses a special technique of energy-dependent correction of the background [10], lowering the limit of detection, and making it useful for environmental studies.

The other type of liquid scintillation spectrometers with higher limit of detection, 2-10 Bq/l (e.g. Hydex 600SL, Tri-Carb series) need to consider tritium enrichment procedure as a must for environmental studies. The enrichment of ^{3}H is usually accomplished using alkaline electrolytic cells with Ni/Ni or mild-steel electrodes, procedure developed in the early 1960s. This procedure employs 250 or 500 mL fixed volume electrolysis cells that are connected to each other in series and placed in a cooler container with regulated temperature around 5^0C. The electrodes are pair of stainless steel and mild steel [11]. In order to increase the electrical conductance, sodium peroxide is added to distilled water sample [12]. When the current is applied to the cell electrodes, the water molecule is decomposed in hydrogen and oxygen gas enriched in stable isotopes, and tritiated water molecule is preferentially and exponentially concentrated in the residual liquid (up to 30-fold, [13]). The electrolyzed water (also containing NaOH) is neutralized (using CO_2 or

$PbCl_2$) and distilled in order to remove salts, followed by addition of a scintillator cocktail for liquid scintillation decay counting.

There are several drawbacks of the alkaline electrolyze procedure. Operational disadvantages include labour intensive procedures for maintenance, careful gravimetric requirements, cleaning and drying of enrichment cell apparatus, as well as the use and disposal of noxious chemicals for the electrolysis and/or neutralization (e.g. Na_2O_2, CO_2, $PbCl_2$). The increasingly higher ^3H enrichments (e.g. >50-fold) sought for contemporary groundwater dating require extreme volume reductions, but these are hampered by the solubility of the electrolyte as supersaturation may be reached in the final stages of electrolysis. In general, alkaline electrolytic procedure remains cumbersome and labour intensive, hampering widespread implementation of ^3H low-level measurements in the routine laboratory practice.

A simpler and attractive alternative to mild-steel or nickel alkaline electrolytic cells are H_2O electrolyzers based on solid polymer electrolyte membranes (PEMs). It is usually used in hydrogen fuel cell [14], and it has very good thermal and chemical stability, mechanical strength, and proton conductivities. The PEM acts like Natrium peroxide added in alkaline electrolysis cell, but without any chemicals dissolved in the water sample. Akin to alkaline electrolysis, positively charged ions migrating to the cathode receive electrons from the external electric power circuit to form hydrogen gas, and the given electrons to the anode by the oxygen molecules, complete the circuit. The PEM cell has some advantages by eliminating chemical residues, distillation of electrolyzed water, and electrode preconditioning necessity [15]. Intensive studies on PEM cell used for ^3H enrichment of environmental water samples are published by Muranaka and Shima [16,17] and later commercialized as the single-sample, Tripure® Tritium Condensation Apparatus (www.permelec.co.jp; not available outside Japan). Wassenaar et al. proposed in 2017 [18] an open access tritium enrichment PEM system, whose components (anode and cathode of PEM produce by De Nora Permelec LTD.) are not available outside Japan. There are still questions about sample memoy effect and robustness of the cell constant k among and between enrichment cells.

Each of the above problems are extesevely presented in this work together with some conclusions. Despite all the present challenges of the environmental tritium measurement, this radionuclide remains one of the important transient tracers used in hydrological studies, or in environmental studies.

Acknowledgements

This work is financed by the Ministry of Research, Innovation and Digitization through Program 1 - Development of the national research and development system, Subprogram 1.2 - Institutional performance - Projects for financing excellence in R&D, Contract no. 19PFE/2021, and PN 23 15 03 01, PN 23 15 03 03, part of Core Program ICSI Lab2Field.

References

[1] Terzer-Wassmuth, S., Wassenaar, L. I., Welker, J. M., & Araguás-Araguás, L. J., Hydrological Processes 35 (6), 2021, doi.org/10.1002/hyp.14254.

[2] Yong Wang, et al., Isotopes in Environmental and Health Studies 58(3), 2022, p.229.

[3] O'Sullivan, R., Schmidt, O., Monahan, F.J., International Dairy Journal 126:105268

[4] IRSN, Institute de Radioprotection et de Surete Nucleaire, Radionuclide Fact Sheet Tritium and the Environment, https://en.irsn.fr/en/research/publications-documentation/ radionuclides-sheets/ environment/pages/tritium-environment.aspx, available April 2023.
[5] UNESCEAR, Report of General Assembly 2016, Annex C- Biological effects of the selected internal emitters -Tritium, 2016, p 258.
[6] Varlam, C., et al., Applied Radiation and Isotopes, 2009 (67), p.812.
[7] Official Journal of the European Union, Commission Regulation (EU) 2017/999.
[8] Salonen L, et al., editor L'Anunziata, M.F., Elsevier Academic Press, 2012, p.625.
[9] Yoon Y., Yongcheol K., Radiation Protection and Research 45(3), 2020, p.142.
[10] Edler R., Radioanalytical Nuclear Chemistry 314, 2017, p.695.
[11] Plastino, W., et al., Radiation Measurements, 42(1), 2007, p.68.
[12] Kumar, B., et. Al., Applied Radiation and Isotopes , 118, 2016, p.80.
[13] Morgenstern, U., Taylor, C.B., Isotopes in Environmental and Health Studies 45, 2009, p. 96.
[14] Carmo, M., et al., International Journal of Hydrogen Energy 38, 2013, p.4901.
[15] Soreefan, A.M., DeVol, T.A., Journal Radioanalytical and Nuclear Chemistry 282, 2009, p. 511.
[16] Muranaka, T., Shima, N., Sato, H., Fusion Science and Technology 48, 2005, p.516.
[17] Muranaka, T., Shima, N., Fusion Science Technology 54, 2008, p. 297.
[18] Wassenaar, L., et al., Isotopes and Environmental Health Studies 54, 2018, p.274.

GEOLOGICAL FIELD TRIP

Gottfried Tichy, Ana-Voica Bojar, Hans-Peter Bojar

Regional route with planned stops

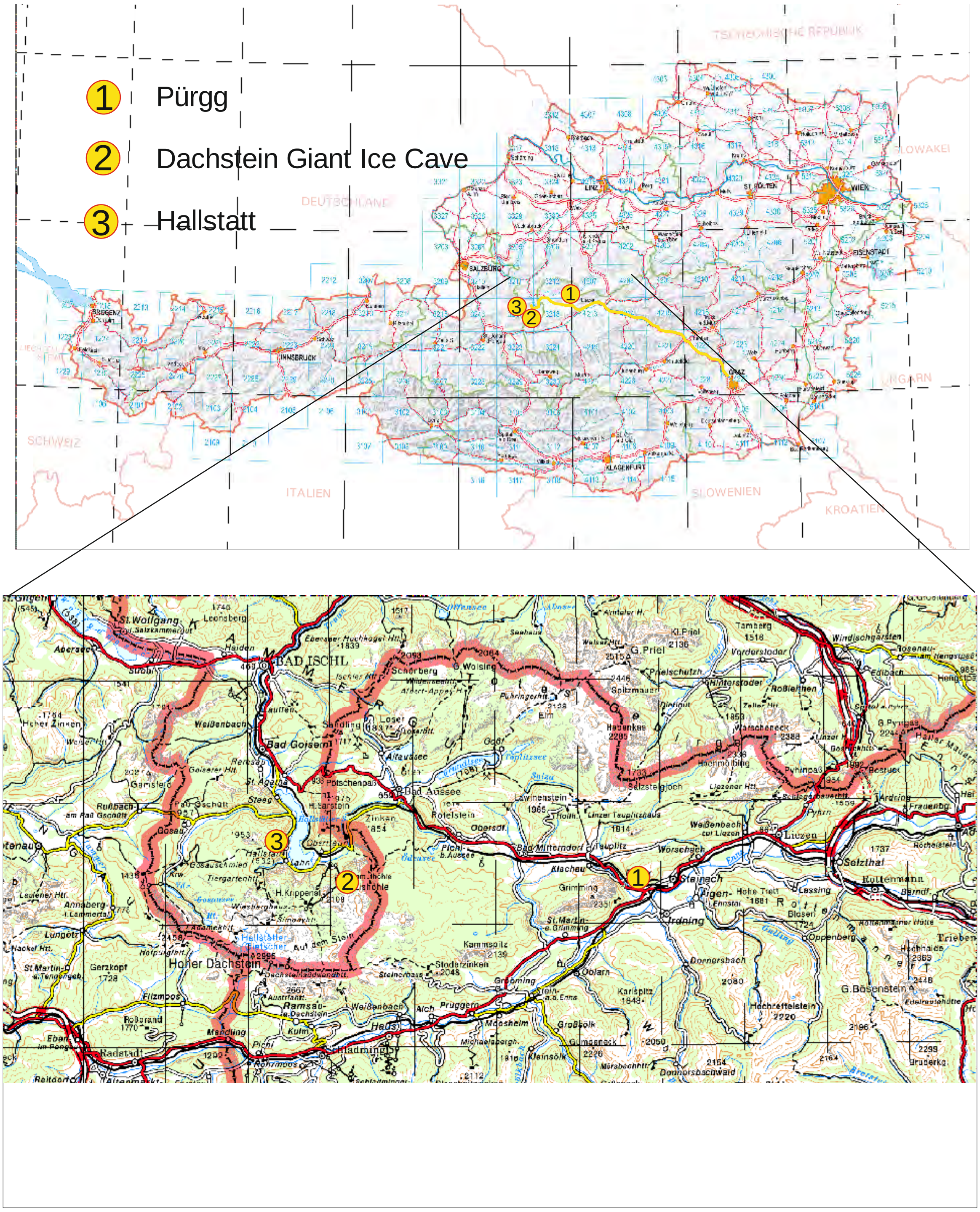

1. PÜRGG

The village of Pürgg-Trautenfels is considered one of the prettiest villages in Styria.
It lies on a small plateau, about 150 m above the valley floor of the Grimmingbach.

1.1. St. George's Catholic Parish Church

The Romanesque church was probably consecrated on July 17th, 1130. The basic structure of the three-nave church is still preserved, but the Gothic makeover was given at the beginning of the 14th century. The church surprises with another nave a mezzanine higher and an additional prayer room, again a few steps up, both discovered after 1945.

St. George's Catholic Parish Church in Pürgg with the Tauplitzalm in the background.
View from the St. John's Chapel (Johanneskapelle)

Tower lute chamber, frescoes

Frescoes from around 1300 were uncovered in 1953. Scenes from the Passion of Christ and from the life of St. Catherine are depicted in two surrounding strips, which is why the room is also called St. Catherine's Chapel.

1.2 St. John's Chapel Pürgg (Johanneskapelle)

A Romanesque chapel is situated on the eastern edge of the plateau, the 786 m high „Purgstall“, on a beautiful vantage point. This chapel is famous for its beautiful and good preserved 12th century frescoes. The Romanesque crucifix on the altar dates from the 13th century.

St John's Chapel (view to the east, the west wall is covered with shingles)

Main nave

Ceiling fresco

Although the first mentioned documents are from 1350, it is assumed that the chapel represents the rest of the former Graunscharn Castle of the Traungauer. The Traungauer were counts, margraves and dukes from the line of the Otakare, who ruled Styria (Margraviate of Steyer) from 1056 to 1192. Due to certain architectural features, it is concluded that it could have been built before 1120. When the Traungau family died out in 1192, the castle was abandoned, and the chapel was probably converted into a memorial chapel. Since the Baroque period, it has served as a Calvary station, which is still indicated today by the three crosses outside on the south wall. A small ridge turret was added to the west side in the Baroque period.

In 1870, during work on the chapel, the painted medieval frescoes were discovered and restored in 1893/1894. Unfortunately, the restoration was carried out improperly, so that damages caused by peeling off occurred after a short time. Apart from the frescoes, which cover almost the entire church interior, there is only a simple altar canteen with a Romanesque crucifix (13th century) from the Pürgg parish church.

The frescoes date from the third quarter of the 12th century. The Traungau Margrave Ottokar III is considered as one of the two donor figures depicted to the left and right of the chancel opening. The performing artists are attributed to the Salzburg Art Circle, although the images indicate that they were familiar with Byzantine art. The frescoes are among the best preserved of this period. A painted curtain forms the base of the frescoes. Above this is the main strip, about two meters high, on which the miracle of the *multiplication of bread* is depicted on the north side and themes relating to the *birth of Christ* are depicted on the south side.

At the western end is the motif of *Aesop's cat-mouse war*. There has been much discussion about the mysterious significance of this representation. The Cat and the Mice is a fable attributed to Aesop (Greek philosopher who lived in the 6th BC), which tells the story of "a house full of mice, and the cat who hunts them. After the cat catches several of them, the remaining mice retreat into their holes. The cat tries to fool them by playing dead, but the mice don't fall for it. The moral of the story is that the wise is not tricked by the innocence of those previously found to be dangerous".

Interestingly, Pliny the Elder, in the *Naturalis Historia* (written between 23-79 AD) notes that Romans consider the mice a prophetic animal, even in state and political issues (the 8th Book included in Volume 3). Pliny lists historical known cases when mice acted accordingly, foreseeing the events.

It is worth to mention that, at the time the chapel was painted (thus in the 12th Century), the compiled stories about animals, as for example those included in the *Physiologus* (published c. 2nd Century AD in Alexandria), had a large circulation across Europe. Being firstly published in Greek, than translated into Latin, the *Physiologus* was translated in German in 1070 AD. Even the *Physiologus* does not contain the "cat and mouse" war episode, it remains the fact that at the time when the chapel was painted, animal allegories and symbols had a large circulation in written and painted form. During the following centuries, in Western Europe, the *Physiologus* continued to be present in the form of the *Bestiary* and the *Liber naturae* (Fiziolog, Bestiar, 2001)

Cat-mouse war, painted representation from the Aesop's fable

In the upper picture strip, the *foolish virgins* (north side) face *the wise ones* (south side). The *sacrifices of Cain and Abel* are depicted next to the triumphal arch. In the decorative band around the triumphal arch, entwined with arabesques, the word Allah, the Arabic term for the one God in all monotheistic religions, can be read repeatedly in Arabic script and with a slight distortion (Tichy & Staley, 2005).

In the chancel, on the east wall, as patrons of the church are depicted *John the Baptist* (left) and *John the Evangelist* (right), while on the side walls are two holy bishops with regional references (*Rupert* and *Virgil*?) and two figures from the Old Testament crowns and scrolls (*David* and *Melchizedek*?) facing each other. The evangelist symbols *bull, lion, eagle* and *man* can be found in the four segments of the flat vault of the choir next to the central representation of *Christ as a lamb* with a cross nimbus and a cross flag.

Throughout the church, the figurative scenes are enriched by a variety of ornamental decorations. Mostly arranged in strips, the ornamentation often imitates marble and fabric patterns or forms plant or purely geometric shapes.

References

https://aesopsfables.wordpress.com/the-cat-the-mice/

Dollwetzel, Ph. (2010): Die romanischen Wandmalereien in der Johanneskapelle in Pürgg-Trautenfels (Steiermark). - Studienarbeit Universität Salzburg, mit zahlreichen Abbildungen.

Fiziolog, Bestiar (2001). Transcriere și note: Cătalina Velculescu, Viorel Guruianu, Manuela Anton. București, Editura Cavallioti, 112 p., ISBN 973-9463-17-7.

Rabensteiner, Ch: & Hensle-Wlasak, H. (1998): Pfarrei Pürgg im Ennstal. - Kunstverlag Hofstetter Ried im Innkreis.

Senft, H. & Senft, W. (2003): Geheimnisvolles Salzkammergut. Magisches, Besonderes, Kurioses und Unbekanntes. – 2. Auflage, 208 S., ill. Leopold Stocker Verlag, Graz.

Tichy, G. & Staley, L. (2003): Arabisches in Salzburg. - Bastei. Zeitschrift des Stadtvereines Salzburg für die Erhaltung und Pflege von Bauten, Kultur und Gesellschaft, 52. Jahrgang, 1. Folge, 42-43, 1 Abb., Salzburg.

Tichy, G. & Staley, L. (2005): Kufische und pseudokufische Inschriften in Salzburg und im europäischen Kontext. - Mitt. Salzburger Landeskunde, 145, 339-362, 4 Taf., Salzburg.

Woisetschläger, K. & Krenn, P. (1982): Die Kunstdenkmäler Österreichs. Dehio-Handbuch Steiermark: (ohne Graz). Hrsg.: Bundesdenkmalamt. Anton Schroll & Co, Wien. [ISBN 3-7031-0532-1], S. 382.

Weiler, I. (1970): Der Katzen-Mäuse-Krieg in der Johanneskapelle auf der Pürgg. - Zeitschrift des Historischen Vereines für Steiermark, 61, 71-82, 5 Abb., Graz.

View from Irdning to Trautenfels Castle and Pürgg (Foto: H. Kowatsch)

2. HALLSTATT

2.1. The city

On the narrow strip of shore between the lake and the steep mountain slope, the houses are crowded close together, some of them even built with piles into the lake. Until the end of the 19th century, Hallstatt could only be reached by boat (from Obertraun or Untersee) or on foot on narrow mule tracks. Between the mountain and the lake, the space has been used to the full. Some of the houses by the lake could only be reached by boat or via the "Oberer Weg"; that is, over a narrow corridor over attics. It was not until 1875 that Hallstatt was made accessible by a road from Gosaumühle (Gosauzwang, to the north-west), which was partially blasted into the rock. In 1966, the double tunnel running west of the village in the mountain was opened for the only road alongside the lake, and since then the west bank has been continuously passable.

View from Hallstatt

Although there is little space for a larger settlement, the area around Hallstatt has been inhabited since the Stone Age. One reason for this must have been the occurrence of salt, the "white gold" which established the prosperity of the former population. This is confirmed by the rich grave goods from the Bronze and Iron Ages which can be studied in the World Heritage Museum in Hallstatt. Both salt and Salina as well as the "salt word - Hall" can be traced back to the Celtic word "sal, sal, salannos" and that means "holy". Salt, the "white gold", was a sacred substance of "Mother Earth" for the Celts, just like gold and iron.

The picturesque location of the place the lake and the grandiose mountains like the Dachstein with its huge cave systems (giant ice cave, mammoth cave) and glaciers attracts a myriad of tourists from all over the world so during the season Hallstatt with its 725 citizens becomes an area of overtourism.

2.1.1. Hallstatt Catholic Parish Church

The parish church of the Assumption of the Virgin Mary, also known as Maria am Berg, is the Roman Catholic parish church of the market town of Hallstatt.

The first Catholic church was built no later than 1150. The tower of this is still preserved. The second, enlarged Romanesque church was consecrated in 1320 and the construction of today's church on the steep rock began in the late Gothic period. The present church room was completed in 1505. After the great fire in 1750, the Romanesque tower received a baroque helmet.

When entering the interior, one sees two winged altars in the double choir. The altar was created as part of the restoration and Gothic revival of the church in the years 1888 to 1895.

2.1.2. The charnel house in the Gothic Michael‘s chapel is located at one of the most beautiful viewpoints in Hallstatt. Since the cemetery is so small, there is no possibility of expansion, and cremation was not allowed in the past, there was always not enough space. The graves were usually reopened between 10 and 15 years after a burial and the skulls, but also the long bones, which took up a lot of space, were removed. There are 1200 skulls in the 12th century ossuary. Of these, 610 are painted, arranged by family and provided with the date of death. The skulls have been painted since 1720.

2.1.3. The Protestant Parish Church (Christ Church) Hallstatt

Two Protestant preachers were already active around 1560 but the new faith was persecuted by the Catholics and thus the Protestant faith could only be lived out in secret. Between 1734 and 1737, Protestant citizens of the Salzkammergut were forced into transmigration to Transylvania and Banat, as so-called Landler. 122 Protestants from Hallstatt are documented as having been deported.

The patents of tolerance issued by Emperor Joseph II allowed Greek Orthodox, Protestants (1781) and Jews (1782) the free private practice of religion - with restrictions. The primacy of the Catholic Church remained. It was not until 1861 that the Protestant churches received full autonomy by the Protestant Patent of Emperor Franz Joseph I. In 1785, the first prayer house was built in Hallstatt, which stood at the mouth of today's Mühlbach. In 1859, two old salt miners' houses were demolished and the new Protestant church in Neo-Romanesque style was built in their place and consecrated in 1863. The building costs of 37,000 guilders were provided by several benefactors and the Gustav Adolf Association.

2.2. Archeology

Hallstatt is home to the world's oldest salt mine. There, in prehistoric times, salt was exclusively extracted by dry mining. The miners cut parallel grooves in the rock with their bronze picks and used them to loosen smaller pieces of salt. Then, salt was carried in sacks down wooden stairs to the shaft and then brought to the surface by ropes in woolen sacks.

The history of the town of Hallstatt in the Upper Austrian Salzkammergut is shaped by the rich salt deposits of the Hallstatt Salt Mountain, which is located above the present lakeside town in the Eastern Alps. “*Hall*” means “salt” in celtic. The salt has been mined since 1500 BC and has brought great wealth to the town. In archaeology, the area of Hallstatt is particularly famous for finds from a burial ground from the early Iron Age, which gave the town its name throughout Europe.

In an extensive burial ground above the village, some 1,300 burials were found, spanning over a period from the older Iron Age 800 to 450 BC (called the Hallstatt period). In addition to the burial ground with its exceptionally rich grave goods, the finds from the prehistoric mines are known worldwide and, thanks to the preservation conditions in the salt mountain, cover an exceptionally broad spectrum. Moreover, a body of a perfectly preserved miner, who died in the 4th century BC, could be recovered in the mining salt in the Kilbwerk in 1734

Traces of over 7000 years of human activity in Hallstatt have so far been found mainly in the Salzberg valley above the present-day town and in the present-day local area around Lake Hallstatt.

The Hallstatt culture was the predominant Western and Central European culture of Late Bronze Age (Hallstatt A, Hallstatt B) from the 12th to 8th centuries BC and Early Iron Age Europe (Hallstatt C, Hallstatt D) from the 8th to 6th centuries BC, developing out of the Urn field culture of the 12th century BC (Late Bronze Age) and followed in much of its area by the La Tène culture.

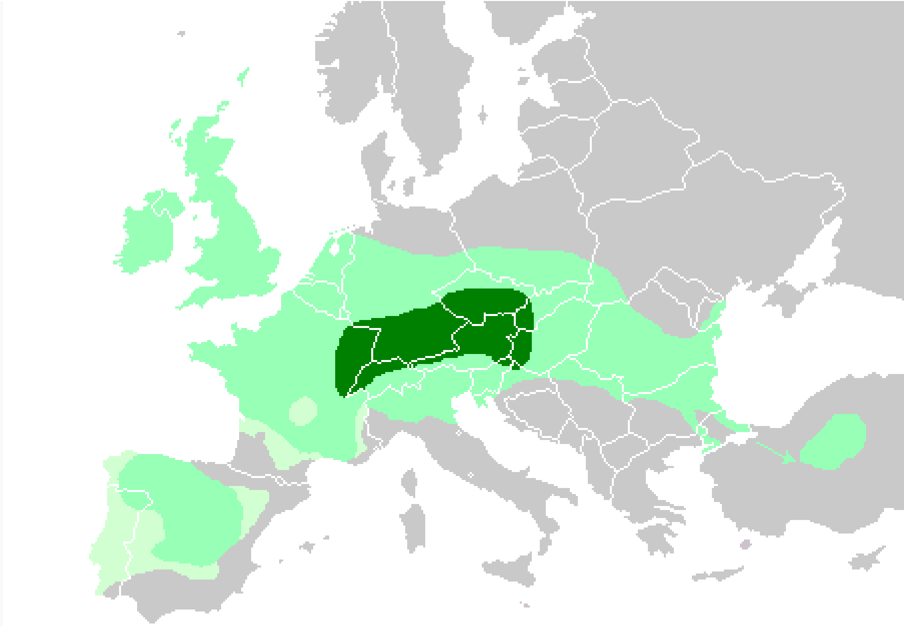

Celtic expansion (https://commons.wikimedia.org/wiki/File:Celtic_expansion.PNG)

Chronology

Bronze Age Central Europe[4]	
Beaker	2600–2200 BC
Bz A	2200–1600 BC
Bz B	1600–1500 v. Chr.
Bz C	1500–1300 v. Chr.
Bz D	1300–1200 BC
Ha A	1200–1050 v. Chr.
Ha B	1050–800 v. Chr.
Iron Age Central Europe	
Hallstatt	
Ha C	800–620 BC
Ha D	620–450 BC

La Tène	
LT A	450–380 BC
LT B	380–250 BC
LT C	250–150 BC
LT D	150–1 BC
Roman period[5]	
B	AD 1–150
C	AD 150–375

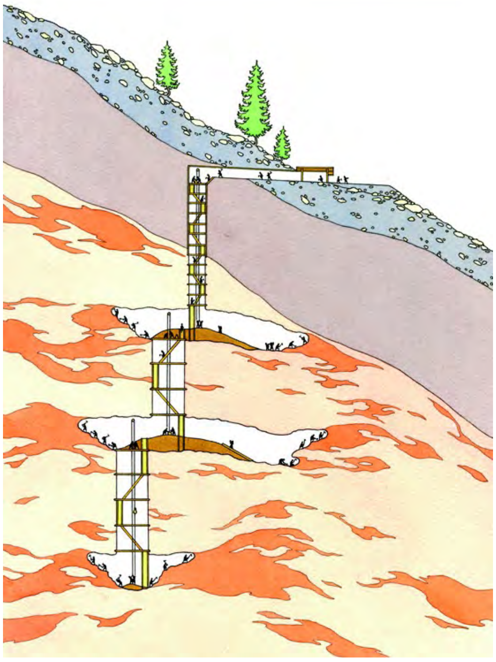

Section of the Hallstatt salt mine. Reconstruction of Bronze Age salt mining at the Christian von Tuschwerk site in Hallstatt.

Grave goods from Hallstatt

World Heritage Museum Hallstatt: Seestraße 56, 4830 Hallstatt Tel: 06134-8280
www.museum-hallstatt.st

2.3. The Hallstatt Lake

In autumn, the circulating lake releases an enormous amount of heat to the surrounding terrain, influencing the local climate. The largest tributary is the Traun-river, which flows into the lake at Obertraun and leaves it at Steeg. In addition to the Gosaubach, which also supplies the lake with water from its 106 km^2 catchment area, the lake is also fed by underground springs from the Dachstein massif with its 150 km^2. After storms or when the snow melts, the water level of the lake can rise sharply (+2 m in 1897; 1.6 m in 1899).

Twelve species of fish live in the lake. A typical fish species for the alpine lakes is the Reinanke (*Coregonus*). It is assumed that the Reinanke reached the Alps from the north with the meltwater streams at the end of the last ice age. However, further migration towards the south was prevented by the Alps. Reinanke stay in open waters and only rarely move into shallow water. They need clear, oxygen-rich water and prefer water temperatures between 10 and 12 degrees Celsius. In the past, the Reinanken were of economic importance, today it is the Seesaibling (*Salvelinus namaycush*, Arctic char) from the North America.

References

Dopsch, H., Heuberger, B. Zeller, K.W. (Red.) (1994): Salz. Salzburger Landesausstellung Hallein Pernerinsel Keltenmuseum 30. April bis 30. Oktober 1994. – 307 S., ill., Salzburger Landesaustellungen, Salzburg.

Husen, van D. (2003): Als unsere Seen Gletscher waren – Die eiszeitliche Entwicklung im Salzkammergut. – In: Weidinger, J.T., Lobitzer, H. & Spitzbart, I.: Beiträge zur Geologie des Salzkammergutes. – Gmundner Geo-Studien, 2, 215-222, Gmunden.

Kern, A., Kowarik, A., Rausch, A.W. & Reschreiter, H. (Hrsg.) (2008): Salz-Reich. 7000 Jahre Hallstatt. – Veröff. Prähistor. Abt., 2, 239 S., Naturhistorisches Museum Wien, Wien.

Leutner, N. (2010): Das Warmwasser am Hallstätter See.- 52 vS., Eigenverlag, Bad Ischl.

Morton. F. (1932): Das "Warme Wasser" am Hallstätter See. - Archiv für Hydrobiologie Bd. XXIV, 543-546, Taf. xxiv, Stuttgart.

Stögner, A. (o.J.): R.-K. Pfarrkirche Hallstatt. - 24 S., ill., OÖ. Landesverlag, Linz.

Urstöger, H.J. (2000): Hallstatt Chronik. Von den Anfängen bis zum Jahr 2000. – 746 S., ill., Musealverein, Hallstatt.

Vancsa-Tironiek, E.M. (1986): Flügelaltar in Hallstatt. -35 S., ill., Verlag Hofstetter-Dia, Ried/Innkreis.

Weidinger, J. (1966): Katholische Pfarrkirche Hallstatt. – 22 S., ill., Oberösterreichische Landesverlag, Linz.

3. THE GIGANT ICE CAVE

The Northern Limestone Alps are heavily karstified and have a myriad of caves. In the Dachstein Mountains alone, 521 caves are known and documented. Among the largest is the Hierlatz Cave (length >75 km) and the Mammut Cave (length: 48 km). Close to the latter is the famous Dachstein Gigant Ice Cave. It is located in the northern part of the Dachstein massif near Obertraun, 76 m above the Schönbergalm in the Schönbergwand-rock wall, within the UNESCO World Heritage area Hallstatt-Dachstein/Salzkammergut.

Dachstein Giant Ice Cave

3.1. History

According to a legend, Peter Gamsjäger from Obertraun discovered the ice cave in 1897 in search of scattered cattle. Alexander Mörk and Prof. Witte penetrated as far as the Great Ice Abyss a few years later and measured its depth. However, it is likely that the cave was known to the locals long before that.

On July 17, 1910, the speleologists Hanna and Hermann Bock from Brno and Georg Lahner from Linz succeeded in exploring deeper the cave for the first time by overcoming the Great Ice Abyss; this day is therefore considered the official time of discovery. Guided tours have been held since 1912. As early as 1928, the cave was equipped with electric lighting, and in 1952 a new entrance was opened.

Since 1951 the cave has been accessible by the Dachstein Krippenstein cable car which brings us to the 745 m higher situated Schönbergalm 1329 m (1345 m). From there the cave can be easily reached in about 20 minutes on foot. An asphalted footpath leads from the Schönbergalm to the artificially opened entrance at 1421 m and after about 800 m guided tour through the cave you come out again at the Great Wind Hole, a natural opening at 1459 m.

3.2. Description of the cave tour

The giant ice cave is located in the banked lagoonal Dachstein Limestone (Upper Triassic: Norian/Rhaetian) and is one of the largest ice caves on earth. It is the most outstanding tourist attraction in the Salzkammergut. Every year over 150,000 people wander through the underground halls: The *King Arthur Cathedral*, the ice-free part of the cave, is littered with huge blocks of rubble that once came loose from the ceiling. Cave bear bones were found here, which is why this area is called the "*bear cemetery*". There we reach the lowest point of the Cave at 1384 m. Behind a weather door we climb up wooden stairs to the "*Little Ice Chapel*" which opens to the "*Parsifal Cathedral*", which has the most beautiful ice formations in the cave (2-6 m ice cover) and after the crystal glacier, the last large hall of the show part of the cave begins with the *Tristandom* with a 15 m thick ice cover. There, a suspension bridge leads over the ice abyss. Alternatively, a path along the cave wall can be chosen. After the Tristandom, the guided tour ends.

3.3. The cause and age of ice formation

The cave system has at least two connections with the outside world at different heights. In winter, warmer cave air rises up through rock crevices and leaves the cave through the upper openings, which are not directly known as such, but are probably located on the high ground between 1600 and 1900 metres. At the same time, cold outside air is drawn in through the lower entrances. In summer, the colder cave air flows out of the lower openings, while warm air flows in from above. In winter, the temperature in the cave follows the outside temperature. It rises quite linearly from the entrance to the cave-in, but without reaching 0 °C. In summer, the warm air is sucked in there and cools down to values around 0 °C inside the mountain,

In general, the flow is out of the cave from December to March, in the cave from July to September, changing frequently in the transition months, the average speed is 4 m/sec. Ice growth depends strongly on the seepage water supply, it mainly occurs at the time of snowmelt on the plateau in the months April to June.

During the summer, but also in winter, there is considerable ice loss. Only in the south-eastern, 340 m long cave branch, running from south-west to north-east, do conditions prevail that allow ice formation. The mass of the cave ice is estimated at **13,000 m³** with a surface area of around **5,000 m².** Since even relatively small climate fluctuations can lead to an increase or melting of the ice, it can be assumed that the cave has already been frozen and de-iced several times during the post-glacial climate fluctuations.

The cave was probably completely ice-free at the end of the "Medieval Climate Optimum" (c. 950 to c. 1250 AD). The formation of ice mainly took place in the period of the modern climate deterioration of the "Little Ice Age" with particularly severe winters from the 16th to the middle of the 19th century.

The Dachstein area shows the largest glaciation in the Northern Limestone Alps. Since the peak of the glacier level in 1850, the glaciers have continuously retreated. Since that time, the Hallstatt Glacier has lost over 1.7 km in length, which is about the half.

4. GEOLOGY

The Eastern Alps are characterized by the presence of three main tectonic units, the Lower, Middle and Upper Austroalpine, which overlie the Penninicum. The Upper Austroalpine unit consists of the Northern Calcareous Alps (NCA) overlying the Greywacke zone and corresponding to the Graz Palaeozoic, Murau Palaeozoic and Gurktal nappe, with evaporitic rocks lacking in the later ones. The Mesozoic NCA belt is detached and thrust along the evaporitic Upper Permian to Lower Triassic Haselgebirge Formation. The sedimentation started in Late Carboniferous or Early Permian times, the youngest sediments being of Eocene age. The NCA are divided into the Bajuvaric, Tirolic and Juvavic nappe complexes.

4.1 Geology of the Dachstein Giant Ice Cave location

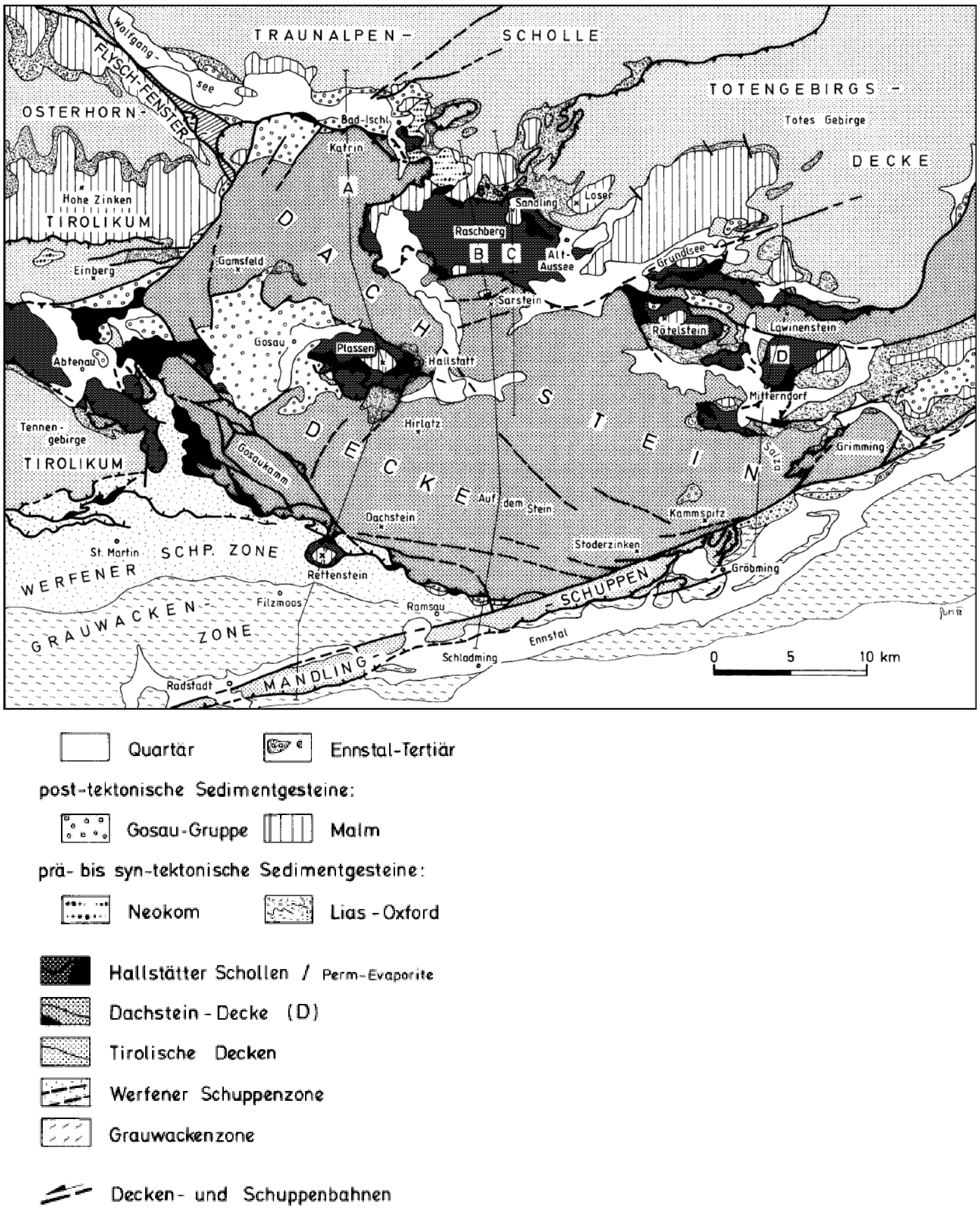

Tectonic overview of the Dachstein region (Scheidleder, 2001)

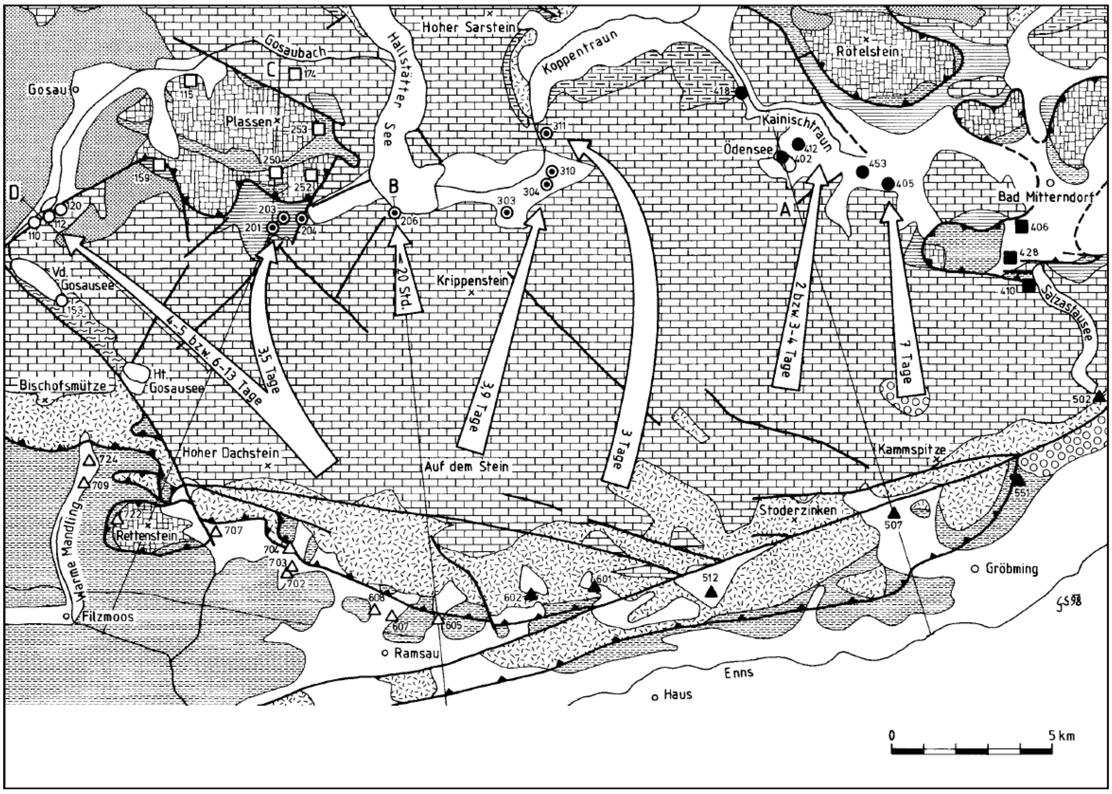

Hydrogeological overview map of the Dachstein area, for figure caption see previous figure (Scheidleder, 2001)

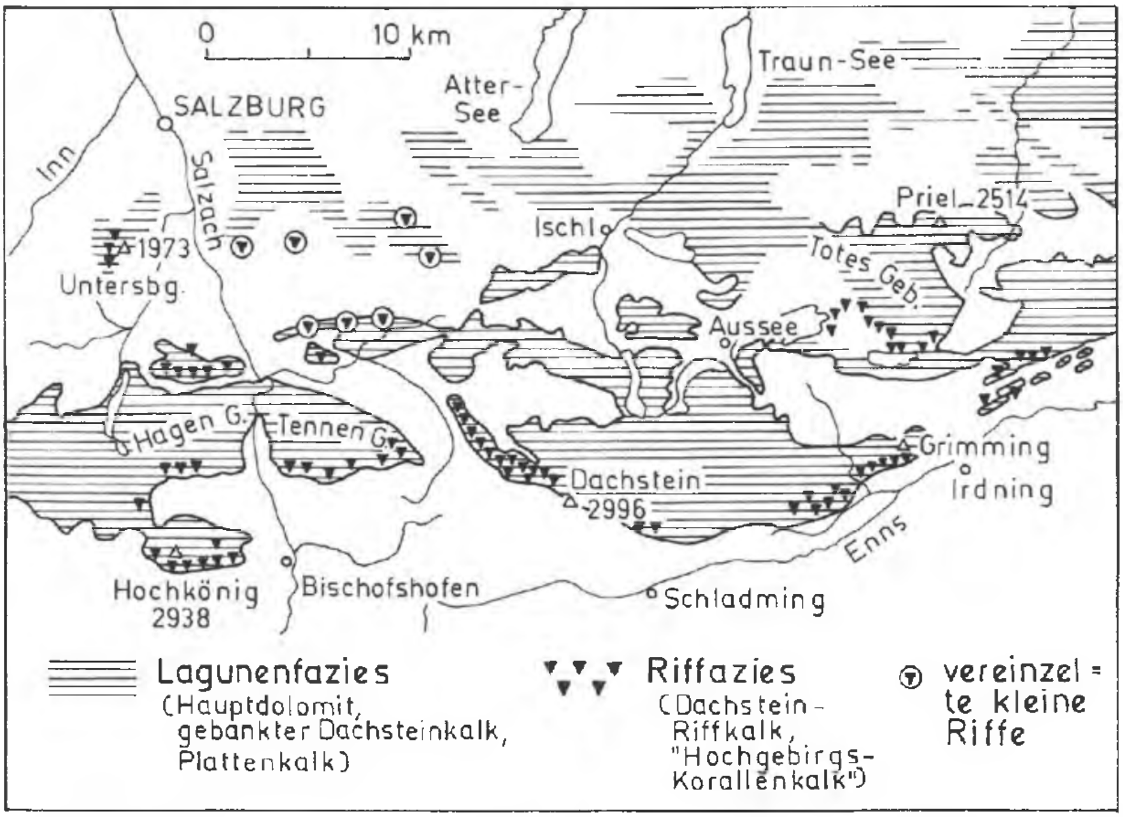

Distribution of Upper Triassic Reefs in the Central Part of the Northern Alps (Flügel, 1981)

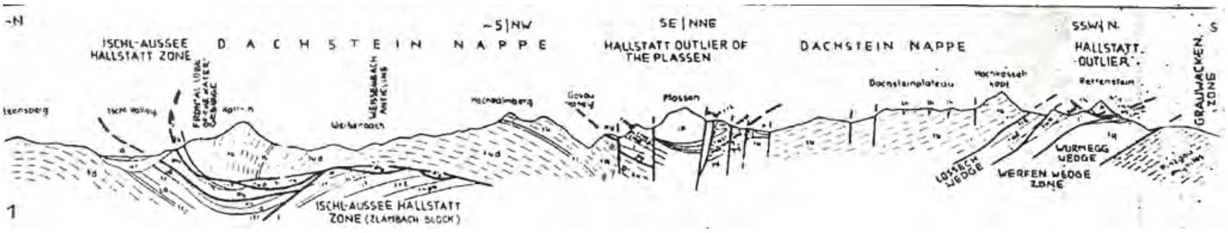

N-S Profile across the Alps (Tollmann, 1976)

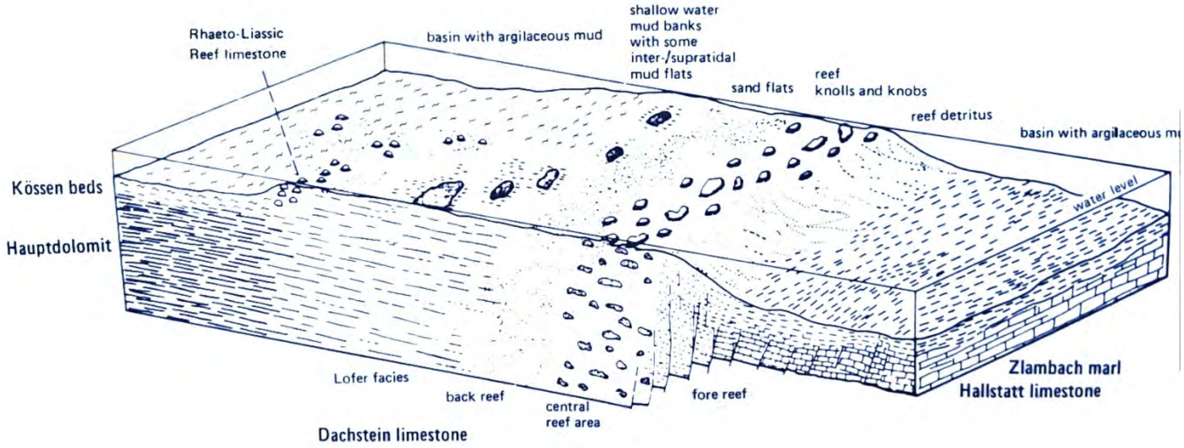

Palaeogeographical interpretation of Upper Triassic sediments before 210 My (Rhät) (Flügel, 1981)

The Dachstein-Formation consists of marine shallow water limestones of the Upper Triassic (Norian to Rhaetian) deposited on the southern margin of the western Tethys and reach a thickness of more than a thousand meters with a high sedimentation rate. Both, the banked lagoon limestone as well as the massive reef limestone were deposited in subtropical latitudes. In the bedded lagoonal limestone, mussels (megalodontids: *Neomegalodon*, *Conchodon* and *Dicerocardium*) and calcareous algae (Dasycladaceae: *Diplopora*, *Heteroporella Solenopora* et al.) are predominant. The main reef builders of the Dachstein reef limestone are corals (*Retiophyllia*, "*Thecosmilia*"; *Astraeomorpha*, *Montlivaltia* et al.) and calcisponges (*Cheilosporites*, *Cryptocoelia*, *Peronidella*, et al.). This geological formation is widespread in the Alps and Carpathians and other Tethyan mountain ranges (e.g. Himalayas).

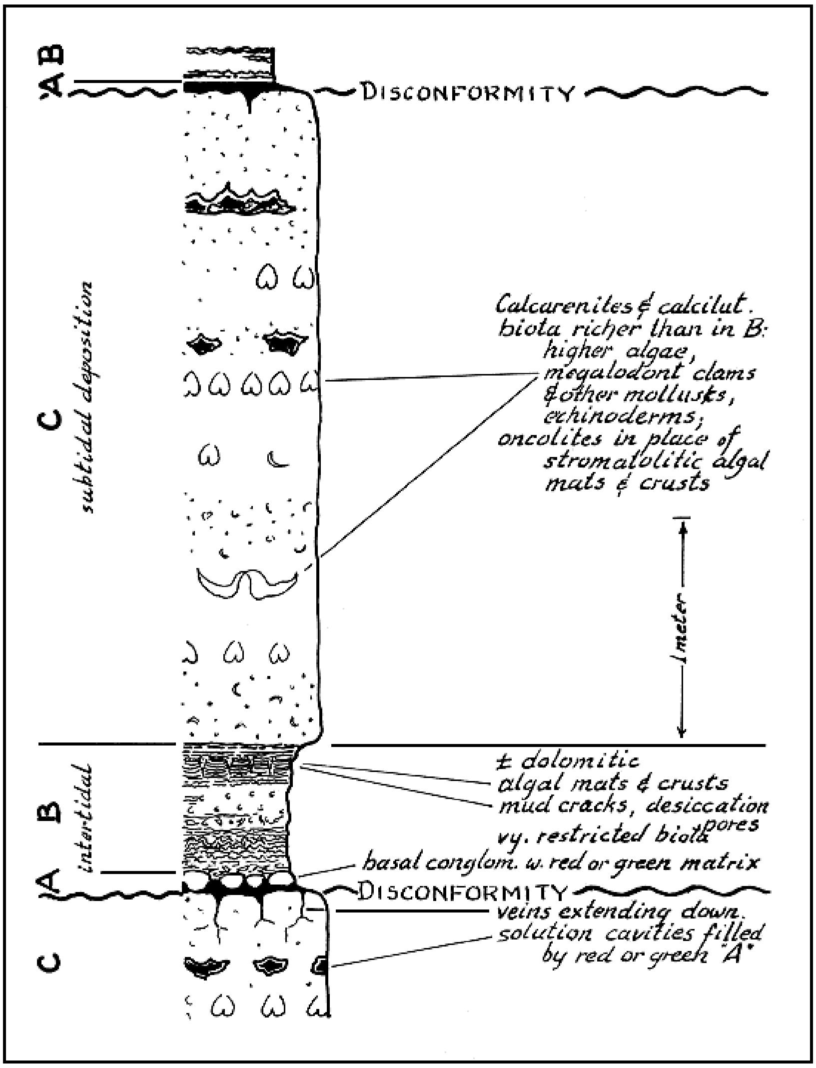

Simplified representation of Lofer cyclothem: **A**) basal, argillaceous member representing reworked residue of weathered material (red or green), commonly confined to cavities in underlying limestone; B) intertidal member of "loferites" with algal mats and abundant desiccation features; C) subtidal "megalodont limestone" member, with cavities produced by desiccation and dissolution succeeding a sea level drop (Fischer, 1964)

Commonly, shallow-water platform carbonates of all ages show repetitive, cyclic patterns. Mechanisms proposed for cycle generation include 1) intrinsic or autocyclic processes and 2) externally imposed or allocyclic processes (Beerbower, 1964), namely eustatic sea-level changes and tectonic pulses (summarized by Enos and Samankassou, 1998). The periodic fluctuation of the Earth's axis inclination, between 22.10 and 24.50 is also considered to drive these cycles, which, for the Dachstein limestones were calculated at 41 kya (Milankovitch cylicity of inclination).

Cross section of Megalodont shells (Zapfe, 1956)

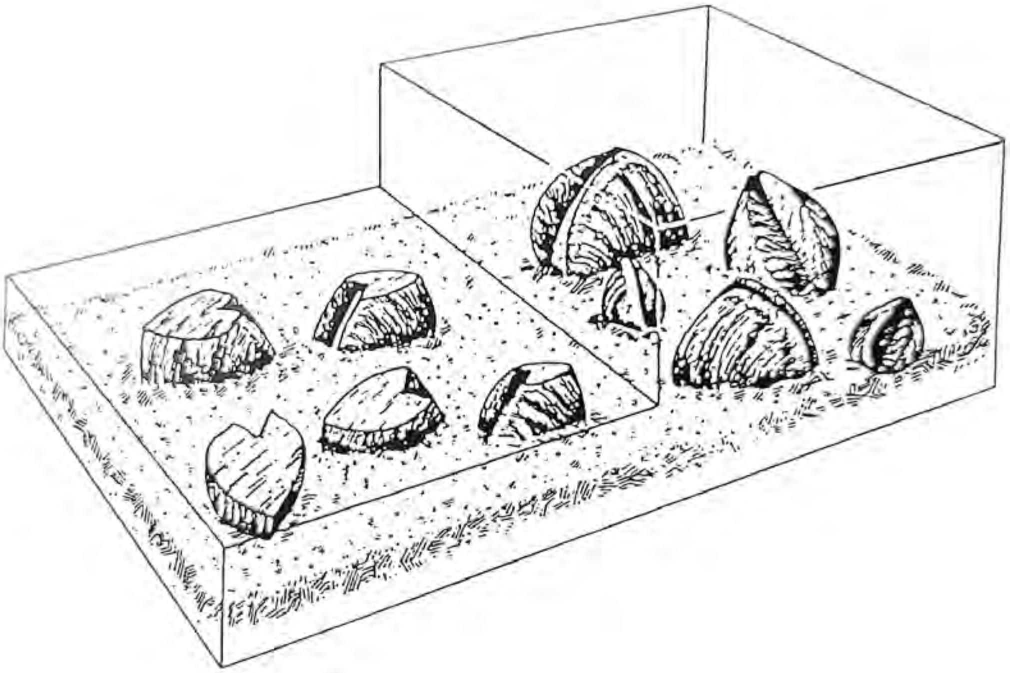

Megalodont pelecypods in life position, Dachstein, (Fischer, 1964)

4.2 Geology of the Hallstatt area

The Hallstatt-Formation is a development of the Hallstatt facies zone in the Northern Limestone Alps. Unlike the overlying shallow water formations, such as the Dachstein limestone, the Hallstatt limestone was formed in basins and associated threshold areas at a depth of about 50 to 200 meters and has a low sedimentation rate.

The sediments are red, grey, white and various shades of micritic limestone with predominantly pelagic fauna and low clay content. The well-known ammonite fauna, is mainly found in layers as well as in syn-sedimentary fissures.

The Hallstatt limestones show a large abundance and diversity of fossils, mainly pelagic cephalopods such as ammonites and nautiloids whose species in the Tethys region often occur worldwide which are used as index fossils. Even gastropod species from Timor can be found in Hallstatt limestone in Austria.

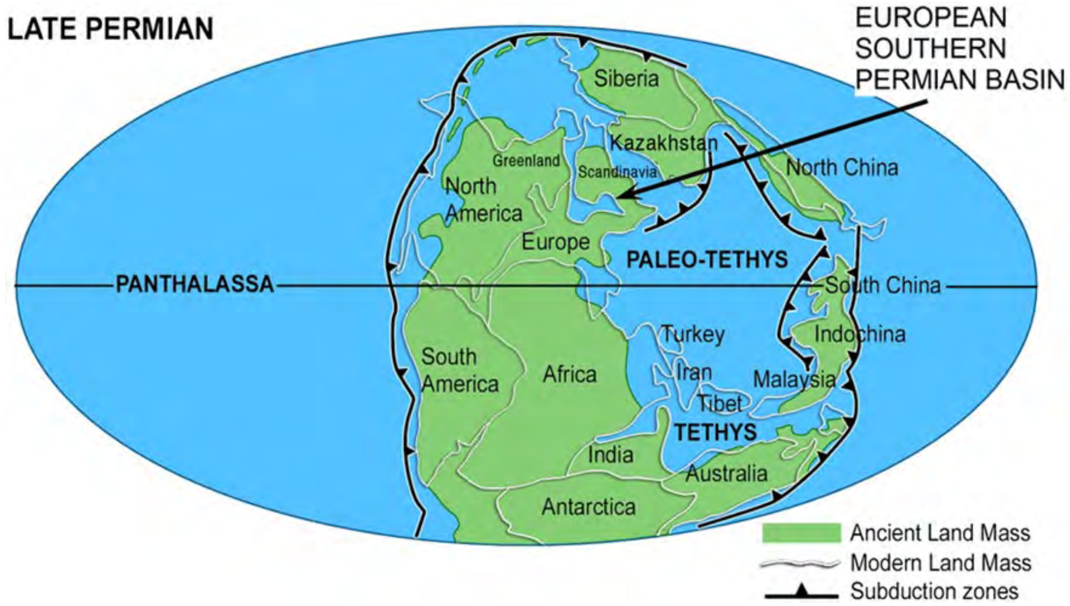

Palaeogeographie of Late Permian (after Scotese, 2002)

4.2.1 The Permian Triassic evaporates

During Phanerozoic times, the concentrations of the main ions present in ocean water as Cl^-, SO_4^{2-}, HCO_3^-, Na^+, K^+, Mg^{2+} and Ca^{2+} have varied significantly. For example, Permian seawater had a SO_4^{2-} concentration similar to that of modern seawater. Sulfate-rich marine waters were generally an exception in the history of the Earth and are restricted to late Precambrian (Vendian), Pennsylvanian–Triassic and Miocene to Quaternary times During such periods, potash deposits formed, which are characterized by the presence of $MgSO_4$ salts, such as polyhalite and kieserite. These periods have alternated with periods characterized by the formation of KCl salts, such as sylvite (KCl), as found in the Cambrian through Mississippian, and Jurassic through Palaeogene.

Sulfate minerals contain besides elements such as calcium, strontium, barium, magnesium and potassium also sulfur, oxygen and, in variable amounts, water. Sulfate evaporitic deposits represent important archives of Earth history, their formation indicating particular basinal and climatic conditions. Isotopic investigations on sulfur and oxygen from sulfate accumulations combined with mineralogical investigations may offer information regarding the origin of fluids, inflows or restricted conditions, evaporative effects, recrystallization and bacterial processes.

The evaporitic Haselgebirge Formation occurs in connection with the Juvavic nappe complex. Some evaporites are also situated in the Tirolic units. The Haselgebirge Formation consists mainly of rock-salt, shales, gypsum and anhydrite and includes the oldest sediments of the NCA. The age of the Haselgebirge Formation, established by using spores and geochronological data is Permian to Early Triassic (Bojar et al., 2018 and references inside).

Some of the conclusions of the isotopic and mineralogical investigations are:

- For the Upper Permian of the Northern Calcareous Alps, the data indicate that the δ34S isotopic composition of sulfates has a maximum ~~maxima~~ of measured values between 11 and 12‰.

The values for the gypsum-type and halite-type deposits are similar, indicating no major fractionation for the different salinity stages of the basin. Bacterial sulfate reduction is supported by the presence of sulfides and sulfur with low and variable $\delta^{34}S$ isotopic composition.

- Lower Triassic, Röt-type sulfates are characterized by a heavy sulfur isotopic composition of c. 26‰. The present study supports the fact that these evaporates were widespread over the entire area of the NCA. Data compilation demonstrates that Röt-type evaporates formed in a large intracratonic stratified sea, with limited connectivity to the ocean.
- The development of the sulfates of Carnian–Norian age from the CAM is more restricted in areal extent, and sulfates are characterized by $\delta^{34}S$ values of c. 15‰.
- The sulfate–sulfide isotope thermometer indicates overprint temperatures of between 215 and 360°C. Microbeam measurements show several generations of sphalerites related to fluctuating liquid chemistry rather than to variation in temperature.

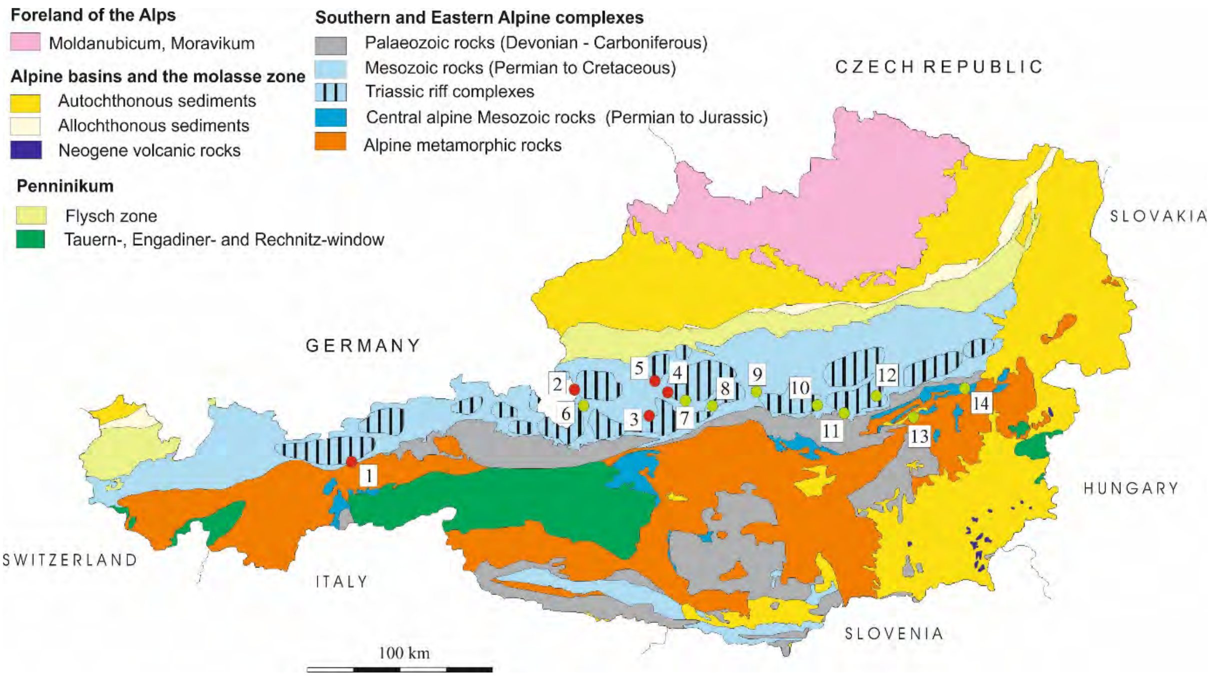

Geological overview of the Eastern Alps showing the distribution of Permian to Triassic sulfate accumulations for which stable isotope compositions were measured. Sulfate accumulations are sometimes associated with salt deposits as for example in Hallstatt (Bojar et al., 2018).

Salt: 1 – Hall in Tirol; 2 – Hallein; 3 – Hallstatt; 4 – Altaussee; 5 – Bad Ischl. Gypsum deposits, Northern Calcareous Alps: 6 – Golling; 7 – Wienern; 8 – Lessern; 9 – Unterlaussa; 10 – Wildalpen; 11 – Tragößß; 12 – Seewiesen. Gypsum deposits, Central Alpine Mesozoic: 13 – Stanz; 14 – Göstritz.

Gypsum, Ca[SO_4]·$2H_2O$; collection Universalmuseum Joanneum

Anhydrite Ca[SO_4], Polyhalite, $K_2Ca_2Mg[SO_4]_4$·$2H_2O$;
collection Universalmuseum Joanneum

Polyhalite, $K_2Ca_2Mg[SO_4]_4$·$2H_2O$, Hallstatt;
collection Universalmuseum Joanneum

Blödite, $Na_2Mg(SO_4)_2 \cdot 4H_2O$, Hallstatt; collection Universalmuseum Joanneum

Langbeinite, $K_2Mg_2[SO_4]_3$, Hallstatt; collection Universalmuseum Joanneum

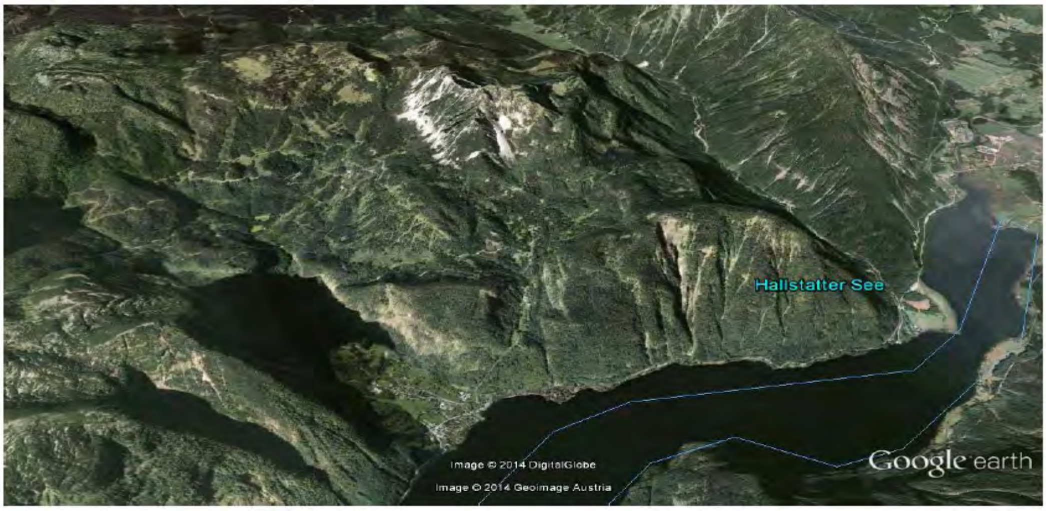

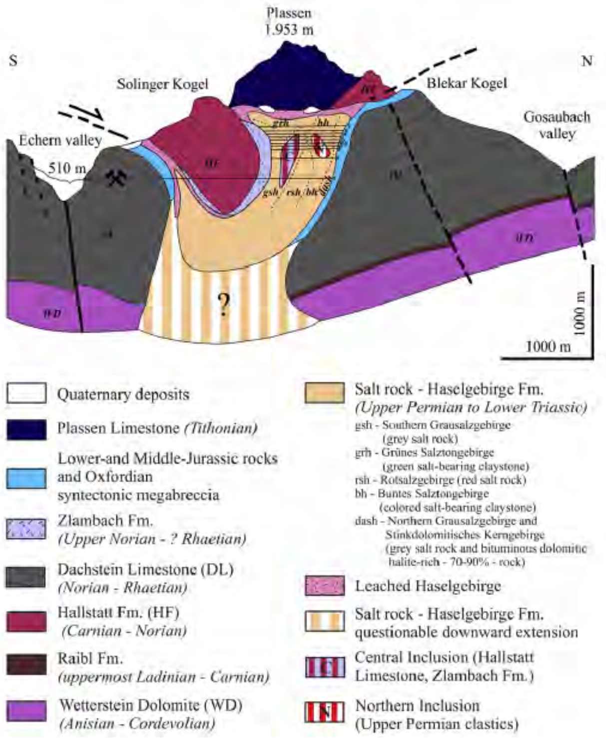

Schematic N-S-trending cross-section through the Hallstatt salt mine (after Schorn, 2013 and references inside)

A further study combined oxygen and sulfate isotope data, with the isotope data of water of crystallization for both gypsum and polyhalite. Generally, in evaporite deposits, minerals precipitate from sea water in reverse order of their solubilities: carbonates first, followed by sulfates, and finally chloride minerals. Polyhalite triple-cationic salt, $K_2Ca_2Mg(SO_4)_4\ 2H_2O$, has a higher solubility than gypsum, polyhalite forming as near end member mineral in evaporite sequences, even after precipitation of halite.

Dehydration temperature of gypsum and polyhalite: Polyhalite loses crystallization water at approximately 285°C, its structure being more stable than that of gypsum, which loses crystallization water at 200°C.

Isotopic composition of water of crystallization and brine: The $\delta^{18}O$ values of calculated brines using water of crystallization (x-axis) versus $\delta^{18}O_{SO4}$ values (y-axis) are displayed in the figure below. Gypsum and polyhalite plot in two distinct groups, with gypsum showing negative oxygen isotope values and polyhalite showing positive values of brines. Considering the measured $\delta^{18}O_{SO4}$ values, the isotopic values of water of crystallisation and the isotherms presented in the figure, we may distinguish between several processes. Oxygen isotopic composition of gypsum shows partial equilibration of sulfate group with local brines, as their $\delta^{18}O_{SO4}$ values are higher than those of the Permian marine sulfate, and this is indicated as “trend 1”. Polyhalites show also a similar trend of partial equilibration between oxygen in the sulfate group with brine oxygen.

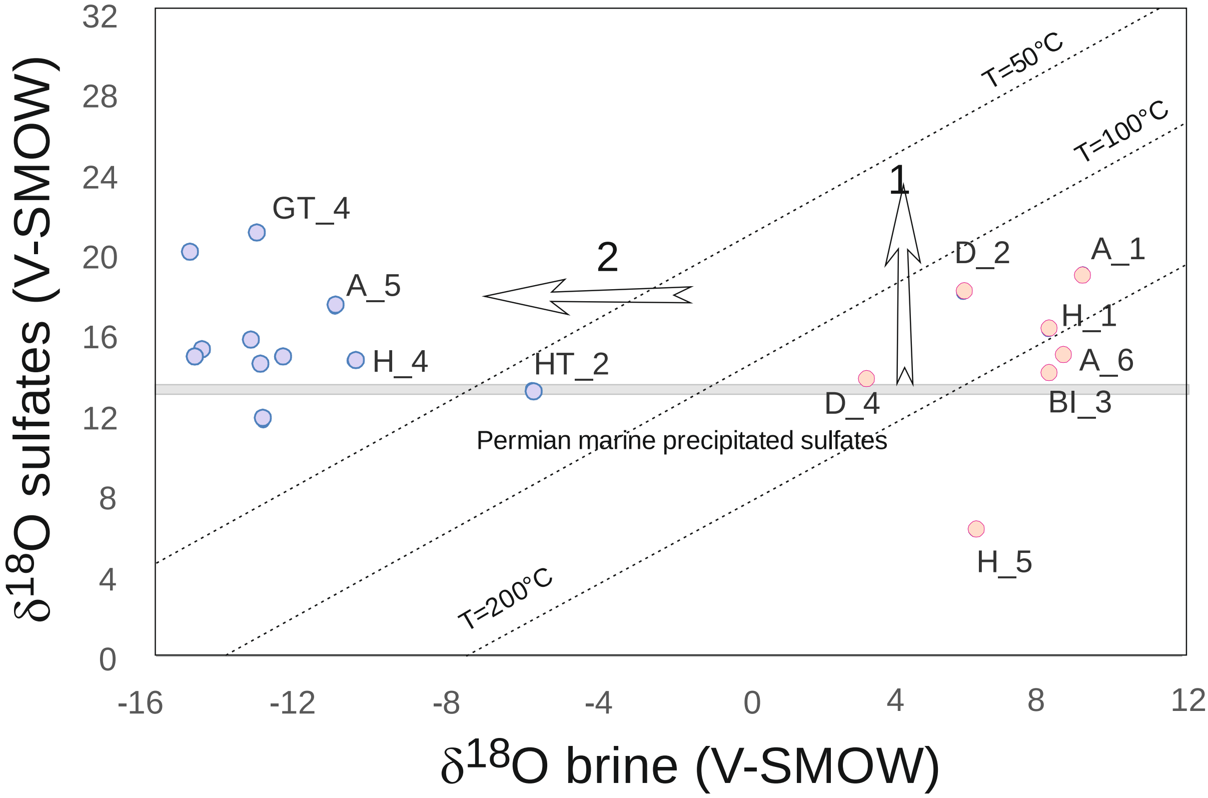

Plot of $\delta^{18}O$ of brines versus $\delta^{18}O_{SO4}$ for the investigated sulfates: blue dots represent gypsum and red polyhalite isotopic compositions. “Trend 1” indicates the thermal event affecting both anhydrite/gypsum and polyhalite $\delta^{18}O_{SO4}$: “trend 2” shows that subsequently crystallization water of gypsum was replaced by meteoric water at low temperature. $\delta^{18}O_{SO4}$ values are the same range for both minerals, gypsum and polyhalite, suggesting that thermal overprint shown by “trend 1” affected both to similar extent. Isotherm calculation was done according to Zeebe (2010). Blue horizontal line represents Permian oxygen isotopic composition in sulfates precipitated from seawater.

Relationship between the measured water of crystallization, calculated brines and local meteoric water line

Alpine overprint temperatures over 200°C were high enough in order to drive dehydration of gypsum to anhydrite. Rehydration to gypsum is possible if fluids are available and temperature falls below the dehydration limit of the mineral. The calculated isotopic compositions of brine (using the oxygen and hydrogen isotopic compositions of gypsum crystallization water) indicate that during rehydration/recrystallization calcium sulfate (gypsum, anhydrite) incorporated meteoric water, as shown in the figure below as “trend 2”. The altitudes from which gypsum samples were collected for this study range between 480 and 970 m. Incorporated meteoric water in gypsum has $\delta^{18}O$ and δD values from -5.7 to -15‰ and -30.9 to-89‰, respectively the isotopic values do not correlate with the altitude of sampling. For similar altitudes, weighted annual mean $\delta^{18}O$ values of present meteoric water are from -10.3 to -10.6‰. These values are higher than those measured for the water of crystallization in the investigated gypsum samples. The water of crystallization for the gypsum samples is also plotting to the left of the Local Meteoric Water Line (LMWL), as the figure below show. It has been documented that late-glacial meteoric water has lower isotopic composition than the late-Holocene one, with $\delta^{18}O_{\text{late-Holocene}} > \delta^{18}O_{\text{late-glacial}}$ by more than 3‰. Moreover, the Younger Dryas period represents the last major period of aquifer refill. In light of these findings, the lower isotopic values of crystallization water of gypsum plotting left of the meteoric water line suggest that meteoric water was incorporated in gypsum in a period cooler and dryer than today, possible during the Younger Dryas, if not earlier. An alternative explanation could consider that gypsum crystallization water records the isotopic signature of meteoric water percolating downward from a much higher elevation than today into subsurface, thereby reaching the sulfate deposit. The incorporation of water characterized by lower isotopic values than present one was put in evidence also for Miocene sulfates.

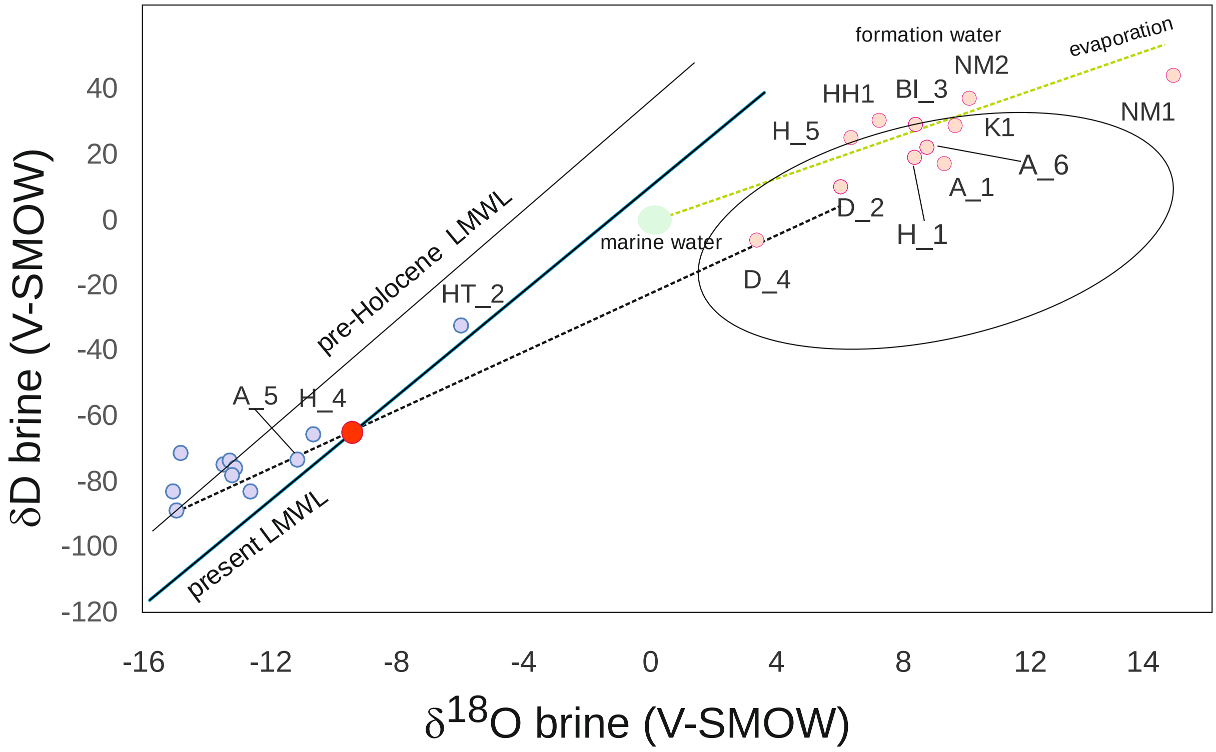

Plot of δD versus $\delta^{18}O$ of brines (blue dots: gypsum crystallization waters; pink dots: polyhalite crystallization waters). The ellipse is displaying the field of syngenetic brines from the Kłodawa salt mine (for details see Dulinski et al., 2014). Other elements displayed are:

- Permian ocean water isotopic composition similar with the present one, Knauth and Beeunas (1986)
- the present Local Meteoric Water Line (LMWL),
- the mean $\delta^{18}O$ value of the present day precipitation (red circle)
- the pre-Holocene meteoric water line showing a similar slope to the present day but with $\delta^{18}O$ mean values with c. 3‰ lower.

- LMWL data according to the IAEA database for the Klagenfurt airport station (IAEA database, 2010), the red point from the LMWL represents the mean value (Bojar et al., 2019).

References geology, paleontology sedimentology

Behm, M. & Hausmann, H. (2007): Eisdickenmessungen in alpinen Höhlen mit Georadar. - Die Höhle, 58, 3-11, Wien.

Bock, H., Lahner, G. & Gaunersdorfer, G. (1913): Höhlen im Dachstein und ihre Bedeutung für die Geologie, Karsthydrographie und die Theorien über die Entstehung des Höhleneises. Dem Andenken weiland Prof. Friedrich Simonys gewidmet. – vii, 151 S., 1 Karte, Verlag f. Höhlenkunde in Österreich: Dt. Vereinsdruckerei, Graz.

Bouchal, R. & Wirth, J. (2001): Höhlenführer Österreich – Über 100 Höhlen mit Skizzen, Plänen, Zugangsbeschreibungen und 150 Fotos. Pichler Verlag, Wien, ISBN 3-85431-234-2.

Enos, P. & Samankassou, E. (1998): Lofer cyclothems revisited (Late triassic, Northern Alps, Austria). Facies, 38, 207–227, Springer Verlag, doi: 10.1007/BF02537366.

Enos, P., & Samankassou, E. (2002). Lateral variations in Dachstein Limestone (Triassic, Austria) (abs). 16th International Sedimentological Congress (Johannesburg, South Africa), Abs. Vol., 88.

Enos, P. and Samankassou, E. (2021): Florida Bay: Modern analogue for Lofer cyclothems? – Sedimentology, 69 (1), DOI: 10.1111/sed.12918

Fernandez, O., Grasemann, B. & Sanders, D. (2022): Deformation of the Dachstein Limestone in the Dachstein thrust sheet (Eastern Alps, Austria). – Austrian Journal of Earth Sciences, 115 (1), 167-190, Wien, doi: 10.17738/ajes.2022.0008

Fischer, A.G. (1964):The Lofer Cyclothems of the Alpine Triassic. - Kansas Geological Survey Bulletin, 169, 107-149, 38 Abb., Lawrence.

Flügel, E. (Ed.) (1981): International Symposium on Triassic Reefs, Erlangen. Guide Book. – 252 S., ill., Institut für Paläontologie der Universität Erlangen-Nürnberg.

Ganss, O., Kümel, F. & Spengler, E. (1954): Erläuterungen zur geologischen Karte der Dachsteingruppe. – Wissenschaftl. Alpenvereinshefte, Heft 15, 82 S., 3 Abb., 6 Taf., Universitätsverlag Wagner, Innsbruck.

Goldhammer, R.K., Dunn, P.A, & Hardie, L.A. (1990): Depositional cycles, composite sea-level changes, cycle stacking patterns, and the hierarchy of stratigraphic forcing: examples from Alpine Triassic platform carbonates.—Geological Society of America Bulletin, 102, 535–562. Boulder.

Haas, J., Lobitzer, H. & Monostori, M. (2007): Characteristics of the Lofer Cyclicity in the type locality of the Dachstein Limestone (Dachstein Plateau, Austria). - Facies 53: 113–126, Springer Verlag.

Haas, J.H. (2008): Excursion 2: Characteristic features of the Lofer cyclicity on the Dachstein Plateau (Austria). Berichte der Geologischen Bundesanstalt, 76, 99-110, Wien.

Henne, P., Krauthausen, B. & Stummer, G. (1994): Höhlen im Dachstein. Derzeitiger Forschungsstand, Anlage der Riesenhöhlensysteme am Dachstein-Nordrand und

Bewertung der unterirdischen Abflußverhältnisse. – Die Höhle, Zeitschrift für Karst- und Höhlenkunde, 45, 48-67. 11 Abb., Wien.

Lobitzer, H. (2013): Geologische Spaziergänge: Rund um den Hallstätter See - Salzkammergut. - Verlag der Geologischen Bundesanstalt in Wien. Wien. [ISBN 978-3-85316-068-8].

Mandl, G.W., Husen, D. van & Lobitzer, H. (2012): Erläuterungen zu Blatt 69: Bad Ischl. – 216 S., 29 Abb., 10 Tab., 4 Falttaf., Geologische Bundesanstalt. Wien.

Pfarr, T. & Stummer, G. (1988): Die längsten und tiefsten Höhlen Österreichs. - Wissenschaftliche Beihefte zur Zeitschrift „Die Höhle“, 35, XXIV+248 S., zahlreich Pläne und Faltpläne.

Richolz, S., Krystyn, L., Hillebrandt, A. v. & Martindale, R. (2012): End-Triassic crisis events recorded in platform and basin of the Austrian Alps. The Triassic/Jurassic and Norian/Rhaetian. - Field Trip Guide 29th IAS Meeting of Sedimentology Schladming/Austria, Journal of Alpine Geology, 54, 323-377, 54 figs., Wien.

Rupp, Ch., Linner, M. & Mandl, G.W. (Redaktion) (2011): Geologische Karte von Oberösterreich 1:200.000, Erläuterungen. - 255 S., 31 Abb., 4 Tab., 9 Farbtaf., Geol. Bundesanst. Wien.

Samankassou, E. & Enos, P. (2019): Lateral facies variations in the Triassic Dachstein platform: A challenge for cyclostratigraphy. – The Depositional Record. The Journal of the International Association of Sedimentology, 5 (3), 469-485, 8 figs., 4 tab., Wiley.

Schauberger, O. (1955): Zur Genese des alpinen Haselgebirges. – Z. dt. Geol. Ges., 105, 736-751, 2 Abb., Taf. 28-30, Hannover.

Scheidleder, E. et al. (2001): Pilotprojekt „Karstwasser Dachstein“: Karsthydrologie und Kontaminationsrisiko von Quellen. – Archiv für Lagestättenforschung, 21, 155 S., 46 Abb., Wien

Schmeidl, H. (1969): Zur pollenanalytischen Altersbestimmung der Eisbildungen In der Schellenberger Eishöhle und in der Dachstein-Rieseneishöhle. - Jahrbuch des Vereins zum Schutze der Alpenpflanzen und -Tiere, 34, 67-84, München.

Tichy, G. (1979): Gastropoden aus den indonesischen Kalkblöcken von Baoen (Baung) in West-Timor (Indonesien). - Beiträge zur Paläontologie von Österreich, 6, 11-121, 1 Abb., 2 Taf., Wien.

Tollmann, A. (1976): Analyse des klassischen nordalpinen Mesozoikums. Stratigraphie, Fauna und Fazies der Nördlichen Kalkalpen. – 580 S., 256 Abb., 3 Taf., Verlag Deuticke, Wien.

Weingartner, H. (Ed.) (2006): Lehrpfad Hallstätter Gletscher. Ein Begleiter durch die Gebirgslandschaft am Dachstein. – 123 S., 61 Abb., Land Oberösterreich, Naturschutzabt., Linz.

Zapfe, H. (1956): Dachsteinkalk und „Dachsteinmuscheln". - Natur und Volk, 87, 87-94, 7 Abb., Frankfurt/M.

References evaporites

Bojar, A.-V., Hałas, S., Bojar, H.-P., Trembaczowski, A., (2018). Late Permian to Triassic isotope composition of sulfates in the Eastern Alps: palaeogeographic implications. - Geological Magazine, 155(4), 797-810.

Bojar, A.-V., Hałas, S., Bojar, H.-P., Trembaczowski, A., (2019). Multiple isotope tracers from Permian-Triassic hydrated sulfates: implications for fluid-mineral interaction

(Traceurs isotopiques multiples à partir de sulfates hydratés de Permien-Trias: implications pour l'interaction fluide-minéral). - Bulletin de la Société Géologique de France 190/11, doi.org/10.1051/bsgf/2019010

Boschetti, T., Cortecci, G., Toscani, L., Iacumin, P. (2011). Sulfur and oxygen isotope compositions of Upper Triassic sulfates from northern Apennines (Italy): paleogeographic and hydrogeochemical implications. Geologica Acta 9, 129-147.

Böttcher, M.E., Brumsack, H.J., Dürselen, D. (2007). The isotopic composition of modern seawater sulfate: I. Coastal waters with special regard to the North Sea. Journal of Marine Geology 67, 73–82.

Canfield, D.E. (2001). Biogeochemistry of Sulphur Isotopes. In: Valley, J.W., Cole, D.R. (eds.), Stable Isotope Geochemistry. Reviews in Mineralogy & Geochemistry 43, 579-606.

Claypool, G.E., Holser, W.T., Kaplan, I.R., Sakai, H., Zak, I. (1980). The age curves of sulfur and oxygen isotopes in marine sulfate and their mutual interpretation. Chemical Geology 28, 199-260.

Chiba, H., Sakai, H. (1985). Oxygen isotope exchange rate between dissolved sulfate and water at hydrothermal temperatures. Geochimica et Cosmochimica Acta 49, 993-1000.

Cortecci, G., Reyes, E., Berti, G., Casati, P. (1981). Sulfur and oxygen isotopes in Italian marine sulfates of Permian and Triassic ages. Chemical Geology 34, 65-79.

Dulinski, M., Rózanski, K., Brudnik, K., Kolonko, P. and Tadych, J., (2014). Isotope monitoring of water appearances in salt mines: The Polish experience. Radioactive Waste Management Committee Natural Analogues for Safety Cases of Repositories in Rock Salt "Salt Club" Workshop Proceedings, 123-132.

Erkan, E. (1989). Die Sulfatlagerstätten der postvariszischen Transgressionsserie in den Ostalpen. Nachrichten der Deutschen Geologischen Gesellschaft 41, 90-91.

Flügel, H.W., Neubauer, F., (1984). Steiermark Geologie der österreichischen Bundesländer in kurzgefassten Einzeldarstellungen. Geologische Bundesanstalt, Vienna, 127 S.

Fontes, J.C., Gonfiantini, R., (1967). Fractionment isotopique de l´hydrogene dans l´eau de crystallization du gypse. Comptes Rendue de l´Academie de Sciences, Paris, 265, 2-4.

Fritz, P., Basharmal, G.M., Drimmie, R.J., Ibsen, J., Qureshi, R.M. (1989). Oxygen isotope exchange between sulfate and water during bacterial reduction of sulfate. Chemical Geology, Isotope Geoscience Section 79, 99-105.

García-Veigas, J., Cendón, D.I., Pueyo, J.J., Peryt, T.M. (2011). Zechstein saline brines in Poland, evidence of overturned anoxic ocean during the Late Permian mass extinction event. Chemical Geology 290, 189-201.

Gawlik, H.-J., Lein, R., Piros, O., Pytel, C. (1999). Zur Stratigraphie und Tektonik des Hallein – Bad Dürrnberger Salzberges – Neuergebnisse auf der Basis von stratigraphischen und faziellen Daten (Nördliche Kalkalpen, Salzburg). Abhandlungen der Geologischen Bundesanstalt 56/2, 69-90.

Gawlik, H.-J., Lein, R., Schlagintweit, F., Suzuki, H., Wegerer, E. (2001). Der Hallstätter Salzberg und sein geologischer Rahmen - Geschichte und Stand der Erforschung, Interpretationen und neue Ergebnisse. Berichte der Geologischen Bundesanstalt 56, 45-49.

Gonfiantini, R., Fontes, J.C. (1963). Oxygen isotopic fractionation in the water of crystallisation of gypsum. Nature 200, 644–646.

Götzinger, M.A., Pak, E. (1983). Zur Schwefelisotopenverteilung in Sulfid- und Sulfatmineralen triadischer Gesteine der Kalkalpen, Österreich. Mitteilungen der Gesellschaft der Geologie- und Bergbaustudenten Österreichs 29, 191-198.

Haditsch, J.G. (1968). Bemerkungen zu einigen Mineralien (Devillin, Bleiglanz, Magnesit) aus der Gips-Anhydrit-Lagerstätte Wienern am Grundlsee. Archiv für Lagerstättenforschung in den Ostalpen 7, 54-76.

Hagenguth, G. (1988). Die Gipsvorkommen bei Edelsdorf im Stanzertal (Steiermark). Archiv für Lagerstättenforschung der Geologischen Bundesanstalt 9, 47-58.

Hałas, S. (1987). Oxygen and sulphur isotope ratios of sulphate minerals in native sulphur deposits. Isotopenpraxis 23/7, 282-283.

Hałas, S., Pluta, I. (2000). Empirical calibration of isotope thermometer $\delta^{18}O$ (SO_4^{2-}) - $\delta^{18}O(H_2O)$ for low temperature brines. ESIR Isotope Workshop V, 1-6 July 2000, Kraków, Poland, Book of Abstracts, 68-71.

Hałas, S., Bojar, A.-V., Peryt, T.M., (2015). Oxygen isotopes in authigenic quartz from massive salt deposits. Chemical Geology, 402, 1-5.

Hałas, S., Krouse, H.R. (1982). Isotopic abundances of water of crystallization of gypsum from the Miocene evaporite formation, Carpathian Foredeep, Poland. Geochimica Cosmochimica Acta, 46, 293-296.

Hardie, L.A. (1996). Secular variation in seawater chemistry: An explanation for the coupled secular variation in the mineralogies of marine limestones and potash evaporites over the past 600 m.y. Geology 24, 279-283.

Holland, H.D. (2005). Sea level, sediments and the composition of seawater. American Journal of Science 305, 220-239.

Holser, W.T. (1977). Catastrophic chemical events in the history of ocean. Nature 267, 403-408.

Holser, W.T., Kaplan, I.R., Sakai, H., Zak, I. (1979). Isotope geochemistry of oxygen in the sedimentary sulfate cycle. Chemical Geology 25, 1-17.

Horita, J. 1989. Stable isotope fractionation factors of water in hydrated saline mineral-brine system. Earth and Planetary Science Letters, 95, 173-179.

IAEA/WMO (2010). Global Network of Isotopes in Precipitation: The GNIP Database, available at: http://www.iaea.org/water (last access: 20 June 2017).

Kajiwara, Y, Krouse, H.R. (1971). Sulfur Isotope partitioning in metallic sulfide systems. Canadian Journal of Earth Sciences 8/11, 1397-1408.

Kampschulte, A., Strauss, H. (2004). The sulfur isotopic evolution of Phanerozoic seawater based on the analysis of structurally substituted sulfate in carbonates. Chemical Geology 204, 255-286.

Knauth, L. P., Beeunas, M. A. (1986). Isotope geochemistry of fluid inclusions in Permian halite with implications for the isotopic history of ocean water and the origin of saline formation waters. *Geochimica et Cosmochimica Acta*, **50/3**, 419-433.

Kirchner, E. (1987). Die Mineral- und Gesteinsvorkommen in den Gipslagerstätten der Lammermasse, innerhalb der Hallstattzone, Salzburg. Jahrbuch Haus der Natur 10, 156-167.

Klaus, W, Pak, E. (1974). Neue Beiträge zur Datierung von Evaporiten des Ober-Perm. Carinthia II 164/84, 79-85.

Kovalevich, V.M., Peryt, T.M., Petrichenko, O.I. (1998). Secular variation in seawater chemistry during the Phanerozoic as indicated by brine inclusions in halite. Journal of Geology 106, 695–712.

Kovalevych, V., Peryt, T.M., Beer, W., Geluk, M., Hałas, S.(2002). Geochemistry of Early Triassic seawater as indicated by study of the Röt halite in the Netherlands, Germany, and Poland. Chemical Geology 182, 549–563

Kucha, H., Schroll, E., Raith J.G., Hałas, S. (2010). Microbial Sphalerite Formation in Carbonate-Hosted Zn-Pb Ores, Bleiberg, Austria: Micro- to Nanotextural and Sulfur Isotope Evidence. Economic Geology 105, 1005-1023.

Leitner, C., Neubauer, F. (2011). Tectonic significance of structures within the salt deposits Altaussee and Berchtesgaden–Bad Dürrnberg, Northern Calcareous Alps. Austrian Journal of Earth Sciences 104/2, 2-21.

Leitner, C., Neubauer, F., Genser, J., Borojevic-Sostaric, B., Rantitsch, G. (2013). ^{40}Ar/^{39}Ar ages of recrystallization of rock-forming polyhalite in Alpine rocksalt deposits. In: Jordan, F., Mark, D.F., Verati C. (eds.), Advances in ^{40}Ar/^{39}Ar Dating: from Archaeology to Planetary Sciences. Geological Society, London, Special Publications 378, 207-244.

Lloyd, R. M. (1968). Oxygen isotope behaviour in the sulfate-water system. Journal of Geophysical Research 73, 6099-6110.

Longinelli, A., Craig, H. (1967). Oxygen-18 variation in sulphate ions in sea water and saline lakes. Science 146, 56-59.

Longinelli, A. (1983). Oxygen-18 and sulphur-34 in dissolved oceanic sulphate and phosphate. In: Fritz, P. and Fontes, J. C. (eds.), The Marine Environment, 219–255. Handbook of Environmental Isotope Geochemistry, Amsterdam, Elsevier.

Longinelli, A., Flora, O. (2007). Isotopic composition of gypsum samples of Permian and Triassic age from the north-eastern Italian Alps. Palaeoenvironmental implications. Chemical Geology 245, 275-284.

Lowenstein, T.K., Hardie L.A., Timofeeff M.N., Demicco R.V. (2003). Secular variation in seawater chemistry and the origin of calcium chloride basinal brines. Geology 31, 857-860. In: Holland H.D., Turekian K.K. (eds.), The Oceans and Marine Geochemistry. Treatise on Geochemistry 2nd Edition, Vol. 8, (), Elsevier, 569-622.

Niedermayr, G., Beran, A., Brandstätter, F. (1989). Diagenetic type magnesits in the Permo-Scythian rocks of the Eastern Alps, Austria. In Möller, P. (ed.), Magnesite Geology, Mineralogy, Geochemistry, Formation of Mg-Carbonates, Monograph Series on Mineral Deposits, Gebrüder Bornträger Berlin Stuttgart, 35-59.

Ohmoto, H. 1986. Stable isotope geochemistry of ore deposits. In: Valley, J.W., Taylor, H.P. Jr., O'Neil, J.R. (eds.), Stable Isotopes in High Temperature Geological Processes. Reviews in Mineralogy 16, 491-560.

Ohmoto, H., Rye, R.O. 1979. Isotopes of sulfur and carbon. In: Barnes, H.L. (ed.), Geochemistry of hydrothermal ore deposits, J. Whiley & Sons, 517-612.

Paytan, A., Kastner, M., Campell, D., Thiemens, M.H. 2004. Seawater sulfur isotope fluctuations in the Cretaceous. Science 304, 1663-1665.

Pak, E., Schauberger, O. (1981). Die geologische Datierung der ostalpinen Salzlagerstätten mittels Schwefelisotopenuntersuchungen. Verhandlungen der Geologischen Bundesanstalt, 185-192.

Payne, J.L., Lehrmann, D.J., Wei, J., Orchard, M.J., Schrag, D.P., Knoll, A.H. (2004). Large perturbations of the carbon cycle during recovery from the end-Permian extinction. Science 305, 506–509.

Peryt, T.M., Hałas, S., Hryniv, S.P. (2010). Sulphur and oxygen isotope signatures of late Permian Zechstein anhydrites, West Poland: seawater evolution and diagenetic constraints. Geological Quarterly 54/4, 387-400.

Postl, W. (1990). Enargit und Parnauit aus dem Gips- und Anhydritbergbau Tragößß-Oberort, Steiermark. In: Niedermayr, G. et al.: Neue Mineralfunde aus Österreich XXXIX. Carinthia II 180/100, 277.

Rey, K., Amiot, Fourel, F., Rigaudier, T., Abdala, F., Day, M.O., Fernandez, V., Fluteau, F., France-Lanord, C., Rubidge, B.S., Smith, R.M., Viglietti, P.A., Zipfel, B., Lecuyer, C. (2015). Global climate perturbations during the Permo-Triassic mass extinctions recorded by continental tetrapods from South Africa. Gondwana Research, http://dx.doi.org/10.1016/j.gr.2015.09.008.

Schauberger, O. (1986). Bau und Bildung der Salzlagerstätten des ostalpinen Salinars. Archiv für Lagerstättenforschung der Geologischen Bundesanstalt 7, 217-254.

Schorn, A., Neubauer, F., Genser, J., Bernroider, M. (2013). The Haselgebirge evaporitic mélange in central Norhtern Calcareous Alps (Austria): part of the Permian to Lower Triassic rift of the Meliata ocean? Tectonophysics 583, 28-48.

Scholle, P.A. (1995). Carbon and sulfur isotope stratigraphy of the Permian and adjacent intervals. In: Scholle, P.A., Peryt, T.M., Ulmer Scholle, D.S. (eds.), The Permian of Northern Pangea, vol. 1, Springer, Berlin, 133–149.

Scotese, C.R., (2002). Paleomap Project. http://www.scotese.com

Seal, R.R., II, Alpers, C.N., Rye, R.O. (2000). Stable isotope systematics of sulfate minerals. In: Sulfate Minerals, Crystallography, Geochemistry and Environmental Significance, Alpers, C.N., Jambor, J.L., Nordstrom, D.K., (eds.). Reviews in Mineralogy & Geochemistry, 40, 541-602.

Spötl, C. (1989). The Alpine Haselgebirge Formation, Northern Calcareous Alps (Austria): Permo-Scythian evaporites in an alpine thrust system. Sedimentary Geology 65, 113-125.

Spötl, C., Pak, E. (1996). A strontium and sulfur isotopic study of Permo-Triassic evaporites in the Northern Calcareous Alps. Chemical Geology 131, 219-234.

Song, H., Wignall, P.B., Tong, J., Bond, D.P.G., Song, H., Lai, X., Zhang, K., Wang, H., Chen, Y. (2012). Geochemical evidence from bio-apatite for multiple oceanic anoxic events during Permian–Triassic transition and the link with end-Permian extinction and recovery. Earth and Planetary Science Letters 353, 12-21.

Strauss, H. (1997). The isotopic composition of sedimentary sulfur through time. Palaeogeography, Palaeoclimatology, Palaeoecology 132, 97-118.

Syverson, D.D., Ono, S., Shanks, W.C., Seyfried, W.E. (2015). Multiple sulfur isotope fractionation and mass transfer processes during pyrite precipitation and recrystallization: An experimental study at 300 and 350°C. Geochimica et Cosmochimica Acta 165, 418-434.

Tollmann, A. (1977). Geologie von Österreich. Band 1. Die Zentralalpen. Deuticke, Wien, 766 pp.

Weber, L. (ed.) (1997). Handbuch der Lagerstätten, der Erze, Industrieminerale und Energierohstoffe Österreichs. Archiv für Lagerstättenforschung der Geologischen Bundesanstalt 19, 607 pp.

Zeebe, R.E. (2010). A new value for the stable oxygen isotope fractionation between dissolved sulfate ion and water. Geochimica et Cosmochimica Acta 74, 818–828.

Geological maps

Ganss, O., Kümel, F. & Spengler, E. (1954): Geologischen Karte der Dachsteingruppe 1: 25.000.

Krenmayr, H.-G., Schnabl, W. & Reitner, J. (Koord.) (2006): Geologische Karte von Oberösterreich 1: 200.000, Geologische Bundesanstalt, Wien.

Mandl, G.W. (1998): Geologische Karte der Dachsteinregion mit Erläuterungen 1: 50.000, und Profile zur geologischen Karte der Dachsteinregion (17 Profile), Geologische Bundesanstalt, Wien.

Mandl, G.W. (2001): Geologische Karte der Dachsteinregion 1: 50.000 mit Erläuterungen. – Archiv für Lagerstättenforschung, Geologische Bundesanstalt, Wien.

Schäffer, G. (1982): Geologische Karte der Republik Österreich 1: 50.000, Bl. 96 Bad Ischl, Geologische Bundesanstalt, Wien. (→mit Erläuterungen: Mandl et al. 2012)

Schubert, G. & Berka, R. (Bearbeitung) (2007): Hydrogeologische Karte von Oberösterreich 1: 200.000. – Geologische Bundesanstalt, Wien.

Spengler, E. (Leitung) u. Bearbeitung von Ganss, O., Kümel, F. & Neumann, G. (1937): Geologische Karte der Dachsteingruppe 1: 25.000, Deutscher Alpenverein u. Verlag Gebrüder Borntraeger, Berlin.

List of participants

Family/First Name	email	Institution	City	Country
Armstrong Garry	sales@sercongroup.com	Sercon Limited	Crewe	UK
Barisevičiūtė Ruta	ruta.bariseviciute@ftmc.lt	State research institute Center for Physical Sciences and Technology	Vilnius	Lithuania
Boglárka Kis	boglarka.kis@ubbcluj.ro	Babes-Bolyai University	Cluj-Napoca	Romania
Bojar Ana-Voica	ana-voica.bojar@plus.ac.at	Salzburg University	Salzburg	Austria
Bojar Hans-Peter	hans-peter.bojar@museum-joanneum.at	Universalmuseum Joanneum, Natural Sciences	Graz	Austria
Bojar Silvia			Graz	Austria
Botoran Oana Romina	oana.dinca@icsi.ro	National Research and Development Institute for Cryogenics and Isotopic Technologies	Râmnicu Valcea	Romania
Böttcher Michael E.	michael.boettcher@io-warnemuende.de	Leibniz Instsitute for Baltic Sea Research, University of Greifswald	Warnemünde	Germany
Bozau Elke	elke.bozau@tu-clausthal.de	IGP, TU Clausthal	Clausthal-Zellerfeld	Germany
Costinel Diana	diana.costinel@icsi.ro	National R&D Institute for Cryogenics and Isotopic Technologies - ICSI Rm.Valcea	Râmnicu Vâlcea	Romania
Czébely Andrea	czebelyandrea@isotoptech.hu	University of Debrecen, Doctoral School of Earth Sciences	Debrecen	Hungary
Czuppon György	czuppon.gyorgy@csfk.org	Research Centre for Astronomy and Earth Sciences	Budapest	Hungary

Deb Sushmita	sushmita.deb@uwr.edu.pl	Institute of Geological Sciences, Wroclaw University	Wrocław	Poland
Drzewicki Wojciech	wojciech.drzewicki@uwr.edu.pl	Institute of Geological Sciences, Wroclaw University	Wrocław	Poland
Făurescu Ionuț	ionut.faurescu@icsi.ro	National Research and Development Institute for Cryogenics and Isotopic Technologies	Râmnicu Vâlcea	Romania
Fórizs István	forizs@geochem.hu	Institute for Geological and Geochemical Research, CSFK	Budapest	Hungary
Futó István	futo.istvan@atomki.hu	Institute for Nuclear Research	Debrecen	Hungary
Gebus-Czupyt Beata	b.gebus@twarda.pan.pl	Institute of Geological Sciences Polish Academy of Sciences	Warsaw	Poland
Green Damon	damon.green@teledyne.com	Teledyne Photon Machines	Kirkby Stephen	UK
Ionete Roxana Elena	roxana.ionete@icsi.ro	National Research and Development Institute for Cryogenics and Isotopic Technologies	Râmnicu Vâlcea	Romania
Jakubiak Marta	marta.jakubiak@uwr.edu.pl	University of Wroclaw	Wroclaw	Poland
Jędrysek Mariusz Orion	mariusz.jedrysek@uwr.edu.pl	University of Wroclaw	Wrocław	Poland
Kanduč Tjaša	tjasa.kanduc@ijs.si	Jožef Stefan Institute	Ljubljana	Slovenia
Kerstel Erik	erik.kerstel@univ-grenoble-alpes.fr	Université Grenoble Alpes, Laboratory for Interdisciplinary Physics	Grenoble	France
Kiss Gabriella	kiss.gabriella@atomki.hu	Institute for Nuclear Research	Debrecen	Hungary

Kozar Logar	Jasmina	Jožef Stefan Institute	Ljubljana	Slovenia
Krztoń Wojciech	krzton@iop.krakow.pl	Institute of Nature Conservation, Polish Academy of Sciences	Kraków	Poland
Kukla Jaroslav	jaroslav.kukla@natur.cuni.cz	Institute for Environmental Studies, Faculty of Science, Charles University	Prague	Czech Republic
László Elemér	laszlo.elemer@atomki.hu	Institute for Nuclear Research	Debrecen	Hungary
Lécuyer Christophe	christophe.lecuyer@univ-lyon1.fr	University Claude Bernard Lyon 1	Villeurbanne	France
Lewicka-Szczebak Dominika	dominika.lewicka-szczebak@uwr.edu.pl	Institute of Geological Sciences, University of Wrocław	Wrocław	Poland
Pușcaș Montana Cristina	montana.puscas@terraanalitic.ro	Terra Analytic	Alba-Iulia	Romania
Moser Bernd	bernd.moser@museum-joanneum.at	Universalmuseum Joanneum, Natural Sciences	Graz	Austria
Neubauer Franz	franz.neubauer@plus.ac.at	Salzburg University	Salzburg	Austria
Pawełczyk Sławomira	slawomira.pawelczyk@polsl.pl	Silesian University of Technology	Gliwice	Poland
Pelc Andrzej	andrzej.pelc@mail.umcs.pl	Maria Curie-Skłodowska University, VAT 712-010-36-92	Lublin	Poland
Pierchala Anna	pierchala@fis.agh.edu.pl	AGH University of Science and Technology	Kraków	Poland
Piotrowska Natalia	natalia.piotrowska@polsl.pl	Silesian University of Technology	Gliwice	Poland
Piper Thomas	t.piper@biochem.dshs-koeln.de	German Sport University Cologne	Cologne	Germany

Pleśniak Łukasz	lukasz.plesniak@uwr.edu.pl	University of Wroclaw, Institute of Geological Sciences	Wroclaw	Poland
Pralle Kerstin	kp@iva-analysentechnik.de	IVA Analysentechnik GmbH & Co. KG	Meerbusch	Germany
Różański Kazimierz	rozanski@agh.edu.pl	AGH University of Krakow	Krakow	Poland
Sarkar Ashish	ashish29s@yahoo.co.in	Retired	Kolkata	India
Sarkar Sudipta	sudiptaashish@yahoo.co.in	Retired	Kolkata	India
Sensuła Barbara	barbara.sensula@polsl.pl	Silesian University of Technology	Gliwice	Poland
Siira Jenniina	jenniina.siira@ruokavirasto.fi	Finnish Food Authority	Helsinki	Finland
Sommerhuber Lamona			Deutschlandsberg	Austria
Strauch Gerhard	gerhard.strauch@ufz.de	Helmholz Center for Environmental Research	Leipzig	Germany
Sulejewski Marek	sulejewskim@yahoo.com	OLD RED	Katowice	Poland
Swinkels Peter	pswinkels@picarro.com	Peter Swinkels	Santa Clara	US
Tichy Gottfried	schnuefferl@gmx.atf	Salzburg University	Salzburg	Austria
Trojanowska-Olichwer Adriana	adriana.trojanowska-olichwer@uwr.edu.pl	University of Wroclaw	Wroclaw	Poland
Tütken Thomas	tuetken@uni-mainz.de	Institut für Geowissenschaften, Univeristät Mainz	Mainz	Germany
Ustrzycka Alicja	alicja.ustrzycka@polsl.pl	Silesian University of Technology	Gliwice	Poland
Vagner Irina	irina.vagner@icsi.ro	Irina Vagner	Râmnicu Vâlcea	Romania
Varlam Carmen	carmen.varlam@icsi.ro	National Research and Development Institute for Cryogenics and Isotopic Technologies	Râmnicu Valcea	Romania

Williams Niel	niel.williams@thermofisher.com	Thermo Fisher Scientific	Hempstead	UK

We thank our SPONSORS

PICARRO

IVA

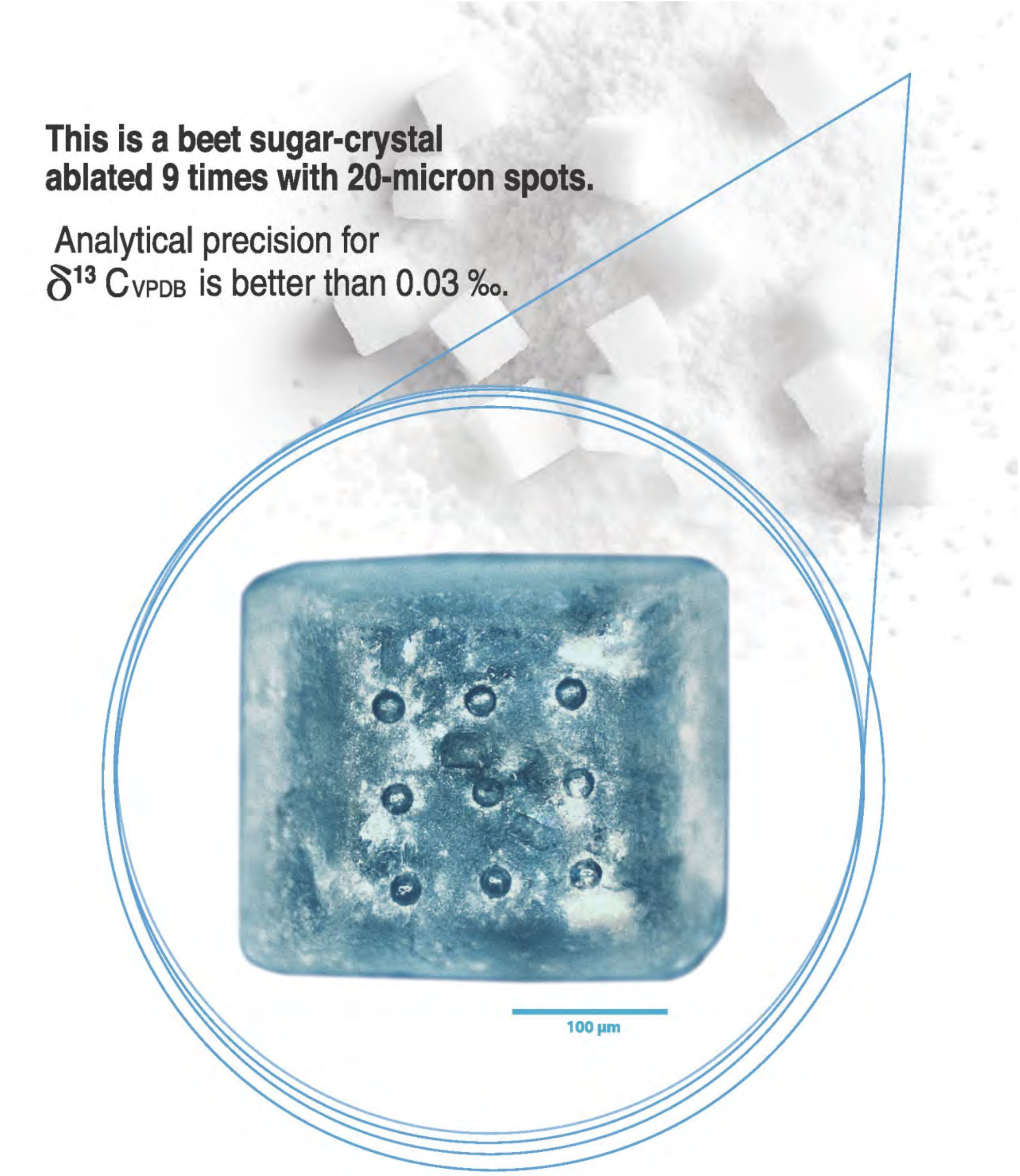
100 μm